Effect of Mercury Speciation on its Transport in Soil and Removal from Produced Water

Submitted in partial fulfillment of the requirements for

the degree of

Doctor of Philosophy

in

Civil and Environmental Engineering

Ke Gai

B.S., Environmental Engineering, China University of Mining & Technology, Beijing

M.S., Environmental Science, University of Chinese Academy of Sciences

Carnegie Mellon University

Pittsburgh, PA

August, 2017

This work is dedicated to my mother and father.

ACKNOWLEDGEMENTS

I would like to express my sincere gratitude to my advisor, Professor Greg Lowry, for his continuous support of my entire study at Carnegie Mellon University, and for his guidance, patience, and kindness. I have been incredibly fortunate to have Greg as my advisor.

I would like to thank the Committee members, Professor David Dzombak, Professor Athanasios Karamalidis, and Dr. Thomas Hoelen, for their valuable comments and advice during both of my Proposal and Thesis Defense.

I am thankful to Thomas for coordinating the financial support from Chevron, providing samples for the experiments, and sending feedbacks throughout the research. Dr. Francisco Lopez-Linares and Dr. Astrid Avellan have also been helpful with the analysis. I am also thankful to Ron Ripper for his experimental support in the lab from placing orders on the chemicals to troubleshooting on the instruments. I would not have been able to have anything done without him. I thank my entire office PH 207C for the great environment and friendliness.

I would also like to take this opportunity to express my deep gratitude to my undergraduate advisor / lifetime mentor, Professor Ma Liqiang, for his kind support and valuable advice. I am also grateful to my advisor for my Master's program, Professor Shi Baoyou. I would not be able to be where I am without them.

I am grateful to have my wonderful family and friends who support me unconditionally.

This research was supported by Chevron Corporation, and the National Science Foundation (NSF) and the US Environmental Protection Agency (EPA) under NSF Cooperative Agreement EF-0830093, Center for the Environmental Implications of Nanotechnology (CEINT). Any opinions, findings, conclusions or recommendations expressed in this thesis are those of the

authors and do not necessarily reflect the views of the NSF or the EPA. This work has not been subjected to EPA review and no official endorsement should be inferred.

ABSTRACT

Mercury (Hg) is distributed globally through atmospheric transport. The broad range of environmental conditions will lead to various possible speciation of mercury, which will ultimately affect the toxicity and transport of mercury. Hg toxicity, transport and speciation have been widely studied. However, information about effects of Hg speciation on its environmental behavior in unsaturated porous media and on its removal from wastewater stream is still limited. The present work contributes towards understanding the impact of Hg speciation on both the transport of Hg species in unsaturated porous media (e.g., surface soil) and removal of Hg species in wastewater streams. This knowledge is necessary to assess the possible environmental risks of Hg in the environment, where different Hg species can exist and have different properties and impacts on water quality and ecosystems.

The first objective of this research was to determine the effect of Hg speciation on its retention in partially saturated soils. The retention of Hg species in model porous media and in real soil was assessed in column breakthrough experiments. Deposition (retention) rates for each Hg species were calculated to evaluate the influence of Hg speciation, porous medium composition and influent solution on the mobility of Hg species in porous media. This study provided information about the relative retention of each Hg species in soils, and identified natural-organic-matter-bound Hg as the most mobile Hg species and that with the greatest potential for vertical migration to groundwater.

The second objective of this research was to determine how Hg speciation affects its ability to be removed from water via adsorption by activated carbon and organoclay. The effects of Hg speciation, water quality parameters and adsorbent type on the removal of Hg were compared to explore the potential removal efficacy and mechanism. The result indicated Hg

removal efficacy was influenced by Hg speciation differently depending on the solution conditions. Therefore, using total dissolved Hg(II) to predict Hg removal efficacy may not provide a reliable estimate of adsorption. Organoclay was shown to have a highly reactive surface and the highest adsorption capacity per unit specific surface area among the tested adsorbents.

The third objective was to determine the Hg speciation in produced water from an oil production well, and to study the influence of Hg speciation on its removal from produced water by adsorbents. Mercury species in a produced water sample were identified as mainly particulate species and hydrophobic species. The removal of the amended Hg species in produced water was measured to evaluate the impact of Hg speciation on its removal. This study showed that produced water composition affected Hg speciation and formed hydrophobic Hg was more difficult to remove than initially added hydrophilic Hg species in produced water.

TABLE OF CONTENTS

LIST OF TABLES

LIST OF FIGURES

Chapter 1. Introduction, Motivation and Objectives

1.1 Mercury in the Environment

Mercury (Hg) is a heavy metal distributed globally through atmospheric transport[1]. Hg can be present in various concentrations in fossil fuels[2, 3], and efficient Hg control devices should be used in specific cases to control releases into the environment from production and processing of fossil fuels. Mercury is released to the environment most commonly as elemental Hg, dissolved or complexed ionic Hg^{2+}, or particulate Hg through natural and anthropogenic processes. Once introduced in environmental systems, mercury can transform between Hg(0) (metallic), Hg(I) (mercurous) and Hg(II) (mercuric) species depending on the redox condition of the ecosystem[4]. Hg(0) is the main form of mercury in the atmosphere due to its high vapor pressure and low water solubility and contributes to the global mercury inputs and transport[5]. In aquatic and terrestrial environment, Hg mainly exists in its ionic form, particularly in its II valence state. Through biotic and abiotic processes[6, 7], inorganic mercury species can also be transformed into organic mercury species (e.g., methyl mercury), which is more toxic than its inorganic form and can bioaccumulate and biomagnify[8-10]. Environmental conditions (e.g., pH and redox) can lead to various possible mercury species, which will ultimately affect their environmental fate and the efficacy of Hg removal technologies. There is limited knowledge about how the speciation of mercury affects its transport in an unsaturated porous medium, and its removal from water by adsorbents. This thesis systematically explores the impact of Hg speciation on these processes.

1.1.1 Hg speciation in water

Mercury speciation in water is complex. In aquatic systems, mercury mainly exists as a mixture of Hg complexes[11-15]. The nature of the mercury species present will depend on the ligands present, and pH and Eh[16-22]. As demonstrated previously[18], mercury is most likely to complex with OH^-, Cl^-, S^{2-} and S-containing functional groups of organic ligands because of their high stability with mercury[23-27]. Soft acids (e.g., Hg^{2+}) react more strongly with soft bases (e.g., RS^-) than with hard bases (e.g., OH^-). Thus, ligands containing thiolate functional groups are expected to complex Hg most strongly (Figure 1). In the absence of sulfide, other ligands such as chloride and hydroxide will dominate the complexation with mercury[4, 19, 20, 28]. Oxygen-containing functional groups such as carboxylic functional or phenolic groups, other than organic S groups, can also act as the primary binding sites for Hg in the absence of reduced sulfur[29]. In the presence of thiol functional groups, the predominant speciation is Hg-$(SR)_x$ species. Thiol groups present in dissolved organic matter (DOM) are therefore likely responsible for the strong binding between Hg and DOM[12, 13].

The presence of Hg species including Hg-dissolved organic matter (DOM) complexes and HgS nanoparticles have been identified in aquatic systems. Revis et al.[30] suggested that ~85% of mercury at East Fork Poplar Creek had been predominately converted to mercuric sulfide (HgS) as a consequence of sulfate reduction in the soils[31, 32]. Hg was correlated with sulfur concentration in soils from that site, bolstering the idea that mercury has been transformed to HgS. It was also shown that mercury-sulfide minerals, cinnabar (α-HgS) and metacinnabar (β-HgS), are the majority of Hg species in mine wastes related to mercury and gold mining[33-35].

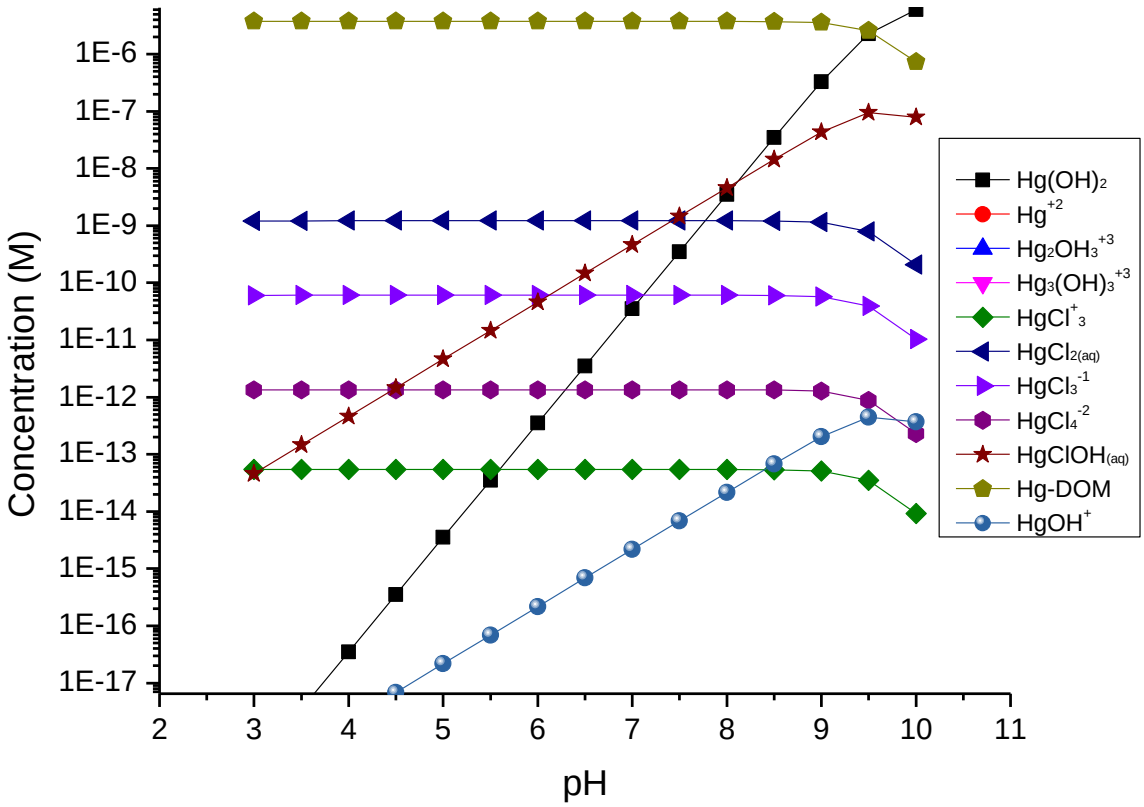

Figure 1. Representative speciation diagram for dissolved Hg(II) species (7.5 µM) under simulated oxic water conditions (0.005 M NaCl, 1mg C/L HA). Visual MINTEQ was used for the simulation of dissolved Hg(II) species (denoted as Hg(II)* in this thesis) by assuming equilibrium was reached. Additional speciation diagrams for dissolved Hg(II) species simulated for our experimental conditions are Figure 3.1 and Figure A4 and A5 in Appendix A. Hg-DOM and HgS nanoparticles under those experimental conditions are assumed to be stable and therefore no Hg speciation diagrams were made for Hg-DOM and HgS nanoparticles.

In addition to inorganic ligands, Hg(II) has a high tendency to be associated with DOM. Both laboratory and modeling studies indicated that more than 90% of inorganic mercury and from 70% to 90% of MeHg in water may be bound with dissolved organic matter (DOM)[19, 20, 28]. Many Hg-impacted aquatic media contain high concentrations of both sulfide and DOM (e.g., in landfill leachate). In these systems, the dominant species are mercury complexes with sulfide and DOM[18], and some metacinnabar nanoparticles have been shown to be present[36-38]. In the presence of DOM formed HgS nanoparticles may prevent aggregation to sizes that are readily sedimented from solution. In laboratory experiments using only DOM (10 mg C/L) and micromolar concentrations of dissolved Hg, HgS primary particle growth was limited to 1-5 nm in diameter, and aggregates of the HgS nanoparticles did not grow beyond a hydrodynamic diameter of about 20-200 nm[36-38].

1.1.2 Hg transport in porous media

Certain Hg-containing wastes may be disposed of in landfills, and vertical transport of Hg in the surrounding vadose zone can impact the groundwater. This is especially true for older landfills, or those in developing countries where appropriate barriers and leachate collection systems are not in place. Sandy (low total organic carbon (TOC)) sites and equatorial (high TOC) sites are also typical porous media in locations where oil and gas are extracted. Most mercury transport studies have usually tracked Hg species by physical size, reporting the dissolved form (< 1 nm), the colloidal form (1 nm – 1 μm) and the particulate form (> 1 μm) of Hg[18]. Although this classification of Hg species into dissolved form (< 1 nm), colloidal form (1 nm – 1 μm) and particulate form (> 1 μm) is practical for analysis and reporting, this definition is not appropriate for modeling the transport of Hg species in porous media. For example, purely dissolved Hg species defined as those that pass through a 0.45 μm filter is not accurate, since HgS

nanoparticles with a small enough diameter would also be described as a dissolved Hg species by this definition. Dissolved inorganic Hg(II) species (e.g., $HgCl_3^-$) can behave differently from dissolved Hg-DOM complexes due to differences in their molecular weight and availability to be adsorbed to solid surface via complexation with surface functional groups on the porous media particles[23, 39]. HgS nanoparticles can behave differently still from the inorganic Hg(II) ions or Hg-DOM in terms of its ability to associate with different ligands and its mobility in soil. The surface charge and macromolecule coating on both nanoparticles and porous media particles can impact the nanoparticle stability in porous media by changing the electrostatic interactions and steric repulsions between the nanoparticles and particles in porous media[40-43]. The effect of Hg speciation, beyond just size, on Hg transport in porous media has not been studied.

Most Hg transport experiments in porous media have been conducted under saturated conditions. However, the porous media in near-surface environments usually remain unsaturated. The porous medium composition (e.g., grain size and TOC content associated with porous media particles) and solution condition (e.g., ionic strength and DOM) are expected to dramatically change the fate of dissolved Hg(II) species, dissolved Hg-DOM complexes and HgS nanoparticles. The influences of these factors in Hg transport are important pieces of knowledge needed to better understand Hg transport in soils. To enhance our understanding of how Hg speciation and porous medium properties may impact its transport in an unsaturated porous medium, column experiments with three controllable variables (i.e., Hg species, porous medium properties, and influent solution chemistry) were conducted under unsaturated conditions to evaluate their impacts of Hg speciation on its transport.

1.1.3 Removal of Hg from wastewater and produced water

Wastewater from various locations may contain elevated levels of Hg that may need to be reduced prior to final disposition. Due to various liable ligands for Hg present in wastewater streams, Hg can form a number of different species in wastewater, e.g., elemental Hg, Hg(II) adsorbed to dissolved organic matter (Hg(II)-DOM), and mononuclear or nanoparticulate HgS[13, 36, 44-50] . Competing ligand exchange-solid phase extraction (CLE-SPE) experiments were used to separate hydrophilic Hg species from hydrophobic Hg species in wastewater streams[51-53]. This method can also qualitatively assess Hg speciation by comparing the binding strength between Hg-ligand complexes present in water with that of the probe ligand and the bond strength of the other Hg species that may be present (e.g., HgS). Natural organic matter (NOM) was shown to associate with Hg(II) species to form hydrophilic Hg(II) complexes, and inorganic sulfide was shown to react with Hg(II) species to form strong hydrophobic Hg(II) species (i.e., mononuclear HgS)[51]. The differences in the hydrophobicity of the Hg species was shown to affect the distribution of Hg species in produced water, which may impact the choice of technologies used for Hg removal from wastewater.

Produced water is water separated from reservoir fluids during crude oil and natural gas production[54]. It can contain dissolved and dispersed hydrocarbons, dissolved salts, formation material, metals and production chemicals. Reported Hg concentrations in the range of 0.1-20,000 ng/g in crude oils[55] with a mean value of ~10 ppb and 10-3,000 ng/g in gas condensate[56] have been reported[57]. Produced water generated from oil and gas field with Hg can contain Hg species and may need to be reduced to meet disposition limits. Due to the low mercury concentrations that are typically encountered in produced waters (less than 1 ppm[58]), Hg speciation is difficult to measure. A three stage filtration systems was developed to identify

organically-bound, elemental, and ionic mercury species in produced water[59]. With abundant hydrocarbons (e.g., carboxylic acid[60], benzothiophene and dibenzothiophene[61]) in produced water, Hg is expected to form Hg(II)-thiol complexes, or potentially HgS nanoparticles. However, the complexation of Hg(II) species in produced water has not been reported in the peer-reviewed literature. Doing so can help to optimize produced water treatment strategies.

A variety of physical and chemical treatments can be used to remove Hg from aqueous streams. These removal processes use methods to remove particle-bound Hg (e.g., filtration) and to adsorb dissolved Hg species, e.g., powder activated carbon treatment, ion exchange, amalgamation, chemical precipitation, electrodeposition, reverse osmosis, photochemical methods, flotation, mechanical filtration, membrane separation, and selective liquid-liquid extraction[48, 62-74]. Complexation-filtration was also studied to remove mercury from waste water[75-77]. Polyethylenimine (PEI), poly(γ-glutamic acid) (γ-PGA)[77] , chitosan[78], xanthate[75, 79-81], xanthate-cationic polymer [e.g., poly(vinylbenzyltrimethylammonium chloride or polythylenimine)] complex [75] and commercially available Nalmet[82] were used as complexing agents to precipitate Hg(II) species. Nanomaterials are also proposed as highly promising materials for Hg removal processes[83, 84].

Adsorbents are most often used to remove remaining dissolved and nanoparticulate Hg from the water after filtration to remove larger particulate Hg species. Particularly, activated carbon is widely used because of its high internal surface area and relatively low cost[85-87]. Sulfurization of activated carbon was shown to be an effective way to enhance the adsorption of either elemental Hg or mercuric ions onto activated carbons[88-91]. Organoclays are another engineered geosorbent with high affinity for metals. They are prepared by adsorption of organic molecules onto the clays and have been used previously in in aqueous Hg adsorption studies[92-94].

Organoclays functionalized by dithiocarbamate[94] and 2-mercapto-5-amino-1,3,4-thiadiazole[93] exhibited strong aqueous Hg(II) adsorption capacity. These studies suggest that the sulfur containing functional groups play an important role in Hg removal from produced water, but the efficacy of these sulfur-modified sorbents in produced water has not been evaluated. Moreover, the effect of mercury speciation on the efficacy of these sorbents has never been studied.

The impact of Hg speciation on the efficacy of sorption-based or filtration-based treatment alternatives is also not well known, especially for produced water. Most studies about mercury removal in aqueous media have been tested using dissolved Hg(II) in the absence of common environmental ligands[95-97]. However, Hg will complex with different ligands (e.g., S^{2-}, Cl^{-} and DOM)[36, 44, 98-101] because of the strong binding constants[11-15]. Also, particulate Hg and particle-bound Hg forms are present in environmental systems[36, 44, 100, 101]. Hg species such as HgS nanoparticles and Hg-DOM complex are likely more difficult to be removed because the porous structure of adsorbents is less accessible for these larger Hg species than for dissolved Hg(II) species.

Water quality parameters (e.g., ionic strength, ionic composition and NOM) and adsorbent properties may affect the efficacy of adsorbents for Hg removal. Ionic strength can affect dissolved Hg(II) speciation and the surface charge of HgS nanoparticles, and divalent cation can be more effective in screening the surface charge of nanoparticles than monovalent cation when humic acid present[102]. These effects may change the adsorption affinity of Hg species onto adsorbents. Activated carbon with a large surface area and pore volume may sorb Hg species better than organoclay (OC) which has a relatively lower surface area. However, the S-containing functional groups on OC can also be reactive with Hg species and therefore enhance the Hg removal from water. Thus it is necessary to assess the performance of

commercial products (especially activated carbon due to its relatively low cost) towards different Hg species (e.g., HgS nanoparticles, Hg(II)-DOM) under different solution conditions and produced water conditions. Better understanding of the role of Hg speciation and solution conditions on its removal will aid in the design of more efficient treatment alternative. A summary of the variables tested and the rationale for testing them in provided in Table 1.

Table 1. Variables tested in Hg removal experiments.

Variables tested and importance	**Impact on Hg species**	**Data gap**
Dissolved organic matter (DOM). DOM is present in process water and wastewaters.	DOM can complex with dissolved Hg(II) species. Sorption of DOM onto HgS NPs or onto sorbents can increase the stability of HgS nanoparticles against aggregation and heteroaggregation by increasing steric repulsions. Hence, DOM is expected to influence the removal of Hg species.	The effect of DOM in the wastewater on the removal of selected Hg species needs to be compared to assess the magnitude of its impact of different Hg species and sorbents.
Ionic strength. Produced water may contain high concentrations of salt.	Increased ionic strength can decrease the activity of dissolved Hg(II) species, reduce the stability HgS nanoparticles by screening its surface charge. Therefore, ionic strength is expected to affect the adsorption of Hg species.	The effect of ionic strength on the removal of Hg^{2+} was widely studied. Its effect on the removal of Hg-DOM and HgS needs to be determined.
Cation type (Na^{+} and Ca^{2+}). Produced water may have different ratios of Ca2+ to Na+ depending on the source.	Ca^{2+} is more effective in screening the surface charge of HgS nanoparticles than Na^{+}. Ca^{2+} also can bridge the DOM onto the adsorbent surface to affect the removal of Hg species.	The effect of cation type on the removal of selected Hg species is not reported.

Table 1 (continued). Variables tested in Hg removal experiments.

Variables tested and importance	**Impact on Hg species**	**Data gap**
Adsorbent type (activated carbon and organoclay). Different adsorbents are available for Hg removal.	Activated carbon has a larger surface area than organoclay due to the porous structure, which could trap additional small-sized Hg species. Also, each may have different surface charge that can affect removal efficiency.	The effect of adsorbent type on the removal of selected Hg species needs to be compared.
Sulfur type and content on adsorbent. Sorbents have different types and amounts of S designed to sequester Hg.	Impregnated sulfur on adsorbents may react with dissolved Hg(II) and Hg-DOM to increase the adsorption. Elemental S may react differently than dithiocarbamate compounds.	The effect of the amount and form of sulfur on adsorbent on the removal of selected Hg species needs to be determined to design better sorbents.
Hg hydrophobicity in produced water. Hydrocarbons in produced water can lead to hydrophobic Hg species.	Hydrophobic Hg species are likely to be associated with the dispersed oil phase (micro emulsions), which could be difficult to remove by adsorbents.	The effect of Hg speciation (hydrophobicity) on its removal from produced water has never been assessed.

These knowledge gaps lead to several important questions concerning the fate of Hg in soil and its removal from produced water and wastewater:

How does Hg speciation impact its transport in unsaturated porous media? How do water chemistry and porous media composition affect the mobility of different Hg species under unsaturated porous media?

How does the speciation of the most relevant Hg species (e.g., Hg-DOM, HgS nanoparticles) in aquatic systems impact its removal from water? How do the adsorbent properties and water chemistry affect the removal of those Hg species? (Possible effects of variables on Hg species are listed in Table 1)

What are the speciation and distribution of Hg in produced water from oil extraction?

How does produced water composition influence the Hg speciation?

How does Hg speciation affect its removal from produced water? (Possible effect of Hg speciation on its removal from produced water is listed in Table 1)

By answering these questions we will better understand the transport and removal of Hg species in soil and water.

1.2 Research Objectives

The overreaching objective of this research was to better understand how Hg speciation and water quality parameters affect Hg fate and removal in natural and engineered systems, with particular focus on systems relevant to the petroleum industry. Three studies were aimed at assessing the impacts of Hg speciation on 1) its transport in porous media, and 2) removal from water streams including petroleum produced water.

Objective 1. Understand how Hg speciation, porous medium properties and water chemistry affects Hg transport in unsaturated soils. The mobility of four important model Hg species in a model unsaturated porous medium and soils was assessed using column breakthrough experiments. Hg species included dissolved Hg(II) species, Hg-DOM, HgS nanoparticles, and elemental Hg. Porous medium included well-characterized sands and a real soil. The influence of ionic strength and background DOM in solution was systematically evaluated. Finally, the impact of the porous medium grain size distribution was assessed. These studies showed that Hg speciation is indeed an import factor affecting their transport in an unsaturated porous medium such as a surface soil.

Objective 2. Evaluate the impact of Hg speciation, adsorbent type and water chemistry on the removal of Hg species from water. The removal of Hg(II), Hg-DOM and HgS nanoparticles from water was measured in batch experiments using commercially available sorbents. The adsorbent types included activated carbon, sulfur impregnated activated carbon and sulfur impregnated organoclay. The effects of ionic strength, ionic composition and the presence of DOM on the removal of Hg species were determined. Hg X-ray absorption spectroscopy was used to evaluate the Hg speciation on the adsorbents. These studies showed that Hg speciation impacts its removal differently dependent on adsorbent type and water chemistry, and that the speciation of Hg on the sorbent is affected by the sorbent properties.

Objective 3. Determine the Hg speciation in produced water and assess the influence of Hg speciation on its removal from produced water. The Hg speciation in produced water samples from an oil well was determined by serial filtration and solid phase extraction experiments. Different Hg species were added to the produced water to study the influence of the produced water hydrocarbons on the speciation of Hg. Removal experiments for added Hg species were conducted to determine how Hg hydrophobicity affects its removal from produced water.

This study, for the first time, systematically evaluated the effect of Hg speciation on its transport in unsaturated porous media including natural soils, and on its removal from water using adsorbents. In this study, pH was fixed at 7.5 in the experiments in chapter 2 and 3 (objective 1 and 2), because the neutral pH fell in the range of reported values for mature landfill leachates[103] and produced waters[58], and this pH also matched the values measured for the produced water samples studied in chapter 4 (objective 3). Evaluation of removal efficiency in treated produced waters provides, for the first time, valuable insights into the mechanisms of

removal of Hg species present in produced water, and helps to identify the removal technologies for final polishing of these waters prior to disposition or reuse. The present work also provides a better understanding of how various representative Hg species respond to the selected environmental systems, and provides insights into optimizing the process steps that may be used to meet treatment requirements as a function of the upstream operating conditions.

1.3 References

1. Boening, D.W., Ecological effects, transport, and fate of mercury: a general review. *Chemosphere* **2000,** *40* (12), 1335-1351.
2. Wilhelm, S.M.; Bloom, N., Mercury in petroleum. *Fuel Processing Technology* **2000,** *63* (1), 1-27.
3. Brown, T.D.; Smith, D.N.; Hargis Jr, R.A.; O'Dowd, W.J., Mercury measurement and its control: what we know, have learned, and need to further investigate. *Journal of the Air & Waste Management Association* **1999,** *49* (6), 1-97.
4. Nriagu, J.O., *The biogeochemistry of mercury in the environment*. 1979: Elsevier/North-Holland Biomedical Press.
5. Galbreath, K.C.; Zygarlicke, C.J., Mercury speciation in coal combustion and gasification flue gases. *Environmental science & technology* **1996,** *30* (8), 2421-2426.
6. Wiatrowski, H.A.; Ward, P.M.; Barkay, T., Novel reduction of mercury (II) by mercury-sensitive dissimilatory metal reducing bacteria. *Environmental science & technology* **2006,** *40* (21), 6690-6696.
7. Benoit, J.M.; Gilmour, C.C.; Mason, R.P.; Heyes, A., Sulfide controls on mercury speciation and bioavailability to methylating bacteria in sediment pore waters. *Environmental science & technology* **1999,** *33* (6), 951-957.
8. Baker, M.R.; Schindler, D.E.; Holtgrieve, G.W.; St. Louis, V.L., Bioaccumulation and transport of contaminants: migrating sockeye salmon as vectors of mercury. *Environmental science & technology* **2009,** *43* (23), 8840-8846.

9. Zhang, X.; Naidu, A.S.; Kelley, J.J.; Jewett, S.C.; Dasher, D.; Duffy, L.K., Baseline Concentrations of Total Mercury and Methylmercury in Salmon Returning Via the Bering Sea(1999-2000). *Marine Pollution Bulletin* **2001,** *42* (10), 993-997.

10. MacCrimmon, H.R.; Wren, C.D.; Gots, B.L., Mercury uptake by lake trout, Salvelinus namaycush, relative to age, growth, and diet in Tadenac Lake with comparative data from other Precambrian shield lakes. *Canadian Journal of Fisheries and Aquatic Sciences* **1983,** *40* (2), 114-120.

11. Haitzer, M.; Aiken, G.R.; Ryan, J.N., Binding of mercury (II) to aquatic humic substances: Influence of pH and source of humic substances. *Environmental science & technology* **2003,** *37* (11), 2436-2441.

12. Haitzer, M.; Aiken, G.R.; Ryan, J.N., Binding of mercury (II) to dissolved organic matter: the role of the mercury-to-DOM concentration ratio. *Environmental science & technology* **2002,** *36* (16), 3564-3570.

13. Ravichandran, M., Interactions between mercury and dissolved organic matter - a review. *Chemosphere* **2004,** *55* (3), 319-331.

14. Hesterberg, D.; Chou, J.W.; Hutchison, K.J.; Sayers, D.E., Bonding of Hg (II) to reduced organic sulfur in humic acid as affected by S/Hg ratio. *Environmental science & technology* **2001,** *35* (13), 2741-2745.

15. Xia, K.; Skyllberg, U.; Bleam, W.; Bloom, P.; Nater, E.; Helmke, P., X-ray absorption spectroscopic evidence for the complexation of Hg (II) by reduced sulfur in soil humic substances. *Environmental science & technology* **1999,** *33* (2), 257-261.

16. Belzile, N.; Lang, C.Y.; Chen, Y.W.; Wang, M., The competitive role of organic carbon and dissolved sulfide in controlling the distribution of mercury in freshwater lake sediments. *Science of the Total Environment* **2008,** *405* (1), 226-238.

17. Drott, A.; Lambertsson, L.; Björn, E.; Skyllberg, U., Importance of dissolved neutral mercury sulfides for methyl mercury production in contaminated sediments. *Environmental science & technology* **2007,** *41* (7), 2270-2276.

18. Liu, G.; Cai, Y.; O'Driscoll, N., Eds. *Environmental chemistry and toxicology of mercury*. **2012,** John Wiley & Sons, Inc., Hoboken, New Jerse.

19. Morel, F.M.M.; Kraepiel, A.M.L.; Amyot, M., The chemical cycle and bioaccumulation of mercury. *Annual review of ecology and systematics* **1998**, 543-566.

20. Ullrich, S.M.; Tanton, T.W.; Abdrashitova, S.A., Mercury in the aquatic environment: a review of factors affecting methylation. *Critical Reviews in Environmental Science and Technology* **2001,** *31* (3), 241-293.

21. Wolfenden, S.; Charnock, J.M.; Hilton, J.; Livens, F.R.; Vaughan, D.J., Sulfide species as a sink for mercury in lake sediments. *Environmental science & technology* **2005,** *39* (17), 6644-6648.

22. Zhong, H.; Wang, W.X., Inorganic mercury binding with different sulfur species in anoxic sediments and their gut juice extractions. *Environmental Toxicology and Chemistry* **2009,** *28* (9), 1851-1857.

23. Schuster, E., The behavior of mercury in the soil with special emphasis on complexation and adsorption processes-a review of the literature. *Water, Air, & Soil Pollution* **1991,** *56* (1), 667-680.

24. Powell, K.J.; Brown, P.L.; Byrne, R.H.; Gajda, T.; Hefter, G.; Sjöberg, S.; Wanner, H., Chemical speciation of Hg (II) with environmental inorganic ligands. *Australian journal of chemistry* **2004,** *57* (10), 993-1000.

25. Schwarzenbach, G.; Widmer, M., Die löslichkeit von metallsulfiden I. schwarzes quecksilbersulfid. *Helvetica chimica acta* **1963,** *46* (7), 2613-2628.

26. Dyrssen, D.; Wedborg, M., The sulphur-mercury (II) system in natural waters. *Water, Air, & Soil Pollution* **1991,** *56* (1), 507-519.

27. Jay, J.A.; Morel, F.M.M.; Hemond, H.F., Mercury speciation in the presence of polysulfides. *Environmental science & technology* **2000,** *34* (11), 2196-2200.

28. Fitzgerald, W.F.; Lamborg, C.H.; Hammerschmidt, C.R., Marine biogeochemical cycling of mercury. *Chemical Reviews-Columbus* **2007,** *107* (2), 641-662.

29. Chai, X.; Liu, G.; Zhao, X.; Hao, Y.; Zhao, Y., Complexion between mercury and humic substances from different landfill stabilization processes and its implication for the environment. *Journal of hazardous materials* **2012**.

30. Revis, N.; Osborne, T.; Holdsworth, G.; Hadden, C., Distribution of mercury species in soil from a mercury-contaminated site. *Water, Air, & Soil Pollution* **1989,** *45* (1), 105-113.

31. Barnett, M.O.; Harris, L.A.; Turner, R.R.; Stevenson, R.J.; Henson, T.J.; Melton, R.C.; Hoffman, D.P., Formation of mercuric sulfide in soil. *Environmental science & technology* **1997,** *31* (11), 3037-3043.

32. Harris, L.; Henson, T.; Combs, D.; Melton, R.; Steele, R.; Marsh, G., Imaging and microanalyses of mercury in flood plain soils of east fork poplar creek. *Water, Air, & Soil Pollution* **1996,** *86* (1), 51-69.

33. Lowry, G.V.; Shaw, S.; Kim, C.S.; Rytuba, J.J.; Brown Jr, G.E., Macroscopic and microscopic observations of particle-facilitated mercury transport from New Idria and Sulphur Bank mercury mine tailings. *Environmental science & technology* **2004,** *38* (19), 5101-5111.

34. Slowey, A.J.; Rytuba, J.J.; Brown Jr, G.E., Speciation of mercury and mode of transport from placer gold mine tailings. *Environmental science & technology* **2005,** *39* (6), 1547-1554.

35. Kim, C.S.; Brown, G.E.; Rytuba, J.J., Characterization and speciation of mercury-bearing mine wastes using X-ray absorption spectroscopy. *Science of the Total Environment* **2000,** *261* (1), 157-168.

36. Ravichandran, M.; Aiken, G.R.; Ryan, J.N.; Reddy, M.M., Inhibition of precipitation and aggregation of metacinnabar (mercuric sulfide) by dissolved organic matter isolated from the Florida Everglades. *Environmental science & technology* **1999,** *33* (9), 1418-1423.

37. Slowey, A.J., Rate of formation and dissolution of mercury sulfide nanoparticles: The dual role of natural organic matter. *Geochimica et Cosmochimica Acta* **2010,** *74* (16), 4693-4708.

38. Deonarine, A.; Hsu-Kim, H., Precipitation of mercuric sulfide nanoparticles in NOM-containing water: Implications for the natural environment. *Environmental science & technology* **2009,** *43* (7), 2368-2373.

39. Dzombak, D.A., *Surface complexation modeling: hydrous ferric oxide*. 1990: John Wiley & Sons.

40. McDowell-Boyer, L.M.; Hunt, J.R.; Sitar, N., Particle transport through porous media. *Water Resources Research* **1986,** *22* (13), 1901-1921.

41. Elimelech, M.; O'Melia, C.R., Kinetics of deposition of colloidal particles in porous media. *Environmental science & technology* **1990,** *24* (10), 1528-1536.

42. Min, Y.; Akbulut, M.; Kristiansen, K.; Golan, Y.; Israelachvili, J., The role of interparticle and external forces in nanoparticle assembly. *Nature materials* **2008,** *7* (7), 527-538.

43. Cerbelaud, M.; Videcoq, A.; Abelard, P.; Pagnoux, C.; Rossignol, F.; Ferrando, R., Heteroaggregation between Al_2O_3 submicrometer particles and SiO_2 nanoparticles: Experiment and simulation. *Langmuir* **2008,** *24* (7), 3001-3008.

44. Lowry, G.V.; Shaw, S.; Kim, C.S.; Rytuba, J.J.; Brown, G.E., Macroscopic and Microscopic Observations of Particle-Facilitated Mercury Transport from New Idria and Sulphur Bank Mercury Mine Tailings. *Environmental science & technology* **2004,** *38* (19), 5101-5111.
45. Ravichandran, M., Interactions between mercury and dissolved organic matter—a review. *Chemosphere* **2004,** *55* (3), 319-331.
46. Mierle, G.; Ingram, R., The role of humic substances in the mobilization of mercury from watersheds. *Water, Air, & Soil Pollution* **1991,** *56* (1), 349-357.
47. Kim, C.S.; Brown Jr, G.E.; Rytuba, J.J., Characterization and speciation of mercury-bearing mine wastes using X-ray absorption spectroscopy. *Science of the Total Environment* **2000,** *261* (1–3), 157-168.
48. Smuleac, V.; Butterfield, D.; Sikdar, S.; Varma, R.; Bhattacharyya, D., Polythiol-functionalized alumina membranes for mercury capture. *Journal of Membrane Science* **2005,** *251* (1), 169-178.
49. Miller, C.L.; Liang, L.; Gu, B., Competitive ligand exchange reveals time dependant changes in the reactivity of Hg–dissolved organic matter complexes. *Environmental Chemistry* **2012,** *9* (6), 495-501.
50. Miller, C.L.; Southworth, G.; Brooks, S.; Liang, L.; Gu, B., Kinetic Controls on the Complexation between Mercury and Dissolved Organic Matter in a Contaminated Environment. *Environmental science & technology* **2009,** *43* (22), 8548-8553.
51. Hsu-Kim, H.; Sedlak, D.L., Similarities between inorganic sulfide and the strong Hg (II)-complexing ligands in municipal wastewater effluent. *Environmental science & technology* **2005,** *39* (11), 4035-4041.
52. Hsu, H.; Sedlak, D.L., Strong Hg (II) complexation in municipal wastewater effluent and surface waters. *Environmental science & technology* **2003,** *37* (12), 2743-2749.
53. Black, F.J.; Bruland, K.W.; Flegal, A.R., Competing ligand exchange-solid phase extraction method for the determination of the complexation of dissolved inorganic mercury (II) in natural waters. *Analytica chimica acta* **2007,** *598* (2), 318-333.
54. Veil, J.A.; Puder, M.G.; Elcock, D.; Redweik Jr, R.J., *A white paper describing produced water from production of crude oil, natural gas, and coal bed methane*, 2004, Argonne National Lab., IL (US).

55. Wilhelm, S.M.; Liang, L.; Cussen, D.; Kirchgessner, D.A., Mercury in crude oil processed in the United States (2004). *Environmental Science & Technology* **2007,** *41* (13), 4509-4514.

56. Bouyssiere, B.; Baco, F.; Savary, L.; Lobinski, R., Méthodes analytiques pour la spéciation du mercure dans les condensats de gaz : évaluation critique et conseils. *Oil & Gas Science and Technology - Rev. IFP* **2000,** *55* (6), 639-648.

57. Wilhelm, S.M., Estimate of mercury emissions to the atmosphere from petroleum. *Environmental Science & Technology* **2001,** *35* (24), 4704-4710.

58. Tibbetts, P.; Buchanan, I.; Gawel, L.; Large, R., *A comprehensive determination of produced water composition*, in *Produced Water* **1992**, Springer. p. 97-112.

59. Alper, H., *Method and system for analyzing concentrations of diverse mercury species present in a fluid medium*, **2014,** Google Patents.

60. Bostick, D.T., *Characterization of soluble organics in produced water*, **2002,** ORNL Oak Ridge National Laboratory (US).

61. Durell, G.; Røe Utvik, T.; Johnsen, S.; Frost, T.; Neff, J., Oil well produced water discharges to the North Sea. Part I: Comparison of deployed mussels (Mytilus edulis), semi-permeable membrane devices, and the DREAM model predictions to estimate the dispersion of polycyclic aromatic hydrocarbons. *Marine Environmental Research* **2006,** *62* (3), 194-223.

62. Biester, H.; Schuhmacher, P.; Müller, G., Effectiveness of mossy tin filters to remove mercury from aqueous solution by Hg (II) reduction and Hg (0) amalgamation. *Water research* **2000,** *34* (7), 2031-2036.

63. Huttenloch, P.; Roehl, K.E.; Czurda, K., Use of copper shavings to remove mercury from contaminated groundwater or wastewater by amalgamation. *Environmental science & technology* **2003,** *37* (18), 4269-4273.

64. Chojnacki, A.; Chojnacka, K.; Hoffmann, J.; Gorecki, H., The application of natural zeolites for mercury removal: from laboratory tests to industrial scale. *Minerals Engineering* **2004,** *17* (7), 933-937.

65. Oehmen, A.; Viegas, R.; Velizarov, S.; Reis, M.A.; Crespo, J.G., Removal of heavy metals from drinking water supplies through the ion exchange membrane bioreactor. *Desalination* **2006,** *199* (1), 405-407.

66. Evangelista, S.M.; DeOliveira, E.; Castro, G.R.; Zara, L.F.; Prado, A.G., Hexagonal mesoporous silica modified with 2-mercaptothiazoline for removing mercury from water solution. *Surface science* **2007,** *601* (10), 2194-2202.

67. Fábrega, F.d.M.; Mansur, M.B., Liquid–liquid extraction of mercury (II) from hydrochloric acid solutions by Aliquat 336. *Hydrometallurgy* **2007,** *87* (3), 83-90.

68. Lopes, C.; Otero, M.; Coimbra, J.; Pereira, E.; Rocha, J.; Lin, Z.; Duarte, A., Removal of low concentration Hg^{2+} from natural waters by microporous and layered titanosilicates. *Microporous and mesoporous materials* **2007,** *103* (1), 325-332.

69. Park, H.G.; Kim, T.W.; Chae, M.Y.; Yoo, I.-K., Activated carbon-containing alginate adsorbent for the simultaneous removal of heavy metals and toxic organics. *Process biochemistry* **2007,** *42* (10), 1371-1377.

70. Vieira, M.A.; Ribeiro, A.S.; Curtius, A.J.; Sturgeon, R.E., Determination of total mercury and methylmercury in biological samples by photochemical vapor generation. *Analytical and bioanalytical chemistry* **2007,** *388* (4), 837-847.

71. Chakrabarty, K.; Saha, P.; Ghoshal, A.K., Separation of mercury from its aqueous solution through supported liquid membrane using environmentally benign diluent. *Journal of Membrane Science* **2010,** *350* (1), 395-401.

72. Olkhovyk, O.; Jaroniec, M., Ordered Mesoporous Silicas with 2,5-Dimercapto-1,3,4-Thiadiazole Ligand: High Capacity Adsorbents for Mercury Ions. *Adsorption* **2005,** *11* (3-4), 205-214.

73. Kostal, J.; Mulchandani, A.; Gropp, K.E.; Chen, W., A temperature responsive biopolymer for mercury remediation. *Environmental science & technology* **2003,** *37* (19), 4457-4462.

74. Mahmoud, M.E.; Gohar, G.A., Silica gel-immobilized-dithioacetal derivatives as potential solid phase extractors for mercury (II). *Talanta* **2000,** *51* (1), 77-87.

75. Swanson, C.L.; Wing, R.E.; Doane, W.M.; Russell, C.R., Mercury removal from waste water with starch xanthate-cationic polymer complex. *Environmental science & technology* **1973,** *7* (7), 614-619.

76. Barron-Zambrano, J.; Laborie, S.; Viers, P.; Rakib, M.; Durand, G., Mercury removal and recovery from aqueous solutions by coupled complexation–ultrafiltration and electrolysis. *Journal of Membrane Science* **2004,** *229* (1), 179-186.

77. Inbaraj, B.S.; Wang, J.S.; Lu, J.F.; Siao, F.Y.; Chen, B.H., Adsorption of toxic mercury(II) by an extracellular biopolymer poly(γ-glutamic acid). *Bioresource technology* **2009,** *100* (1), 200-207.

78. Kuncoro, E.P.; Roussy, J.; Guibal, E., Mercury Recovery by Polymer‐Enhanced Ultrafiltration: Comparison of Chitosan and Poly(Ethylenimine) Used as Macroligand. *Separation Science and Technology* **2005,** *40* (1-3), 659-684.

79. Kolattukudy, P.E.; Purdy, R.E., Identification of cutin, a lipid biopolymer, as significant component of sewage sludge. *Environmental science & technology* **1973,** *7* (7), 619-622.

80. Macchi, G.; Marani, D.; Majone, M.; Coretti, M., Optimization of mercury removal from chloralkali industrial wastewater by starch xanthate. *Environmental Technology* **1985,** *6* (1-11), 369-380.

81. Campanella, L.; Cardarelli, E.; Ferri, T.; Petronio, B., Mercury removal from petrochemical wastes. *Water research* **1986,** *20* (1), 63-65.

82. Braden, M.L.; Lordo, S.A., *Removal of mercury and mercuric compounds from crude oil streams*, **2013,** Google Patents.

83. Lisha, K.; Pradeep, T., Towards a practical solution for removing inorganic mercury from drinking water using gold nanoparticles. *Gold Bulletin* **2009,** *42* (2), 144-152.

84. Lo, S.-I.; Chen, P.-C.; Huang, C.-C.; Chang, H.-T., Gold Nanoparticle–Aluminum Oxide Adsorbent for Efficient Removal of Mercury Species from Natural Waters. *Environmental science & technology* **2012,** *46* (5), 2724-2730.

85. Namasivayam, C.; Kavitha, D., Removal of Congo Red from water by adsorption onto activated carbon prepared from coir pith, an agricultural solid waste. *Dyes and pigments* **2002,** *54* (1), 47-58.

86. Kadirvelu, K.; Thamaraiselvi, K.; Namasivayam, C., Removal of heavy metals from industrial wastewaters by adsorption onto activated carbon prepared from an agricultural solid waste. *Bioresource technology* **2001,** *76* (1), 63-65.

87. Hadi, P.; To, M.-H.; Hui, C.-W.; Lin, C.S.K.; McKay, G., Aqueous mercury adsorption by activated carbons. *Water research* **2015,** *73*, 37-55.

88. Korpiel, J.A.; Vidic, R.D., Effect of Sulfur Impregnation Method on Activated Carbon Uptake of Gas-Phase Mercury. *Environmental science & technology* **1997,** *31* (8), 2319-2325.

89. Liu, W.; Vidic, R.D.; Brown, T.D., Optimization of high temperature sulfur impregnation on activated carbon for permanent sequestration of elemental mercury vapors. *Environmental science & technology* **2000,** *34* (3), 483-488.
90. Wang, J.; Deng, B.; Wang, X.; Zheng, J., Adsorption of aqueous Hg (II) by sulfur-impregnated activated carbon. *Environmental Engineering Science* **2009,** *26* (12), 1693-1699.
91. Cai, J.H.; Jia, C.Q., Mercury removal from aqueous solution using coke-derived sulfur-impregnated activated carbons. *Industrial & engineering chemistry research* **2010,** *49* (6), 2716-2721.
92. Dias Filho, N.L.; do Carmo, D.R., Study of an organically modified clay: selective adsorption of heavy metal ions and voltammetric determination of mercury (II). *Talanta* **2006,** *68* (3), 919-927.
93. Filho, N.L.D.; Carmo, D.R.d.; Rosa, A.H., Selective sorption of mercury (II) from aqueous solution with an organically modified clay and its electroanalytical application. *Separation Science and Technology* **2006,** *41* (4), 733-746.
94. Say, R.; Birlik, E.; Erdemgil, Z.; Denizli, A.; Ersöz, A., Removal of mercury species with dithiocarbamate-anchored polymer/organosmectite composites. *Journal of hazardous materials* **2008,** *150* (3), 560-564.
95. Krishnan, K.A.; Anirudhan, T.S., Removal of mercury(II) from aqueous solutions and chlor-alkali industry effluent by steam activated and sulphurised activated carbons prepared from bagasse pith: kinetics and equilibrium studies. *Journal of hazardous materials* **2002,** *92* (2), 161-183.
96. Elhami, S.; Shafizadeh, S., Removal of Mercury (II) using modified Nanoclay. *Materials Today: Proceedings* **2016,** *3* (8), 2623-2627.
97. Thielke, M.; Bultema, L.; Brauer, D.; Richter, B.; Fischer, M.; Theato, P., Rapid Mercury(II) Removal by Electrospun Sulfur Copolymers. *Polymers* **2016,** *8* (7), 266.
98. Schuster, E., The behavior of mercury in the soil with special emphasis on complexation and adsorption processes-a review of the literature. *Water Air & Soil Pollution* **1991,** *56* (1), 667-680.
99. Hsu, H.; Sedlak, D.L., Strong Hg(II) Complexation in Municipal Wastewater Effluent and Surface Waters. *Environmental science & technology* **2003,** *37* (12), 2743-2749.

100. Hurley, J.P.; Benoit, J.M.; Babiarz, C.L.; Shafer, M.M.; Andren, A.W.; Sullivan, J.R.; Hammond, R.; Webb, D.A., Influences of watershed characteristics on mercury levels in Wisconsin rivers. *Environmental science & technology* **1995,** *29* (7), 1867-1875.
101. Ravichandran, M.; Aiken, G.R.; Reddy, M.M.; Ryan, J.N., Enhanced dissolution of cinnabar (mercuric sulfide) by dissolved organic matter isolated from the Florida Everglades. *Environmental science & technology* **1998,** *32* (21), 3305-3311.
102. Chen, K.L.; Elimelech, M., Influence of humic acid on the aggregation kinetics of fullerene (C 60) nanoparticles in monovalent and divalent electrolyte solutions. *Journal of colloid and interface science* **2007,** *309* (1), 126-134.
103. Kjeldsen, P.; Barlaz, M.A.; Rooker, A.P.; Baun, A.; Ledin, A.; Christensen, T.H., Present and long-term composition of MSW landfill leachate: a review. *Critical Reviews in Environmental Science and Technology* **2002,** *32* (4), 297-336.

Chapter 2. Mobility of Four Common Mercury Species in Model and Natural Unsaturated Soils

2.1 Abstract

Mercury (Hg) occurs as a myriad of species in environmental media, each with different physicochemical properties. The influence of Hg speciation on its transport in unsaturated soils is not well studied. Transport of four Hg species (dissolved inorganic Hg (II) species, a prepared Hg(II)-Dissolved Organic Matter (DOM) complex, Hg(0), and HgS nanoparticles) was measured in sand and soil packed columns with partial water saturation under simulated rainfall (low ionic strength solution without DOM) and landfill leachate (high DOM content and high ionic strength) influent conditions. The Hg(II)-DOM species had the highest mobility among the four Hg species evaluated, and HgS particles (~230 nm hydrodynamic diameter) had the poorest mobility, for all soil and influent conditions tested. The addition of 2 wt% clay particles to sand greatly retarded the transport of all Hg species, especially under simulated rainfall. DOM in the column influent facilitated the transport of all four Hg species in model and natural soils. For simulated rainfall, the transport trends observed in model sands were consistent with those measured in a sandy soil, except that the mobility of dissolved inorganic Hg(II) species was significantly lower in natural soils. For simulated rainfall, Hg transport was negligible in a high organic content (~3.72 wt%) soil for all species except Hg-DOM. This work suggests that the Hg-DOM species presents the greatest potential for vertical migration to groundwater, especially with DOM in the influent solution.

2.2 Introduction

Mercury (Hg) is one of the most toxic heavy metals in humans[1] and ecological receptors[2]. Anthropogenic activities produce various forms of gaseous Hg (~80%-90%) and particulate Hg (~10%)[3, 4] that are released into air but ultimately find their way into terrestrial and aquatic systems[5]. In soils and subaquatic sediment, Hg can be present as or form various inorganic and organic complexes[6-12], the distribution of which will depend on parameters such as available ligands, pH, E_h, and time. This distribution of Hg species ultimately affects the bioavailability and toxicity of Hg[10] and likely influences the mobility of Hg in unsaturated soils, which dictates the potential for groundwater impact.

Based on reported equilibrium constants for Hg ligands and the typical concentrations of Hg(II) and ligands in environmental systems, Hg(II) is most likely to form complexes with S^{2-}, OH^-, Cl^- and S-containing functional groups of organic ligands[13-17]. Revis et al.[18] suggested that ~85% of Hg present in the floodplain soils of East Fork Poplar Creek (Oak Ridge, Tennessee, USA) is present as mercuric sulfide (HgS) as a consequence of sulfate reduction in the soils. Studies[19, 20] using soil from the site bolstered the argument that Hg has been transformed to HgS by correlating the total Hg and sulfur concentration. The mercury-sulfide minerals cinnabar (α-HgS) and metacinnabar (β-HgS) are the primary species in Hg and gold mining waste rocks and calcines[21-23]. In addition to inorganic ligands, Hg(II) has high affinity for metal-binding groups associated with natural organic matter (NOM)[16, 24-26]. Both laboratory and modeling studies indicated that in some lakes more than 90% of inorganic Hg may be bound with dissolved organic matter (DOM)[9, 10, 27]. Therefore, HgS and Hg-DOM are good surrogate species for mobility testing in soils.

Hg in landfill leachate is one potential source of Hg into the environment, especially for unlined landfills. Hg is associated with both the solid phase (680-750 ng/g) and the liquid phase (260-300 ng/L) of landfill leachate[28]. Landfill leachate commonly contains high concentrations of sulfide and DOM, so the dominant Hg species in leachate can be assumed to be HgS and Hg-DOM. It is likely that some or all of the HgS is present as metacinnabar nanoparticles[29-31]. In the presence of DOM, HgS nanoparticles forming from solution may be stabilized against aggregation[32]. Particle growth was shown to stop at 1-5 nm in diameter and aggregates were stabilized at sizes on the order of 20-200 nm[29-31, 33] with DOM present. Dissolution of HgS nanoparticles could also be promoted by DOM interaction with the HgS nanoparticle surface[34, 35]. In an anoxic environment, elemental Hg(0) can also be produced as a result of Hg(II) reduction by humic acids[36] or by microorganisms with metal reduction capabilities[37]. However, it has been shown that ionic Hg is the dominant Hg form in typical landfill leachate[28].

The relative transport of Hg in a porous medium has been proposed based on size classification: particulate (> 1 μm), colloidal (1 nm – 1 μm) and dissolved forms (< 1 nm) of Hg[8]. In a porous medium, it was postulated that transport of dissolved Hg species would be limited due to adsorption to solids and transport of particulate Hg species would also be limited due to filtration of large particles (>>1 μm). This suggests that colloidal (nanoparticulate) forms of Hg may be the most mobile species in a porous medium, and that conditions that favor colloid (nanoparticle) transport may also favor Hg transport. Previous laboratory column studies using mine tailings from a Hg mine in Central California showed that cinnabar and metacinnabar nanoparticles were the dominant mobile Hg forms in in those tailings[21, 22]. In addition to HgS colloids, it has been suggested that Hg(II) associated with colloidal material is a mechanism for mobilization of Hg in watersheds[38-43]. In a recent study, Zhu et al.[44] showed that kaolinite,

used as a model environmental colloid, enhanced Hg transport in saturated porous media. The presence of low molecular weight organic acids can further enhance colloidal transport of Hg because the organic compounds can strongly adsorb to colloid surfaces[45], enhancing mineral dissolution[46] and inhibiting particle deposition by altering the surface properties of the released colloids[47]. Slowey et al.[48] found that organic acids produced by plants promoted the transport of colloid-associated Hg from mine tailings piles.

These prior works suggest that high DOM concentrations may facilitate the transport of Hg species in a porous medium, but that the degree of enhancement will depend on the Hg speciation as well as the presence and mobility of clay in the porous medium. However, little fundamental information exists about the influence of Hg speciation on its transport in porous media, especially under extreme solution conditions (e.g., landfill leachate containing high ionic strength and high DOM). In this study, the mobility of four environmentally relevant Hg species in four types of unsaturated porous media was evaluated in column experiments. Hg species studied included β-HgS nanoparticles, dissolved inorganic Hg(II) species (denoted as Hg(II)*), Hg-DOM, and dispersed Hg(0) colloid-sized droplets. Transport was systematically evaluated for simulated rainfall, i.e., low ionic strength and no DOM, and for simulated landfill leachate, i.e., high ionic strength and high DOM. We hypothesize that Hg transport will be highly dependent on speciation, with particulate Hg species being generally less mobile than dissolved species under unsaturated flow conditions. We also hypothesize that the presence of fine particles (silt and clay sized particles) in sands and in natural soils will limit Hg transport.

2.3 Materials and Methods

Mercuric chloride (ACS grade), mercuric nitrate (ACS grade), Na_2S, Sodium 4-(2-hydroxyethyl)piperazine-1-ethanesulfonate (HEPES), and humic acid sodium salt were purchased from Sigma-Aldrich. NaCl was obtained from Fisher Scientific. Cysteine (98%) was obtained from Alfa Aesar. An Hg standard solution (1 ppm, Brooks Rand Labs) was used for calibration. Bromine monochloride, hydroxylamine and stannous chloride were purchased from Brooks Rand Labs and were used according to EPA method 1631. Commercially available sand (Unimin #50 sand) with sieve size fractions between 0.074 mm and 0.3 mm, and kaolin clay (MP biomedicals) was used as packing material in the column experiments. Both sand and clay particles were washed with 1 N nitric acid to remove impurities, followed with multiple DI water (ultrapure Milli-Q water) rinses to remove residual acid before use. Trace metal grade hydrochloride acid and nitric acid were used to digest column effluent samples and column solids prior to Hg analysis.

Transport was also evaluated in two natural samples. One sample collected from Alameda Point, CA contained approximately 79 wt% sand (>50 μm), 7 wt% silt (2 μm<x<50 μm) and 14 wt% clay sized particles (<2 μm), based on their sedimentation rate in a water column. The pH of this material in DI water was 8.5. Total organic carbon (TOC) was determined by a commercial lab (Test America, Pittsburgh, PA) and was below the detection limit of 0.009 wt%. Therefore, this material represents a low TOC sandy porous medium. An organic-rich soil sample was collected in Pittsburgh, PA. This soil was washed with DI water ~10 times to remove the Hg present in the samples prior to addition of any Hg species as measured by EPA method 1631. DI water rinsing was used rather than chemical treatments to maintain the original characteristics of the soil (e.g., organic content). Total Hg was measured on all soil/sand samples.

No detectable Hg was found so they were not rinsed. The washed soil was air-dried in a fume hood for a week. Particles larger than 1mm were removed. The air-dried soil was gently ground and the fraction between 0.3 mm to 1 mm was collected. The composition of this soil was 25 wt% sand, 50 wt% silt and 25 wt% clay. The pH of this soil in DI water was 7.6, and the TOC was determined to be 6.2 wt%. This represents a high organic soil.

2.3.1 Hg(II)* and Hg-DOM Stock Solution Preparations

Dissolved inorganic Hg(II) (denoted as Hg(II)*) stock solution was prepared by dissolving $HgCl_2$ in DI water to yield 0.1 mM Hg. The solution was acidified to pH=1.9 with 1 N nitric acid to prevent formation of less soluble Hg species such as $Hg(OH)_2$ or Hg_2Cl_2O. A Hg-DOM stock was prepared by mixing a humic acid (HA) stock solution and a Hg(II)* stock solution. HA stock solution was prepared by dissolving 500 mg HA sodium salt in 1 L DI water in a foil-wrapped glass bottle. The mixture was allowed to sit quiescently for a month and the top 500 mL of the solution was filtered through a 0.2 filter and used as the HA stock solution (181 mg carbon per liter) as determined by TOC analysis (O·I·Analytical Model 1010 Total Organic Carbon Analyzer). A 200 µL aliquot of the Hg(II)* stock solution and 1 mL of the HA stock solution were mixed in a centrifuge filter tube (3KDa MWCO). The mixture was then centrifuged at 5000 rpm for 15 min. The solution that was retained on the 3kDA MWCO filter was washed by adding DI water and centrifuging repeatedly until the Hg concentration of the filtrate was equivalent to the DI water, i.e., background. Washed retentate was collected from several filters using the same procedure, composited, and used as the Hg-DOM stock solution for transport studies. The Hg concentration in the Hg-DOM stock was measured as 9.4 mg/L.

2.3.2 Hg(0) Stock Solution Preparation

A Hg(0) stock solution was prepared by first adding a small droplet (~20 µL) of liquid elemental Hg into 100 mL N_2 purged DI water, then the mixture was sonicated for 5 min using a probe sonicator and allowed to settled over night. The upper solution was collected and used as the Hg(0) stock solution. The Hg(0) concentration of the stock was measured by diluting into N_2-purged DI water and directly purging Hg(0) to the Hg analyzer (Brooks-Rand Model MERX). To avoid artifacts from oxidation, the Hg(0) stock solution was used in column experiments immediately after its preparation. Several Hg(0) stock solutions were prepared during the study, having an average concentration of 15.1 ± 0.9 mg/L. The total Hg concentration in the stock solution was also measured to determine if a significant fraction of the Hg(0) was oxidized in the preparation process. The total Hg concentration was always ~10% higher than the Hg(0) concentration. The excess Hg was considered to be oxidized to Hg(II) species. We also calculated both Hg(0) and total Hg concentration in the column experiment effluent immediately after each fraction was collected, and the results showed the same trend. Thus, significant oxidation of elemental Hg(0) during the column experiments was not observed. The hydrodynamic diameter and electrophoretic mobility of the Hg(0) fine droplets in 5 mM NaCl at pH=7.5 were determined by time-resolved dynamic light scattering (DLS) (ALV, Germany) and Zetasizer Nano ZS (Malvern, UK), respectively.

2.3.3 HgS Nanoparticle Synthesis

HgS nanoparticles were synthesized in aqueous solution using a previously published method[31]. All stock solutions were prepared using filtered (<0.2 µm) DI water. The Hg stock solution was prepared by dissolving $HgCl_2$ or $Hg(NO_3)_2$ in 0.1 N HCl solutions to provide a 10

mM total Hg solution. The sulfide stock solution was prepared by dissolving Na_2S in N_2 purged DI water. A cysteine stock solution (5 mM) and HEPES buffer (40 mM, pH 7.5) solution were also prepared in N_2 purged DI water. The HgS nanoparticle synthesis was conducted in an anaerobic glovebox to prevent oxidation of the experimental sulfide solutions. For the synthesis of HgS nanoparticles, an aliquot of the cysteine stock solution was added into 0.2 μm filtered HEPES buffer (40 mM, pH 7.5) to give a 200 μM cysteine solution. An aliquot of the Hg stock solution was then added to provide an initial Hg(II) concentration of 100 μM. The β-HgS nanoparticle precipitation was then initiated by adding S(-II) (equimolar to Hg(II)) to the solution, and allowing it to react quiescently for two days. The precipitated HgS nanoparticles were centrifuged, washed with DI water three times, and then used as the HgS nanoparticle stock suspension (26.5 mg Hg/L) for column studies. The hydrodynamic diameter of the HgS nanoparticles and the stability of the particles against aggregation in the different column influent solutions were measured using DLS. The electrophoretic mobility of HgS nanoparticles was measured in 5 mM NaCl at pH=7.5.

2.3.4 Column Breakthrough Experiments

Transport of Hg(II)*, Hg-DOM, Hg(0) and HgS nanoparticles was evaluated in 9 cm × 2.5 cm glass columns (Ace Glass, Vineland, New Jersey). Porous media included the Unimin sand, Unimin sand amended with 2 wt% kaolin clay, and two natural soils (described above). The soil from Alameda Point was gently ground and sieved, and the particle aggregates with sieve size fractions between 0.074 mm and 0.3 mm was used for the column study. The 0.3 mm to 1 mm size fraction of the organic rich soil contained a higher fraction of silt and clay particles that made the column impermeable to flow. To provide a hydraulic conductivity similar to the sand and the Alameda Point soil (based on observed flow rate for the same inlet pressure), a

fraction of the larger minerals (>1 mm) initially removed from the soil were ground, and the 0.3 mm to 1 mm size fraction was acid washed and rinsed with DI water, and then added to the soil with a weight ratio of 2:3. Assuming that this mineral fraction was very low in organic content, the TOC for the packed soil is ~3.72 wt%. These two soil types were selected to represent the typical sites of interest to oil companies, sandy (low TOC) sites and equatorial (high TOC) sites.

Column transport studies used two influent solutions to determine the mobility of Hg species in these media. One solution representing rain water had a low ionic strength and contained no DOM. This solution was prepared by dissolving 0.005 mol NaCl in 1 L DI water and adjusting the solution pH to 7.5 with $NaHCO_3$. The second solution was a high ionic strength high DOM concentration solution designed to mimic a mature landfill leachate. Landfill leachate composition varies greatly depending on many factors (e.g., age of the landfill, waste type, seasonal weather variation)[49-53], and the organic matter such as humic substances becomes dominant in mature landfill leachates[54]. The simulated leachate solution was prepared by dissolving NaCl and humic acid in DI water to obtain an initial concentration of 200 mM NaCl and 500 mg/L HA. The humic acid used here was from Sigma-Aldrich and may not represent every DOM type in real leachates. The stock solution was then filtered through a 0.2 μm filter and the pH was adjusted to 7.5 by 0.01 N HCl and 0.01 N NaOH as needed. Over a 4 month period, the stock solution was stored quiescently in the dark and the pH was regularly adjusted to 7.5 by adding 0.01 N HCl and 0.01 N NaOH as needed. After confirming that the pH of the stock solution was stable at 7.5, the upper 800 mL of the stock solution was used as influent solution. The DOM concentration was 147 mg carbon per L determined by TOC analysis.

The columns were wet-packed with the sand, sand-clay mixture, or natural media. The soil bulk density, hydraulic conductivity and porosity of porous media were determined under

saturated condition. The columns were then drained to create an unsaturated porous medium. Solutions were introduced at the top of the columns using a piston pump (FMI, Syosset, NY), effluent was collected from the bottom of the column. The flow rate was set to maintain partially saturated conditions in the column. A 5 mM NaCl solution was flowed through the column to equilibrate the solids and solution in the column, and to attain a stable degree of water saturation. After confirming that the unsaturated column conditions were maintained at the desired water saturation and flow rate, a tracer test using 20 mM NaCl and an in-line conductivity detector was conducted to determine the effective porosity, average linear velocity of the water, and dispersion in the column (Table 2 and Figure A1). The similar hydraulic conductivity, breakthrough curves, and coefficient of hydrodynamic dispersion suggest no significant difference of water distributions among the column media. The properties of the unsaturated porous media are summarized in Table 2.

Table 2. Measured Properties of the Unsaturated Porous Media Used in this Study.

Column medium	$\boldsymbol{\rho_b}$ **Soil bulk density (g/cm^3)**	$\boldsymbol{K^a}$ **Hydraulic conductivity (cm/s)**	$\boldsymbol{n}$ **Porosity (Degree of water saturation)**	$\boldsymbol{D_L}$ **Coefficient of hydrodynamic dispersion (cm^2/s)**	$\boldsymbol{v_x}$ **Average linear velocity (cm/s)**	$\boldsymbol{n_e}$ **Effective porosity**
#50Sand	1.45	0.0082	0.32(0.85)	0.001	0.0046	0.27
#50Sand + Clay	1.40	0.0075	0.34(0.91)	0.003	0.0041	0.31
Low TOC natural medium	1.55	0.0026	0.32(0.90)	0.001	0.0043	0.29
High TOC natural medium	1.12	0.0011	0.41(0.94)	0.006	0.0033	0.38

[a] Measured at 20°C.

Prior to adding the Hg species, each column was equilibrated with the influent solution that would be used for that test. An equilibration time of over a month was needed for both of the natural media packed columns to provide a stable column flow, degree of saturation, and absence of particles in the column effluent prior to adding the Hg species. After equilibration, the top layer of column media (1 cm) was homogeneously mixed with Hg species under investigation. In each case, a total Hg concentration of 0.43 μg/g was added to simulate the Hg background concentration in a landfill[28]. The appropriate influent solution was then flowed through the column at a rate of 0.37 mL/min. The flow was continued until breakthrough of Hg was observed and the effluent concentration had returned to baseline (11 pore volumes), or for 11 to 15 pore volumes for cases where no Hg breakthrough was observed. The effluent Hg concentration was measured every 0.1 pore volume for the first 2 pore volumes, every 0.2 pore volume for the following 3 pore volumes, and every 0.5 pore volume for the effluent after 5 pore volumes. The breakthrough experiments were conducted in duplicate for all Hg species and under all column conditions using the model sands, and were duplicated for the Hg(II)* species under all column conditions in the natural media. Reproducibility was good, with the deviation of breakthrough percentage for all Hg species less than 4%.

Total Hg in the column effluent was quantified using cold vapor atomic fluorescence spectroscopy (CVAFS) according to EPA Method 1631. For HgS nanoparticles and for Hg-DOM, effluent samples were first digested with aqua regia before analysis. For Hg(0), the sample was directly purged into the analyzer for measurement of Hg(0). Hg breakthrough curves were plotted to evaluate the mobility of Hg species. Hg deposition profiles were also measured as described below.

2.3.5 Hg Deposition Profiles

At the end of each column experiment, 1-cm layers of column medium was sampled, digested and measured for total Hg. This provides an estimate of Hg transport even if no measurable Hg breakthrough is observed. It also provides an ability to calculate a total Hg mass balance (retained Hg plus effluent Hg) in each experiment. Each column was divided into nine 1-cm long segments. The material from each layer was removed from the column and digested using 40 mL aqua regia overnight in glass vials, and the digestate was analyzed for total Hg. The background Hg concentrations for sand, sand-clay mixture, and natural soils were also measured by digesting the column material without loading Hg species. For Hg(0) species, the Hg(0) concentration was assumed to be 0.9 of the total Hg concentration after subtracting the background Hg concentrations of the porous medium. The overall recoveries of total Hg ranged from 85% to 106% for all experiments.

2.3.6 Hg Deposition Rate

Deposition (retention) rate is a quantitative indicator that can be used to compare the transport behavior for each Hg species under the different conditions tested. The deposition rate was calculated using two methods. First, the overall deposition rate (denoted as $k_{d,overall}$) under each column condition was calculated from Hg breakthrough data using equation 2.1[55],

$$k_{d,overall} = -\frac{1}{t_p}\ln\left[\frac{q}{N_0}\int_0^{t_f} C(t)dt\right] \qquad \text{(eqn 2.1)}$$

where $k_{d,overall}$ (min^{-1}) is the deposition rate coefficient, t_p (min) is the average travel time, t_f (min) is the time at which Hg species have been completely washed out of the column, q (mL/min) is the volumetric flow rate, N_0 is the total Hg injected (µg), and $C(t)$ is the Hg in effluent solution at time point t (µg /L). For some Hg species a significant fraction of the Hg remained in the top 1-

cm of the column where it was added. Due to this heterogeneity for some of the Hg species, the overall deposition rate calculated from eqn 1 will overestimate the deposition rate of the mobile fraction of Hg. Therefore, a deposition rate for the mobile species was also calculated from the deposition profiles using eqn 2.2,

$$L = -\frac{v_p}{k_d}\ln(\frac{C}{C_0}) \qquad \text{(eqn 2.2)}$$

where, L (cm) is the maximum travel distance, v_p (cm/min) is the pore water velocity calculated using eqn 2.3,

$$v_p = \frac{q}{n_e A} \qquad \text{(eqn 2.3)}$$

where, n_e is effective porosity, which is calculated by multiplying the porosity of the column with the degree of water saturation. A (cm^2) is cross section area. In eqn 2, C/C_0 is calculated from a Hg mass balance for each column subsection up to the section of the column where Hg was higher than background. C_0 was the mobile Hg concentration determined from the difference in mass of Hg in the upper layer at the end of the experiment compared to what was initially emplaced in the top layer of the column (Figure A2). The slope of a plot of ln(C/C_0) vs. L yields k_d^{-1} (Figure A3), the inverse of the deposition rate coefficient (eqn 2). This deposition rate applies only to the mobile fraction of Hg (denoted as $k_{d,mobile}$). We report both $k_{d,overall}$ and $k_{d,mobile}$ because they provide a range of estimates of the mobility of these Hg species present in soils at the concentrations evaluated. $k_{d,overall}$ represents the upper bound estimate, while $k_{d,mobile}$ presents the most conservative (lower bound) estimate of deposition of a mass of Hg added to the system.

2.4 Results and Discussion

2.4.1 Speciation of Dissolved Inorganic Hg(II) Species

The dissolved Hg(II) speciation under the two influent solution conditions was calculated using Visual MINTEQ ver. 3.0 (Figures A4 and A5). The results suggest that dissolved Hg(II) is mainly a mixture of $HgClOH_{(aq)}$ (47%), $HgCl_{2(aq)}$ (39%) and $Hg(OH)_{2(aq)}$ (11%) under the simulated rain water condition. In simulated leachate the added Hg(II) is calculated to be predominantly complexed with DOM (> 99%).

2.4.2 Prepared Hg-DOM Characteristics

For the specifically prepared Hg-DOM sample, the Hg to DOM molar ratio for the Hg-DOM stock was calculated by determining the Hg concentration and the DOM concentration in the washed Hg-DOM sample. The calculated Hg to DOM molar ratio was 0.00007±0.00001 mol Hg/mol C. The sulfur to carbon molar ratio in the HA is estimated to be in the range of 0.0056:1 to 0.024:1 based on previous reports[56-58]. Assuming this C:S ratio, The ratio of Hg to S in the Hg-DOM ranged from 0.0029:1 to 0.0125:1. Due to the high affinity of Hg(II) for S(-II) in DOM, it is likely that Hg in the Hg-DOM stock is primarily bound with DOM through reduced sulfur groups.

2.4.3 Prepared Hg(0) Characteristics

The size and charge of dispersed Hg(0) species were determined in the water containing 5 mM NaCl at pH=7.5. The hydrodynamic diameter of Hg(0) droplets was measured by DLS as 488 ± 88 nm. The electrophoretic mobility of Hg(0) was -1.46 ± 0.08 μm cm/Vs.

2.4.4 HgS Nanoparticle Characteristics

The size, charge, and aggregation state of HgS nanoparticles can affect their transport behavior. Synthesized HgS nanoparticles were polydisperse with a mean hydrodynamic diameter of ~230 nm as measured by DLS in water containing 5 mM NaCl at pH=7.5 (Figure A6). Under the same solution conditions, the electrophoretic mobility of HgS nanoparticles was -1.10 ± 0.11 μm cm/Vs. The hydrodynamic diameter of the HgS particles was also determined by DLS in the two column influent solutions. The measured hydrodynamic diameter did not significantly increase in the presence of 5 mM NaCl, or in the presence of 200 mM NaCl plus 147 mg carbon per L DOM, suggesting that the solution conditions did not promote aggregation of the particles (Figure A7). The absence of aggregation at 200 mM NaCl suggests that the organic carbon added may sterically stabilize the HgS nanoparticles[59-61].

2.4.5 Hg Transport in Unsaturated Porous Media

The mobility of four Hg species was first evaluated in a simple well sorted sand column using the simulated rainfall influent solution. The breakthrough curves and deposition profiles for each Hg species under these conditions are shown in Figure 2.1a and 2.1b, respectively. The breakthrough curves indicate that the speciation of Hg affects Hg transport in the column under simulated rainfall conditions. Transport of the two soluble Hg species, Hg(II)* and Hg-DOM, showed similar breakthrough behavior with much of the mobile fraction being eluted in less than 2.5 pore volumes. More Hg(II)* eluted (39%) compared to Hg-DOM (25%) (Figure 2.1a). This suggests greater adsorption of Hg-DOM to the clean (acid washed) sand surfaces than Hg(II)*. The Hg deposition profiles are consistent with this assertion (Figure 2.1b). Hg(II)* was relatively evenly distributed throughout the column solids whereas the Hg-DOM showed an approximately

exponential decrease from the column inlet to the column outlet. The relatively low adsorption of Hg(II)* to the model sand suggests a deficient number of surface hydroxide sites favorable for adsorption. These sites are removed through acid-washing the sand[62].

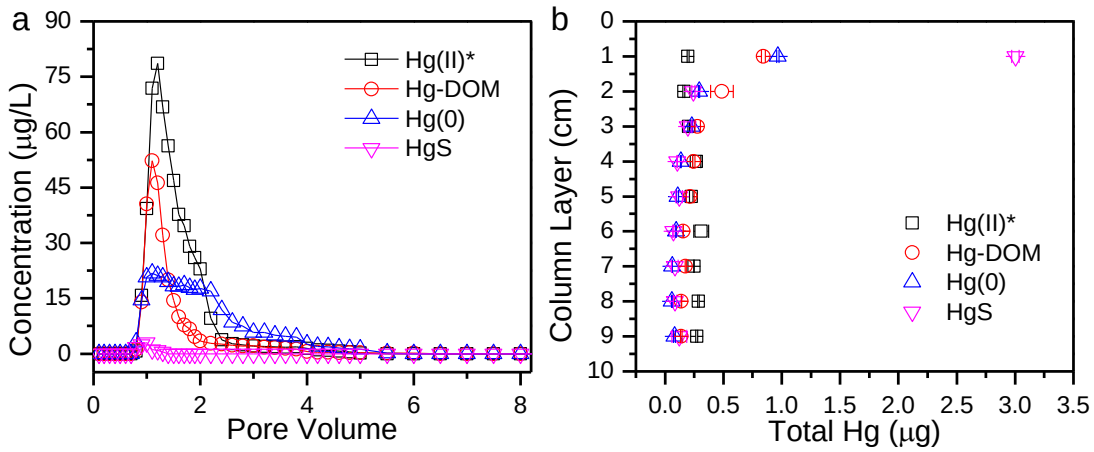

Figure 2.1. Breakthrough curves (a) and deposition profiles (b) for the four different Hg species in the unsaturated sand column. Column size: 9 cm × 2.5 cm; medium: #50 Unimin sand; Pore volume: 22.4 ± 1.8 mL; Influent solution: 5 mM NaCl, pH 7.5. Lines are not models fits of data. They are only meant to guide the eye. Horizontal Error bars are the standard deviation of measured Hg concentration. Breakthrough curves for all of the other media used are provided in supporting information.

Hg(0) was present in the sample as colloidal droplets and was also found to be mobile under these influent conditions, with about 25% of the total Hg(0) being eluted from the column. However, it took more than 5 pore volumes for the Hg(0) to move through the column, indicating greater holdup within the column compared to Hg(II)* and Hg-DOM species. In sharp

contrast, the HgS nanoparticles were relatively immobile. Only about 1% of HgS nanoparticles were collected in the column effluent after 11 pore volumes. The column deposition profiles indicate that much of the particulate Hg species, Hg(0) and HgS nanoparticles, remained in the top 1-cm of the column where they were emplaced. This suggests very limited transport for a significant fraction of these particulate Hg species. Since our prepared HgS nanoparticles were polydisperse with an average hydrodynamic diameter around 230 nm, it is possible that the largest particles are strained or filtered by the sand, but a small fraction of the HgS particles were mobile. It is also likely that some of the nanoparticles were captured by the air-water interface[63, 64]. The number of particles eluted was too low to measure by DLS so the particle size distribution of the eluted particles could not be determined.

The second set of transport experiments used simulated landfill leachate. The initial mobilization and subsequent deposition of soluble and particulate Hg species may be affected differently by high ionic strength and presence of DOM. For example, dissolved Hg can become strongly associated with DOM via -S and -O functional groups on the organic matter[13, 16, 17, 65, 66], and organic acids can favor the transport of HgS nanoparticles[48]. However, high ionic strength may promote attachment of the nanoparticles to the porous medium, thereby limiting transport.

Using simulated leachate as influent water greatly increased the mobility of all four of the Hg species tested (Figure 2.2a). In all cases except HgS nanoparticles, >88% of the mass of the Hg species was eluted from the sand column under these conditions. For HgS nanoparticles the presence of high DOM increased elution to 12% from only 0.4% without DOM. The HgS nanoparticles were not aggregated in the 200 mM NaCl + 147 mg carbon per L DOM influent solution (Figure A7), so the dissolved organic matter may have coated the sand surfaces and

prevented deposition of HgS nanoparticles on the sand. This is most likely a result of steric repulsions between the DOM coated HgS particles and the DOM-coated sand surfaces given that the high ionic strength of the solution (200 mM) limits electrostatic repulsive forces[67]. The increased Hg(II)* transport is due to its complexation with the added DOM. It was expected that the prepared Hg-DOM species should behave the same as Hg(II)* in the presence of high DOM concentration. This appears to be the case as both Hg(II)* and Hg-DOM species elute to a similar degree (Figure 2.2a) and have nearly identical deposition profiles (Figure A8d).

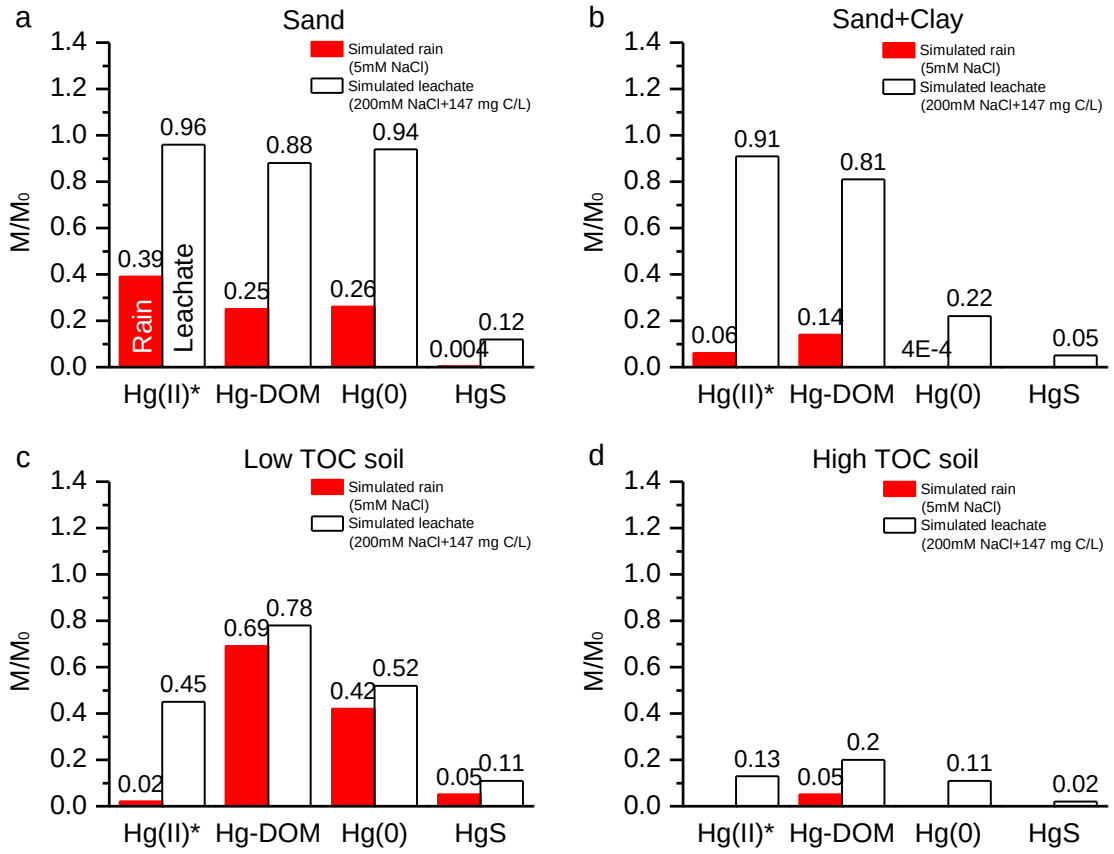

Figure 2.2. Fraction of mass of each Hg species transported through the 9cm x 2.5cm column in each porous medium evaluated (a) Unimin sand; (b) Unimin sand + clay; (c) Low TOC soil from Alameda point, CA; (d) High TOC soil from Pittsburgh, PA.

The deposition profile in Figure A8d also shows that with DOM in the influent, HgS nanoparticles can be detected in the lower layers of the column whereas HgS was practically immobile without DOM in the influent solution (Figure A8b).

Most natural media are not uniform in size, but instead contain a clay-sized fraction that can alter the pore space in the porous medium. The presence of only 2 wt% clay particles in sand has been shown to significantly decrease the transport of iron nanoparticles through these Unimin sands[68]. When 2 wt% of kaolin clay was mixed with the #50 Unimin sand, the transport of all of the Hg species in simulated rainwater was significantly decreased (Figure 2.2b-red bars) compared to sand only (Figure 2.2a-red bars). The greatest effect of clay particles on Hg transport was observed for the colloidal species, HgS and Hg(0). Addition of clay effectively prevented transport of these species for up to 11 pore volumes of solution flowed through the column. The deposition profiles show that nearly all of HgS nanoparticles remained in the top 1-cm layer when clay particles were present. The presence of clay particles also significantly hindered Hg(0) transport. Due to the relatively large particle size of the HgS nanoparticles (hydrodynamic diameter of ~200 nm) and the Hg(0) droplets (hydrodynamic diameter of ~500 nm) and the angular shape of the porous medium grains, straining or retention of colloids in flow stagnation zones are possible mechanisms of removal for these Hg species[69-73]. The deposition profiles (Figure A9b) indicate that Hg(0) transport was retarded by the clay but it penetrated the porous medium more than the HgS nanoparticles. The difference in behavior could be, in part, a result of the density difference between liquid Hg(0) (13.5 g/cm^3) and β-HgS (7.8 g/cm^3), and in part to the differences in structure. Hg(0) droplets do not have rigid crystal structure like HgS nanoparticles. With the higher downward gravity-driven force and its liquid nature, Hg(0) droplets are able to breakthrough through some porous structures that HgS cannot. Some

breakthrough may also be attributed to dissolved Hg(0) species. The clay fines also significantly decreased the transport of the soluble Hg species, Hg(II)* and Hg-DOM, but less than for the particulate Hg species (Figure 2.2). It also retarded the breakthrough time of Hg(II)* (Figure A9a). This lower transport suggests that these soluble Hg species are adsorbing to the high surface area clay particles. At natural pH under the rain water condition, Hg(II)* mainly exists as HgClOH and $Hg(OH)_2$ (Figure A4), which can form XO-$HgOH^+$ species with the surface functional groups XOH (X = Al or Si) on the porous media particles[74]. This is consistent with the deposition profiles (Figure A9b) that show higher mass of Hg in the column solids compared to sand alone. Previous studies have demonstrated that clay particles have good adsorption capacity for heavy metals[75-77].

In simulated leachate solution the breakthrough of all Hg species was also decreased with the addition of clay particles to the sand. However, the effect of clay particles was greater on the particulate Hg species compared to the soluble Hg species (Figure 2.2a and 2.2b). The eluted masses of HgS and Hg(0) species were decreased by more than 50% due to the presence of 2% kaolinite clay. Despite the higher mobility of all Hg species in the sand-clay porous medium using simulated leachate compared to simulated rain water, the character of the deposition profiles for each Hg species are similar in both cases (Figure A9). The colloidal Hg species were largely deposited in the top portion of the column, whereas the soluble Hg species were deposited along the length of the column.

The transport of the four Hg species under simulated rainfall influent was measured in a low TOC natural sandy porous medium (Alameda Point, CA). In this low TOC sandy soil, the greatest transport was observed for Hg-DOM and the lowest transport was observed for HgS nanoparticles (Figure 2.2c). This is consistent with observations in the model soils. Notable

differences were the low elution of Hg(II)* species in the natural soil compared to model soils, and the relatively higher elution of Hg(0) species in the natural soil compared to model soils. The sandy medium contains more fines compared with Unimin sand, and therefore has more surface area available for adsorption of Hg(II)* species. Deposition profiles are consistent with this assertion and indicate that Hg(II)* species are adsorbed to the soil particles in the top few centimeters of the soil (Figure A10b). It is also possible that organic matter and metal-binding functional groups on the surfaces of the natural medium provide an affinity for the Hg(II)*, limiting its transport[78]. The transport of Hg(0) species was higher than expected based on the results using model soils. Reasons for the greater than expected transport of Hg(0) species are unclear.

The transport of all tested Hg species was increased in simulated landfill leachate compared to simulated rain water (Figure 2.2c). Particularly for Hg(II)*, the breakthrough increased from 2% to 45%. In Figure A10c, the breakthrough curve of Hg(II)* shows that the Hg(II)* was detected in the effluent fractions for five pore volumes. The deposited amount of Hg(II)* in the top layers of the sandy medium was also significantly decreased compared with rainwater influent (Figure A10d). These results suggest that complexation between Hg(II)* ions and DOM in this porous medium leads to a decreased attachment of Hg(II)* onto the porous medium particle surfaces, and subsequent increase in transport.

Hg transport through a soil with high TOC content was also evaluated to determine if the trends in transport behavior observed in columns packed with model sands and low TOC content soil also apply to high TOC soils. In simulated rainwater, only Hg-DOM showed detectable breakthrough after 11 pore volumes (Figure 2.2d and A11a). Breakthrough of Hg-DOM was lower than for the low organic soil, with a maximum concentration being about one order of

magnitude lower than observed for the low TOC soil. The trend is consistent with the other column conditions where Hg-DOM is the most mobile Hg species. The deposition data demonstrated that all of the Hg species except Hg-DOM primarily remained in the top 1 cm of the column (Figure A11b). The results indicate that particulate Hg species (e.g., Hg(0) and HgS nanoparticles) had very limited transport in this organic rich porous medium using simulated rainwater. It also suggests that Hg(II)* can be strongly associated with particle-associated organic matter in this soil matrix[79], likely through interaction between Hg(II)* and reduced organic S groups of the soil organic matter[80].

In simulated landfill leachate, the mobility of Hg species was enhanced (Figure 2.2d). The deposition of Hg species in the top layer of the column was also lower compared to the low ionic strength influent solution (Figure A11d). The enhanced transport of Hg species indicates that DOM facilitates the transport of all Hg species even in a high (particulate) TOC content soil, as was observed with the model sands and low TOC natural medium.

2.4.6 Hg Removal Efficiency in Unsaturated Porous Media

Figure 2.3 shows a summary of the deposition rate coefficients for the mobile fraction of Hg species (i.e., $k_{d,mobile}$). The deposition rate coefficients calculated from the breakthrough curves (i.e., $k_{d,overall}$) and for the mobile fraction of the Hg species as measured from the deposition profiles (i.e., $k_{d,mobile}$) are also provided in Table A1. The $k_{d,mobile}$ of each Hg species was decreased for simulated leachate compared to the simulated rainfall for all tested media, indicating that the introduction of DOM facilitated the transport of Hg species in porous media despite the higher ionic strength. In natural media, Hg-DOM has the lowest deposition rate coefficient among the assessed Hg species, indicating that Hg-DOM will be more mobile than the other Hg species. The high $k_{d,mobile}$ of Hg(II)* ions in both natural media using simulated rain

water suggests a limited transport of Hg(II)* in natural media, as has been previously suggested[8, 79]. This analysis suggests that mobility of Hg species is quite low in natural soils; <<1m is needed to remove 99.99% of the Hg for all species in the high TOC soil for any condition, and only ~3 to 6 m is needed to remove the most mobile species (Hg-DOM) in the low TOC natural soil, under rainfall and leachate conditions, respectively.

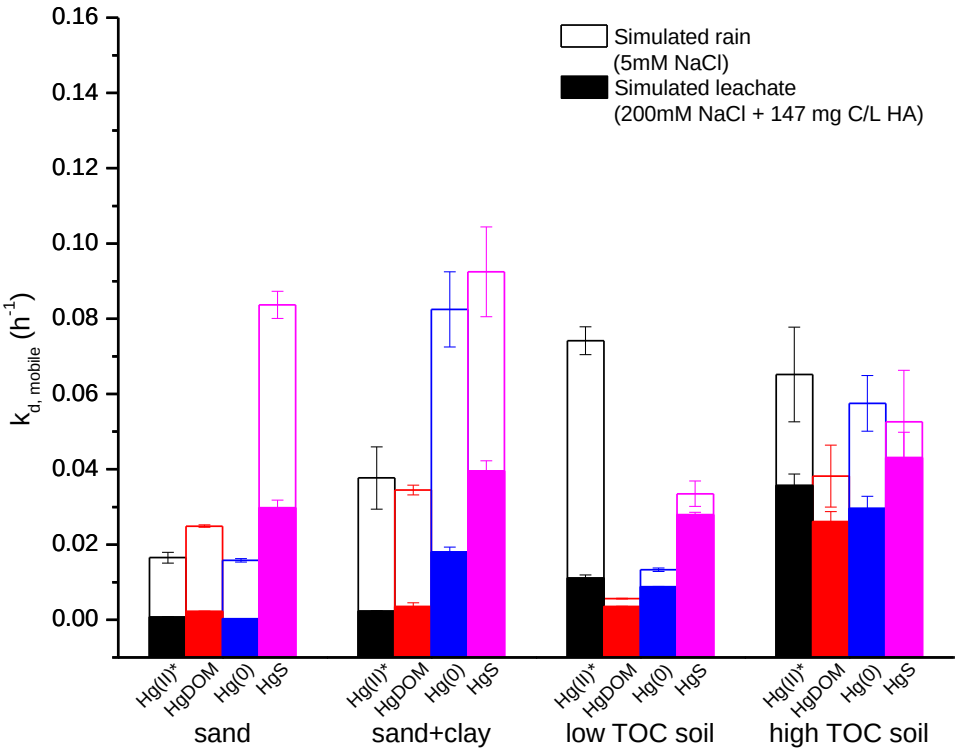

Figure 2.3. Calculated deposition rate coefficients, $k_{d,mobile}$, for each of the Hg species in the four types of unsaturated porous media evaluated: sand, sand + clay, low TOC soil, and high TOC soil. Both influent water types are shown: simulated rainfalls are open bars, simulated landfill leachate are closed bars. In all cases, the deposition rates were lower in the simulated leachate compared to simulated rain water.

The lower mobility in the high TOC soil compared to the low TOC soil could be from greater deposition onto the particulate TOC in the soil, but may also be due to permeability differences between the two soil types despite efforts to use similar particle sizes and to match flow rates through the column.

2.5 Implications for Hg Transport and Risk

Overall, this study indicates that the speciation of Hg greatly affects its mobility in partially water-saturated porous media. While Hg(II)* shows a relatively high mobility in model sands, its mobility is significantly lower in natural soils due to a high affinity for adsorbing Hg(II)*. Addition of clay particles to the model sands greatly retarded the transport of Hg species, especially under low ionic strength and low DOM influent conditions that represent rainfall. The clay particles in the medium are highly effective at retarding the transport of particulate Hg species, but less effective on dissolved Hg species, especially with high DOM in the column influent. Hg-DOM consistently has high transportability in model porous media and in natural media, suggesting that this Hg species has the greatest potential mobility in the environment. Synthesized 230 nm sized HgS nanoparticles show limited mobility in general, and was consistently the least mobile compared with other Hg species tested here. The breakthrough behavior and eluted mass for Hg(0) was distinct from the other Hg species, which may suggest that a slow but continual transport of separate phase liquid elemental Hg(0) is possible in porous media, or that dissolved elemental Hg(0) is being mobilized to some degree. This study demonstrates that although Hg species transport differently through commercial sands and natural media, the introduction of dissolved organic matter in the influent solution will increase the mobility of all relevant Hg species in environmental media. The results also suggest that Hg-DOM transport in well sorted sandy media with high dissolved organic matter flow through (e.g.,

landfill with mature leachate flow through) presents the greatest potential risk of vertical migration.

While these studies were performed using well-characterized influent and porous media, the findings here can be cautiously extended to inform mobility of Hg in different environment. For example, in organic rich media with some clay-sized particle content (e.g., freshwater wetland soils), poor mobility of Hg species is expected due to clay fines, and high TOC content of the porous medium, even though considerable DOM is present. Similarly, limited transport of Hg species are expected in coastal areas (e.g., coastal lagoon) because of the low DOM content in sea water.

Importantly, these findings suggest that the speciation of Hg in a soil or sediment and the permeability and organic content of the soil must be determined to assess the potential for migration. Finally, it suggests that transformations of the Hg species (e.g., sulfidation to form β-HgS or complexation with organic matter) after its introduction to the environment may change the mobility of the Hg over time.

2.6 References

1. Clarkson, T.W.; Magos, L.; Myers, G.J., The toxicology of mercury - Current exposures and clinical manifestations. *N. Engl. J. Med.* **2003,** *349* (18), 1731-1737.
2. Boening, D.W., Ecological effects, transport, and fate of mercury: a general review. *Chemosphere* **2000,** *40* (12), 1335-1351.
3. Street, D.G.; Hao, J.M.; Wu, Y.; Jiang, J.K.; Chan, M.; Tian, H.Z.; Feng, X., Anthropogenic mercury emission in China. *Atmos. Environ.* **2005,** *39*, 7789-7806.
4. Pacyna, E.G.; Pacyna, J.M.; Fudala, J.; Strzelecka-Jastrzab, E.; Hlawiczka, S.; Panasiuk, D., Mercury emissions to the atmosphere from anthropogenic sources in Europe in 2000 and their scenarios until 2020. *Sci. Total Environ.* **2006,** *370* (1), 147-156.

5. Eckley, C.S.; Blanchard, P.; McLennan, D.; Mintz, R.; Sekela, M., Soil-Air Mercury Flux near a Large Industrial Emission Source before and after Closure (Flin Flon, Manitoba, Canada). *Environ. Sci. Technol.* **2015,** *49* (16), 9750-9757.

6. Belzile, N.; Lang, C.Y.; Chen, Y.W.; Wang, M., The competitive role of organic carbon and dissolved sulfide in controlling the distribution of mercury in freshwater lake sediments. *Sci. Total Environ.* **2008,** *405* (1), 226-238.

7. Drott, A.; Lambertsson, L.; Björn, E.; Skyllberg, U., Importance of dissolved neutral mercury sulfides for methyl mercury production in contaminated sediments. *Environ. Sci. Technol.* **2007,** *41* (7), 2270-2276.

8. Liu, G.; Cai, Y.; O'Driscoll, N., Eds. *Environmental chemistry and toxicology of mercury*. **2012,** John Wiley & Sons, Inc., Hoboken, New Jerse.

9. Morel, F.M.M.; Kraepiel, A.M.L.; Amyot, M., The chemical cycle and bioaccumulation of mercury. *Annu. Rev. Ecol. Syst.* **1998**, 543-566.

10. Ullrich, S.M.; Tanton, T.W.; Abdrashitova, S.A., Mercury in the aquatic environment: a review of factors affecting methylation. *Crit. Rev. Env. Sci. Tec.* **2001,** *31* (3), 241-293.

11. Wolfenden, S.; Charnock, J.M.; Hilton, J.; Livens, F.R.; Vaughan, D.J., Sulfide species as a sink for mercury in lake sediments. *Environ. Sci. Technol.* **2005,** *39* (17), 6644-6648.

12. Zhong, H.; Wang, W.X., Inorganic mercury binding with different sulfur species in anoxic sediments and their gut juice extractions. *Environ. Toxicol. Chem.* **2009,** *28* (9), 1851-1857.

13. Schuster, E., The behavior of mercury in the soil with special emphasis on complexation and adsorption processes-a review of the literature. *Water Air Soil Pollut.* **1991,** *56* (1), 667-680.

14. Powell, K.J.; Brown, P.L.; Byrne, R.H.; Gajda, T.; Hefter, G.; Sjöberg, S.; Wanner, H., Chemical speciation of Hg (II) with environmental inorganic ligands. *Aust. J. Chem.* **2004,** *57* (10), 993-1000.

15. Schwarzenbach, G.; Widmer, M., Die löslichkeit von metallsulfiden I. schwarzes quecksilbersulfid. *Helv. Chim. Acta* **1963,** *46* (7), 2613-2628.

16. Dyrssen, D.; Wedborg, M., The sulphur-mercury (II) system in natural waters. *Water Air Soil Pollut.* **1991,** *56* (1), 507-519.

17. Jay, J.A.; Morel, F.M.M.; Hemond, H.F., Mercury speciation in the presence of polysulfides. *Environ. Sci. Technol.* **2000,** *34* (11), 2196-2200.

18. Revis, N.W.; Osborne, T.R.; Holdsworth, G.; Hadden, C., Distribution of mercury species in soil from a mercury-contaminated site. *Water Air Soil Pollut.* **1989,** *45* (1), 105-113.
19. Barnett, M.O.; Harris, L.A.; Turner, R.R.; Stevenson, R.J.; Henson, T.J.; Melton, R.C.; Hoffman, D.P., Formation of mercuric sulfide in soil. *Environ. Sci. Technol.* **1997,** *31* (11), 3037-3043.
20. Harris, L.A.; Henson, T.J.; Combs, D.; Melton, R.E.; Steele, R.R.; Marsh, G.C., Imaging and microanalyses of mercury in flood plain soils of east fork poplar creek. *Water Air Soil Pollut.* **1996,** *86* (1), 51-69.
21. Lowry, G.V.; Shaw, S.; Kim, C.S.; Rytuba, J.J.; Brown Jr, G.E., Macroscopic and microscopic observations of particle-facilitated mercury transport from New Idria and Sulphur Bank mercury mine tailings. *Environ. Sci. Technol.* **2004,** *38* (19), 5101-5111.
22. Slowey, A.J.; Rytuba, J.J.; Brown Jr, G.E., Speciation of mercury and mode of transport from placer gold mine tailings. *Environ. Sci. Technol.* **2005,** *39* (6), 1547-1554.
23. Kim, C.S.; Brown, G.E.; Rytuba, J.J., Characterization and speciation of mercury-bearing mine wastes using X-ray absorption spectroscopy. *Sci. Total Environ.* **2000,** *261* (1), 157-168.
24. Skyllberg, U., Competition among thiols and inorganic sulfides and polysulfides for Hg and MeHg in wetland soils and sediments under suboxic conditions: Illumination of controversies and implications for MeHg net production. *J. Geophys. Res* **2008,** *113*, G00C03.
25. Haitzer, M.; Aiken, G.R.; Ryan, J.N., Binding of mercury (II) to aquatic humic substances: Influence of pH and source of humic substances. *Environ. Sci. Technol.* **2003,** *37* (11), 2436-2441.
26. Haitzer, M.; Aiken, G.R.; Ryan, J.N., Binding of mercury (II) to dissolved organic matter: the role of the mercury-to-DOM concentration ratio. *Environ. Sci. Technol.* **2002,** *36* (16), 3564-3570.
27. Fitzgerald, W.F.; Lamborg, C.H.; Hammerschmidt, C.R., Marine biogeochemical cycling of mercury. *Chem. Rev.* **2007,** *107* (2), 641-662.
28. Flores, É.L.M.; Paniz, J.N.G.; Flores, É.M.M.; Pozebonb, D.; Dressler, V.L., Mercury speciation in urban landfill leachate by cold vapor generation atomic absorption spectrometry using ion exchange and amalgamation. *J. Braz. Chem. Soc* **2009,** *20* (9), 1659-1666.

29. Ravichandran, M.; Aiken, G.R.; Ryan, J.N.; Reddy, M.M., Inhibition of precipitation and aggregation of metacinnabar (mercuric sulfide) by dissolved organic matter isolated from the Florida Everglades. *Environ. Sci. Technol.* **1999,** *33* (9), 1418-1423.

30. Slowey, A.J., Rate of formation and dissolution of mercury sulfide nanoparticles: The dual role of natural organic matter. *Geochim. Cosmochim. Acta* **2010,** *74* (16), 4693-4708.

31. Deonarine, A.; Hsu-Kim, H., Precipitation of mercuric sulfide nanoparticles in NOM-containing water: Implications for the natural environment. *Environ. Sci. Technol.* **2009,** *43* (7), 2368-2373.

32. Aiken, G.R.; Hsu-Kim, H.; Ryan, J.N., Influence of dissolved organic matter on the environmental fate of metals, nanoparticles, and colloids. *Environ. Sci. Technol.* **2011,** *45* (8), 3196-3201.

33. Pham, A.L.-T.; Morris, A.; Zhang, T.; Ticknor, J.; Levard, C.; Hsu-Kim, H., Precipitation of nanoscale mercuric sulfides in the presence of natural organic matter: Structural properties, aggregation, and biotransformation. *Geochim. Cosmochim. Acta* **2014,** *133*, 204-215.

34. Waples, J.S.; Nagy, K.L.; Aiken, G.R.; Ryan, J.N., Dissolution of cinnabar (HgS) in the presence of natural organic matter. *Geochim. Cosmochim. Acta* **2005,** *69* (6), 1575-1588.

35. Ravichandran, M.; Aiken, G.R.; Reddy, M.M.; Ryan, J.N., Enhanced dissolution of cinnabar (mercuric sulfide) by dissolved organic matter isolated from the Florida Everglades. *Environ. Sci. Technol.* **1998,** *32* (21), 3305-3311.

36. Gu, B.; Bian, Y.; Miller, C.L.; Dong, W.; Jiang, X.; Liang, L., Mercury reduction and complexation by natural organic matter in anoxic environments. *Proc. Natl. Acad. Sci. U.S.A.* **2011,** *108* (4), 1479-1483.

37. Barkay, T.; Liebert, C.; Gillman, M., Environmental significance of the potential for mer (Tn21)-mediated reduction of Hg2+ to Hg0 in natural waters. *Appl. Environ. Microbiol.* **1989,** *55* (5), 1196-1202.

38. Mierle, G.; Ingram, R., The role of humic substances in the mobilization of mercury from watersheds. *Water Air Soil Pollut.* **1991,** *56* (1), 349-357.

39. Watras, C.J.; Morrison, K.A.; Bloom, N.S., Chemical correlates of Hg and Methyl-Hg in northern Wisconsin lake waters under ice-cover. *Water Air Soil Pollut.* **1995,** *84* (3), 253-267.

40. Gustin, M.S., Are mercury emissions from geologic sources significant? A status report. *Sci. Total Environ.* **2003,** *304* (1), 153-167.

41. Benoit, J.M.; Gilmour, C.C.; Mason, R.P.; Heyes, A., Sulfide controls on mercury speciation and bioavailability to methylating bacteria in sediment pore waters. *Environ. Sci. Technol.* **1999,** *33* (6), 951-957.

42. Stordal, M.C.; Santschi, P.H.; Gill, G.A., Colloidal pumping: Evidence for the coagulation process using natural colloids tagged with 203Hg. *Environ. Sci. Technol.* **1996,** *30* (11), 3335-3340.

43. Babiarz, C.L.; Hurley, J.P.; Hoffmann, S.R.; Andren, A.W.; Shafer, M.M.; Armstrong, D.E., Partitioning of total mercury and methylmercury to the colloidal phase in freshwaters. *Environ. Sci. Technol.* **2001,** *35* (24), 4773-4782.

44. Zhu, Y.; Ma, L.Q.; Gao, B.; Bonzongo, J.; Harris, W.; Gu, B., Transport and interactions of kaolinite and mercury in saturated sand media. *J. Hazard. Mater.* **2012**.

45. Evanko, C.R.; Dzombak, D.A., Influence of structural features on sorption of NOM-analogue organic acids to goethite. *Environ. Sci. Technol.* **1998,** *32* (19), 2846-2855.

46. Duckworth, O.W.; Martin, S.T., Surface complexation and dissolution of hematite by C_1-C_6 dicarboxylic acids at pH= 5.0. *Geochim. Cosmochim. Acta* **2001,** *65* (23), 4289-4301.

47. Leong, Y.K.; Scales, P.J.; Healy, T.W.; Boger, D.V.; Buscall, R., Rheological evidence of adsorbate-mediated short-range steric forces in concentrated dispersions. *J. Chem. Soc.-Faraday Trans.* **1993,** *89* (14), 2473-2478.

48. Slowey, A.J.; Johnson, S.B.; Rytuba, J.J.; Brown Jr, G.E., Role of organic acids in promoting colloidal transport of mercury from mine tailings. *Environ. Sci. Technol.* **2005,** *39* (20), 7869-7874.

49. Baig, S.; Coulomb, I.; Courant, P.; Liechti, P., Treatment of Landfill Leachates: Lapeyrouse and Satrod Case Studies. *Ozone: Science & Engineering* **1999,** *21* (1), 1-22.

50. Lema, J.; Mendez, R.; Blazquez, R., Characteristics of landfill leachates and alternatives for their treatment: a review. *Water, Air, and Soil Pollution* **1988,** *40* (3-4), 223-250.

51. Renou, S.; Givaudan, J.G.; Poulain, S.; Dirassouyan, F.; Moulin, P., Landfill leachate treatment: Review and opportunity. *Journal of hazardous materials* **2008,** *150* (3), 468-493.

52. Kjeldsen, P.; Barlaz, M.A.; Rooker, A.P.; Baun, A.; Ledin, A.; Christensen, T.H., Present and long-term composition of MSW landfill leachate: a review. *Critical Reviews in Environmental Science and Technology* **2002,** *32* (4), 297-336.

53. Christensen, T.H.; Kjeldsen, P.; Bjerg, P.L.; Jensen, D.L.; Christensen, J.B.; Baun, A.; Albrechtsen, H.-J.; Heron, G., Biogeochemistry of landfill leachate plumes. *Applied geochemistry* **2001,** *16* (7), 659-718.

54. Chian, E.S.; Dewalle, F.B., Sanitary landfill leachates and their leachate treatment. *Journal of the Environmental Engineering Division* **1976,** *102* (2), 411-431.

55. Kretzschmar, R.; Barmettler, K.; Grolimund, D.; Yan, Y.; Borkovec, M.; Sticher, H., Experimental determination of colloid deposition rates and collision efficiencies in natural porous media. *Water Resour. Res.* **1997,** *33* (5), 1129-1137.

56. Gismera, M.J.; Procopio, J.R.; Sevilla, M.T., Characterization of mercury–humic acids interaction by potentiometric titration with a modified carbon paste mercury sensor. *Electroanal.* **2007,** *19* (10), 1055-1061.

57. Sachs, S.; Bernhard, G., Humic acid model substances with pronounced redox functionality for the study of environmentally relevant interaction processes of metal ions in the presence of humic acid. *Geoderma* **2011,** *162* (1), 132-140.

58. Zhang, L.; Li, A.; Lu, Y.; Yan, L.; Zhong, S.; Deng, C., Characterization and removal of dissolved organic matter (DOM) from landfill leachate rejected by nanofiltration. *Waste Manage.* **2009,** *29* (3), 1035-1040.

59. Louie, S.M.; Tilton, R.D.; Lowry, G.V., Effects of Molecular Weight Distribution and Chemical Properties of Natural Organic Matter on Gold Nanoparticle Aggregation. *Environ. Sci. Technol.* **2013,** *47* (9), 4245-4254.

60. Saleh, N.; Sirk, K.; Liu, Y.; Phenrat, T.; Dufour, B.; Matyjaszewski, K.; Tilton, R.D.; Lowry, G.V., Surface modifications enhance nanoiron transport and NAPL targeting in saturated porous media. *Environ. Eng. Sci.* **2007,** *24* (1), 45-57.

61. Lecoanet, H.F.; Bottero, J.-Y.; Wiesner, M.R., Laboratory assessment of the mobility of nanomaterials in porous media. *Environ. Sci. Technol.* **2004,** *38* (19), 5164-5169.

62. Bradl, H.B., Adsorption of heavy metal ions on soils and soils constituents. *J. Colloid Interface Sci.* **2004,** *277* (1), 1-18.

63. Chen, L.; Sabatini, D.A.; Kibbey, T.C., Role of the air–water interface in the retention of TiO_2 nanoparticles in porous media during primary drainage. *Environ. Sci. Technol.* **2008,** *42* (6), 1916-1921.

64. Wan, J.; Tokunaga, T.K., Partitioning of clay colloids at air–water interfaces. *J. Colloid Interface Sci.* **2002,** *247* (1), 54-61.

65. Ravichandran, M., Interactions between mercury and dissolved organic matter - a review. *Chemosphere* **2004,** *55* (3), 319-331.

66. Chai, X.; Liu, G.; Zhao, X.; Hao, Y.; Zhao, Y., Complexion between mercury and humic substances from different landfill stabilization processes and its implication for the environment. *J. Hazard. Mater.* **2012,** *209*, 59-66.

67. Chen, K.L.; Elimelech, M., Influence of humic acid on the aggregation kinetics of fullerene (C_{60}) nanoparticles in monovalent and divalent electrolyte solutions. *J. Colloid Interface Sci.* **2007,** *309* (1), 126-134.

68. Kim, H.J.; Phenrat, T.; Tilton, R.D.; Lowry, G.V., Effect of kaolinite, silica fines and pH on transport of polymer-modified zero valent iron nano-particles in heterogeneous porous media. *J. Colloid Interface Sci.* **2012,** *370* (1), 1-10.

69. Bradford, S.A.; Simunek, J.; Bettahar, M.; van Genuchten, M.T.; Yates, S.R., Modeling colloid attachment, straining, and exclusion in saturated porous media. *Environ. Sci. Technol.* **2003,** *37* (10), 2242-2250.

70. Tufenkji, N.; Miller, G.F.; Ryan, J.N.; Harvey, R.W.; Elimelech, M., Transport of Cryptosporidium oocysts in porous media: Role of straining and physicochemical filtration. *Environ. Sci. Technol.* **2004,** *38* (22), 5932-5938.

71. Li, X.; Scheibe, T.D.; Johnson, W.P., Apparent decreases in colloid deposition rate coefficients with distance of transport under unfavorable deposition conditions: A general phenomenon. *Environ. Sci. Technol.* **2004,** *38* (21), 5616-5625.

72. Tong, M.; Johnson, W.P., Excess Colloid Retention in Porous Media as a Function of Colloid Size, Fluid Velocity, and Grain Angularity. *Environ. Sci. Technol.* **2006,** *40* (24), 7725-7731.

73. Johnson, W.P.; Li, X.; Yal, G., Colloid Retention in Porous Media: Mechanistic Confirmation of Wedging and Retention in Zones of Flow Stagnation. *Environ. Sci. Technol.* **2007,** *41* (4), 1279-1287.

74. Sarkar, D.; Essington, M.; Misra, K., Adsorption of mercury (II) by kaolinite. *Soil Science Society of America Journal* **2000,** *64* (6), 1968-1975.

75. Bhattacharyya, K.G.; Gupta, S.S., Adsorption of a few heavy metals on natural and modified kaolinite and montmorillonite: a review. *Adv. Colloid Interface Sci.* **2008,** *140* (2), 114-131.

76. Sarkar, D.; Essington, M.E.; Misra, K.C., Adsorption of mercury (II) by kaolinite. *Soil Sci. Soc. Am. J.* **2000,** *64* (6), 1968-1975.

77. Farrah, H.; Pickering, W.F., The sorption of mercury species by clay minerals. *Water Air Soil Pollut.* **1978,** *9* (1), 23-31.

78. Schuster, E., The behavior of mercury in the soil with special emphasis on complexation and adsorption processes-a review of the literature. *Water Air & Soil Pollution* **1991,** *56* (1), 667-680.

79. Yin, Y.; Allen, H.E.; Huang, C.P.; Sparks, D.L.; Sanders, P.F., Kinetics of mercury (II) adsorption and desorption on soil. *Environ. Sci. Technol.* **1997,** *31* (2), 496-503.

80. Skyllberg, U.; Bloom, P.R.; Qian, J.; Lin, C.M.; Bleam, W.F., Complexation of mercury(II) in soil organic matter: EXAFS evidence for linear two-coordination with reduced sulfur groups. *Environ. Sci. Technol.* **2006,** *40* (13), 4174-4180.

Chapter 3. Impact of Hg Speciation on its Removal from Water by Activated Carbon and Organoclay

3.1 Abstract

Mercury exists as different species in water depending on the type of dissolved constituents that are present. Each species has different properties and therefore Hg speciation is expected to affect its removal by adsorbents. This study assessed the removal of selected mercury species, including dissolved Hg(II) species (denoted Hg(II)*), Hg-dissolved organic matter (DOM) complexes, and HgS nanoparticles, by activated carbon, sulfur-modified activated carbon, and organoclay adsorbents. The effect of solution ionic strength, ionic composition, and DOM content on the removal of each Hg species was also evaluated. The removal of Hg(II)* and HgS nanoparticles was reduced by adding DOM into the solution, and increasing ionic strength decreased the removal of Hg(II)* species. On a surface area-normalized basis, the organoclay removed all of the Hg species better than the activated carbon samples. However, organoclay was more susceptible to fouling by NOM in the water. This indicates that using dissolved Hg(II) as a model species for assessing removal efficiency may not provide reliable estimates. Therefore, both the expected Hg speciation and the water quality parameters (NOM content, ionic strength, and ionic composition) need to be considered when designing sorbent based emission controls to meet Hg removal. Hg X-ray absorption spectroscopy results indicate that the surface of the organoclay is highly reactive with the adsorbed Hg species, resulting in the formation of a β-HgS phase for adsorbed Hg-DOM. This study provides insights into the mechanisms of removal of Hg-DOM, the most relevant Hg species due to the ubiquity of NOM in environmental samples, for organoclay and activated carbons.

3.2 Introduction

Wastewater from industrial processes may contain low concentrations of Hg. Depending on the Hg concentrations, some Hg may need to be removed to comply with local regulations. A range of Hg species can exist in environmental and wastewater streams, e.g., Hg(II) bound to dissolved organic matter (Hg-DOM), HgS nanoparticles[1-7]. A number of physical and chemical treatments are used or have been proposed to remove these Hg species from aqueous streams. Removal processes include methods to remove particle-bound Hg (e.g., filtration) and to adsorb dissolved Hg species, (e.g., powder activated carbon treatment, ion exchange, amalgamation, chemical precipitation, electrodeposition, reverse osmosis, photochemical methods, flotation, mechanical filtration, membrane separation, and selective liquid-liquid extraction)[7-20]. The efficacy of any particular treatment process will likely depend on the speciation of Hg, the water properties, and the sorbent properties, and is generally determined using a site-specific treatability study. Improved understanding of the impact of Hg speciation and water chemistry on its removal from water will help in making decisions about what types of sorbents to consider for a desired removal.

After filtration to remove particulate Hg species, sorbents are often used to remove remaining nanoparticulate and dissolved Hg from the water. Many different adsorbents have been evaluated for their ability to remove specific mercury species from water. These include experimental, higher cost, high affinity sorbents like Au nanoparticles[21] or aluminum oxide supported Au nanoparticles[22] that form Au-Hg amalgams[23, 24], and mesoporous silica materials functionalized with 2,5-dimercapto-1,3,4-thiadiazole ligands with adsorption capacity above 1g Hg/1g adsorbent[18]. Chelating fibers[25, 26], ion-exchange materials[27-29], thiol-functionalized materials[30-34], activated carbons[26, 35-41] and organoclay[42-44] have all been used to remove

dissolved inorganic Hg species from water. Although these experimental sorbents are interesting to consider, low cost sorbents like activated carbon have also been shown to also be highly effective[35-41]. In this study, we focus on the behavior of three low cost and widely used sorbent materials: activated carbon, sulfur-impregnated activated carbon, and organoclay.

Activated carbon is a porous material usually produced via carbonization of carbonaceous material followed by either physical or chemical activation process[45]. Because of its high internal surface area and relatively low cost, activated carbon is widely used for the removal of heavy metals and organic compounds from wastewater effluents[46-48]. Sulfurization of activated carbon was shown to be an effective way to enhance gaseous elemental Hg adsorption onto activated carbons[49, 50]. Elemental sulfur in those materials can react with the carbon surface to form disulfide, thiophene, sulfoxide and sulfone groups to increase the affinity of activated carbon to aqueous phase mercuric ions[51, 52]. Enhanced aqueous mercury adsorption was also observed for carbon disulfide treated activation carbon[53]. Organoclays are an engineered geosorbent with high affinity for metals. They are prepared by adsorption of organic molecules onto the clays and have been used previously in in aqueous Hg adsorption studies[42-44]. Dithiocarbamate functional groups incorporated onto organoclay was shown to have a maximum adsorption capacity of 158 mg g^{-1} for Hg(II)[43]. A 2-mercapto-5-amino-1,3,4-thiadiazole modified organoclay also exhibited strong aqueous Hg(II) adsorption capacity[42].

The efficacy of sorbents for mercury removal from water is generally tested using dissolved Hg^{2+} species in deionized water, e.g., a test solution containing $HgCl_2$ or $HgNO_3$. However, in environmental media, dissolved Hg^{2+} species are not likely to be the predominant Hg species. Rather, Hg will form complexes with various ligands (e.g., HS^-, Cl^- , SO_4^{2-}, and DOM)[54]. Strong interaction between Hg^{2+} and DOM are expected in aquatic systems because of

the abundance of DOM in natural waters and the strong Hg(II)-DOM binding constants[4, 55-58]. Also, particulate Hg and particle-bound Hg forms are often detected in environmental samples[1, 3, 59, 60]. This includes nanoparticulate HgS species that may not be effectively removed by filtration[61]. Each of these Hg species has different physicochemical properties, and therefore their removal by commercial sorbents (especially activated carbon due to its relatively low cost) can reasonably be expected to depend on this speciation.

A portion of mercury that may potentially be present in extracted crude oil and gas can distribute to wastewater streams leaving separation units in production and refining operations [62]. These wastewater streams often contain dissolved salts, with chloride salts of Na^+ and Ca^{2+} being most abundant[63, 64]. The ionic composition of water can affect the removal of Hg(II)* by changing Hg speciation[65, 66]. It can also affect the behavior of nanoparticulate HgS species through screening of electrostatic repulsions between particles and sorbents[67]. Thus, the ionic strength and ion types are also expected to play a role in the removal process for different Hg species.

In this study, Hg removal experiments were conducted to assess the impacts of Hg speciation on its removal by various sorbents with different water compositions. Dissolved inorganic Hg(II) species (Hg(II)*), Hg(II)-DOM, and HgS nanoparticles were selected as model Hg species due to their prevalent use in efficacy testing or existence in aqueous environments and wastewater streams [1, 6, 68]. The efficacy of three commercially available adsorbents for each Hg species was determined in batch experiments. Sulfur-impregnated activated carbon was compared with activated carbon without sulfur to evaluate the effect of additional sulfur on Hg removal. Removal with activated carbon was also compared with organoclay. Organoclay is a commercially available chemically-modified natural clay with high affinity for heavy metals[69-

71]. The presence of DOM, ionic strength and two abundant cations (Na^+ and Ca^{2+}) were also compared. The present work provides a better understanding of how various representative Hg species will respond to selected environmental parameters, and provides insight into optimizing the Hg removal process steps needed to meet discharge requirements as a function of the upstream operating conditions.

3.3 Materials and Methods

3.3.1 Characterization of Adsorbents

The removal efficiency of the three Hg species was measured using three commercially available adsorbents. The adsorbents included activated carbon (D/S React-A, Calgon Corporation, Pittsburgh, PA) (denoted as AC), sulfur-impregnated activated carbon (HGR, 4X10, Calgon Corporation, Pittsburgh, PA) (denoted as CSC) and sulfur-impregnated organoclay (MR2, CETCO Hoffman Estates, IL) (denoted as OC). Comparison across these sorbents allowed us to assess the influence of sulfur impregnation on the performance of activated carbon and enables a direct comparison of performance between organoclay and activated carbon sorbents.

To eliminate differences in performance due to mass transfer limitations, each adsorbent was ground and dry sieved to create a size fraction between 74-150 μm, which was used for the adsorption experiments. The N_2-BET surface area was measured using a Quantachrome Nova 2000e (Quantachrome Instruments, USA). The adsorbents (activated carbon, sulfur-impregnated activated carbon and organoclay) were analyzed without further treatment other than heating to 60°C in an oven overnight to remove adsorbed water prior to the N_2-BET measurement. Depending on the specific surface area of the adsorbents, 100-200 mg adsorbent was weighed for the analysis. Just before BET measurement, the samples were degassed at 200°C for 5 hours and

then weighed again. Nitrogen adsorption and desorption experiments were conducted after the samples were cooled to 25°C. Specific surface area was calculated by the multipoint BET method, and pore volume was calculated by the BJH method. To qualitatively assess the phase of sulfur present and to qualitatively assess differences in the carbon structure of the activated carbon samples, X-ray diffraction (XRD) spectra of adsorbents were collected using a X'Pert Pro MPD X-Ray Diffractometer (Panalytical) with Cu-Kα radiation (45kV, 20mA) in a scanning range of 15°-90° 2θ. Elemental analysis was performed to determine the sulfur content of the adsorbents. Electrophoretic mobility of the adsorbents was measured under solution conditions matching the removal experiments using a Zetasizer Nano ZS (Malvern, UK).

3.3.2 Preparation and Characterization of Hg Species

We used dissolved inorganic Hg(II) (denoted as Hg(II)*), Hg(II)-DOM and HgS nanoparticles as representative Hg species presenting different properties and, presumably, different affinities for the sorbents. The preparation of Hg(II)* and Hg(II)-DOM stock solutions was described previously[72]. Briefly, 0.1 mM Hg(II)* stock was prepared by dissolving $Hg(NO_3)_2$ in Millipore water. Hg(II)-DOM stock was prepared by saturating humic acid (HA) (Sigma-Aldrich) solution with Hg(II)* stock and equilibrating for several weeks. Then the Hg(II)-DOM species was collected using a 3KDa filter. HgS nanoparticles were synthesized with a microwave technique[73]. First, 16 mg of mercury acetate and 4 mg of thiourea were dissolved in 50 mL Milli-Q ultrapure water and sealed in a Teflon container. The solution was heated using a microwave digester (Mars 5, CEM Corporation) at 300 W for 10 minutes. After cooling, the synthesized black particles were centrifuged, decanted, and re-suspended in Millipore water five times to remove excess reagents. The particles were then suspended in Millipore water using a probe sonicator and stored as a particle suspension at 4°C until use. Transmission electron

microscopy (TEM) images of synthesized HgS nanoparticles were obtained using a H7100 Hitachi TEM microscope to estimate the average particle size. The hydrodynamic radius was monitored using dynamic light scattering (DLS) (ALV, Germany). The particles remained stable against aggregation for 10 hours with a ~150 rpm magnetic stirring under the solution conditions used in the Hg removal experiments (described next). XRD measurement for HgS nanoparticles was performed under the same condition as for adsorbents to analyze their crystal structure.

3.3.3 Hg Removal Experiments

The removal rate of each Hg species was determined in stirred (~150 rpm) Teflon beakers. For each adsorbent, 2 ± 0.1 mg was added to 15mL of solution in Teflon beakers, and the solution pH was adjusted to 7.5 ± 0.05 using 0.1 N HCl or 0.1 N NaOH without added buffer. The pH of each solution was also measured at the end of the experiment, and no significant change of pH was observed. The adsorbent dispersion was placed under vacuum to saturate the adsorbent pore spaces with water before adding the Hg species. This procedure helps to homogenize the system with respect to available surface area for each sorbent, and facilitates comparison between the sorbents. After saturating the sorbents with water, either 100 ppb Hg(II)*, 100 ppb Hg(II)-DOM, or 100 ppb HgS nanoparticles were injected into the reactors. These initial concentrations were selected to achieve approximately 50% removal based on preliminary testing. This ensures that the final concentration of Hg in solution is measureable. Aliquots were sampled at different time points over four hours. Four hour experiments were selected based on the typical contact time of common powdered activated carbon processes[74]. Prior to analyzing the water for total Hg, the adsorbents were allowed to settle quiescently for 2 min at each sampling time point to separate unadsorbed Hg species (especially HgS nanoparticles) from Hg species associated with adsorbents. The relatively large sorbent particles

settled out readily. Hg(II)* species and Hg(II)-DOM were directly measured in water samples according to EPA method 1631 using a mercury analyzer (Brooks-Rand Model MERX). HgS particles were digested using aqua regia over night before total Hg analysis.

Experimental solution conditions were used to look at the influence of *i)* ionic strength, *ii)* the presence of dissolved organic matter and *iii)* the cation type, on the removal of Hg species. Each condition was studied at two specific concentrations, resulting in six experimental solutions. The salt concentrations, and presence and absence of DOM used in this study fall in the range of salinity and DOM reported for wastewater or produced waters[75]. The mercury speciation in these solutions was modeled using Visual MINTEQ by assuming that equilibrium conditions were reached. The Hg(II)-DOM species was estimated by assuming $K_{DOM} = 10^{23.4}$ L kg^{-1} at neutral pH[56].

The Hg removal rate constants and mechanisms were evaluated by fitting the experimental data of Hg loss vs. time using a pseudo second order kinetic model (equation 3.1). The pseudo second order kinetic model often gives better fitting results compared with simpler models such as first or second order models[76] because adsorbents rarely have a homogeneous surface structure and diffusion effects and chemical reactions are usually inseparable[77].

$$\frac{t}{q_t} = \frac{1}{k{q_e}^2} + \frac{t}{q_e} \qquad \text{(eqn 3.1)}$$

In eqn 3.1, q_t (mg/g) is the amount of Hg species adsorbed at time t (h), q_e (mg/g) is the amount of Hg species adsorbed at equilibrium, and k (g mg^{-1} h^{-1}) is the pseudo second order adsorption rate constant. The fitting results are shown in Table B1. Although the pseudo second order models showed high correlation coefficients in this study and several other Hg removal studies[78, 79], it may be less valid in the case of HgS removal than the removal of the other two

Hg species because heteroaggregation between adsorbent particles and HgS nanoparticles was expected to be the main removal mechanism. Student-Newman-Keuls test was applied using SAS software to compare the fitted values (k and q_e) across each group.

3.3.4 X-ray Adsorption Spectroscopy (XAS) Experiments

XAS experiments were conducted to assess the speciation of Hg on adsorbents exposed to Hg(II)* and Hg-DOM solutions. To ensure sufficient Hg on the adsorbents for XAS analysis, Hg was adsorbed to provide a concentration of ~500 ppm. The samples were prepared by the same procedure described earlier, except that an initial Hg concentration of 6 mg/L and 100 mg adsorbent was used. Duplicates for each Hg species-adsorbent combination were generated to provide sufficient sample mass. To remove poorly bound Hg species, the Hg-loaded adsorbents were centrifuged and re-suspended in Milli-Q ultrapure water five times. The washed adsorbents were freeze-dried, and the Hg concentration on adsorbents was measured by digesting the material with aqua regia and measuring the digestate with the Hg analyzer. The rest of the freeze-dried sample was pressed into pellets, and sealed into Kapton tape. The Hg speciation was determined using XAS at the Hg L(III) absorption edge (12,282 eV) on beamline 11-2 at the Stanford Synchrotron Radiation Lightsource (SSRL). All measurements were conducted at liquid nitrogen temperature (~77K) using a slow cooling method[35] to identify elemental Hg if it existed on the samples. Both transmission and fluorescence spectra were collected. Monochromator and internal energy calibration was made using a $HgCl_2$ salt reference using SIXpack software suite[36], version 0.68.13. XAS scans were then background subtracted with E_0 defined as 12,284 eV, converted to frequency (k) space using a spline range of 0 to 11 $Å^{-1}$, and weighted by k^3. To assess Hg speciation, linear combination fitting (LCF) was performed. LCF allows identifying the components significantly contributing to the extended X-ray absorption fine structure

(EXAFS) spectra of a sample. LCF was performed on k-space, constrained between k = 1 – 9 $Å^{-1}$, using a library of 18 Hg model compounds (Figure B1 for the list and spectra of model compounds).

3.4 Results and Discussion

3.4.1 Characteristics of Adsorbents

Characteristics of the adsorbents are shown in Table 3. BET surface area results show that both activated carbon samples had a surface area that was more than 2 orders of magnitude higher than for the organoclay. Thus, the activated carbon samples had a significantly larger internal surface area compared to the organoclay. The BJH pore volume of sulfur impregnated activated carbon is more than six times lower than for activated carbon, suggesting that the sulfur present on the internal surface of the carbon[80] has reduced the pore volume. This is consistent with the relatively large amount of S present (~14 wt%) in the sulfur impregnated activated carbon (Table 3). It was also showed that the S as S_8 was weakly bonded in macropores and S as S_2 and S_6 was strongly bonded in micropores[49]. The microporous structures in activated carbon could be accessible for the smaller sized dissolved inorganic Hg(II) species[81], but potentially less accessible to larger Hg compounds such as Hg-DOM and HgS nanoparticles.

The impregnated sulfur in the OC and CSC sorbents are designed to increase the affinity for Hg[49]. For the CSC material, the manufacturer indicates that the sulfur is distributed in a thin layer over the internal surface area of the particles[80]. This sulfur-impregnated activated carbon was shown to be highly effective for the removal of elemental mercury from gas phase because of its sulfur content[82]. However, it is unclear if the sulfur in the internal micropore space of materials will be available and have an affinity to aqueous phase Hg species. Different from the

sulfur impregnated activated carbon, the organoclay surface is functionalized to increase the affinity of organoclay for a range of heavy metals, including Hg[71]. It has a lower sulfur content than the CSC, but still contains a significant amount of S (~5 wt%) that is available for reaction with adsorbed Hg as discussed later in the paper. The exact speciation of sulfur in the OC and CSC is proprietary. XRD results (Figure B1) indicate a small fraction of crystalline sulfur on organoclay, but not on the CSC.

Table 3. Characteristics of activated carbon and organoclay adsorbents.

Adsorbent	**AC**	**CSC**	**OC**
BET surface area (m^2/g)	690	610	2.4
BJH surface area (m^2/g)	79	7.4	1.9
BJH Pore volume (cc/g)	0.13	0.02	0.015
Sulfur content (%)	0.8	13.9	4.7

3.4.2 Characteristics of Hg Species

Synthesized HgS nanoparticles were characterized by XRD, TEM and DLS. XRD (Figure B1) indicates that the crystal form of synthesized HgS nanoparticles matched metacinnabar (β-HgS). An average particle size of 10 nm was calculated by measuring HgS particle sizes in TEM images (Figure B2). However, the mean hydrodynamic particle radius was centered on 20 nm determined by DLS (Figure B3), suggesting that particles were aggregating to some degree in the aqueous phase. Hg-DOM characterization was included in our previous study[72]. A Hg/C molar ratio of 0.00007 mol Hg/mol C was determined for the prepared Hg-DOM species. Unlike β-HgS nanoparticles and Hg-DOM species, Hg(II)* species were expected

to depend more on the solution conditions. The calculated Hg(II)* speciation in each solution is shown in Figure 3.1. The Hg-DOM species is the dominant Hg species when 1 mg/L DOC was present. At lower ionic strength in the absence of DOC, Hg speciation is primarily HgClOH and $HgCl_2$(aq), with $Hg(OH)_2$ and $HgCl_3^{-1}$ as minor species. As the ionic strength increases, the various $HgCl_x^{2-x}$ are the predominant species.

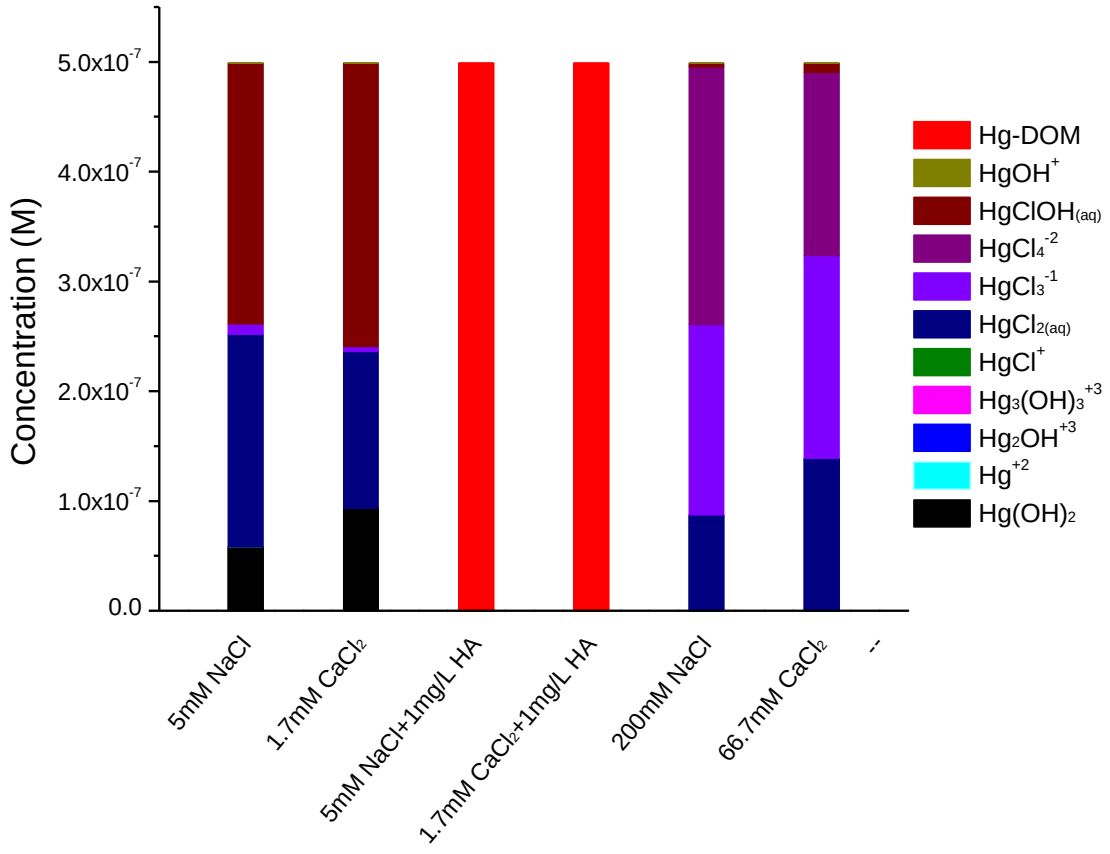

Figure 3.1. Hg speciation expectation under the different Hg removal experimental solution conditions used in this study. Visual MINTEQ was used for the simulation by assuming equilibrium was reached. Simulation conditions matched the parameters used in Hg removal experiments.

3.4.3 Effect of NOM on the Removal of Each Hg Species

The effect of DOM in solution on the removal of the three different Hg species was compared in both NaCl and $CaCl_2$ solution conditions, respectively (Figure 3.2). Fitting results of these data using the pseudo second order kinetic model are provided in Table B1. The presence of DOM (1 mg C/L of HA) (Figure 3.2 open symbols) generally decreased the removal extent of Hg(II)* species and HgS nanoparticles on all adsorbents relative to removal without DOM added to the solution (Figure 3.2 open symbols). Organoclay (blue triangles) is more affected by the presence of DOM in solution than activated carbon sorbents. For organoclay, both the rate of uptake and the adsorbed mass was lower with added DOM than without. Moreover, the data were not fit well with the pseudo second order model for Hg(II)* removal using organoclay with added DOM in the solution, suggesting a different removal process may be involved for organoclay with DOM present.

Organoclays are known to have high affinity for DOM[83], so DOM in the solution might be fouling the surface sites on organoclay and slowing down the adsorption of Hg(II)* species. The addition of DOM in the solution also reduced the removal rate and extent of β-HgS nanoparticles by organoclay. DOM is expected to adsorb onto both the organoclay and the β-HgS nanoparticles, and thus decrease their heteroaggregation rate by increasing the steric repulsion[84]. Compared with organoclay, the impact of added DOM on activated carbon is less significant. It suggests either a relatively lower affinity between DOM and these activated carbon samples compared to organoclay, or a greater abundance of reactive sites on activated carbon compared to organoclay. This is consistent with the significantly higher surface area measured for activated carbon compared to the organoclay.

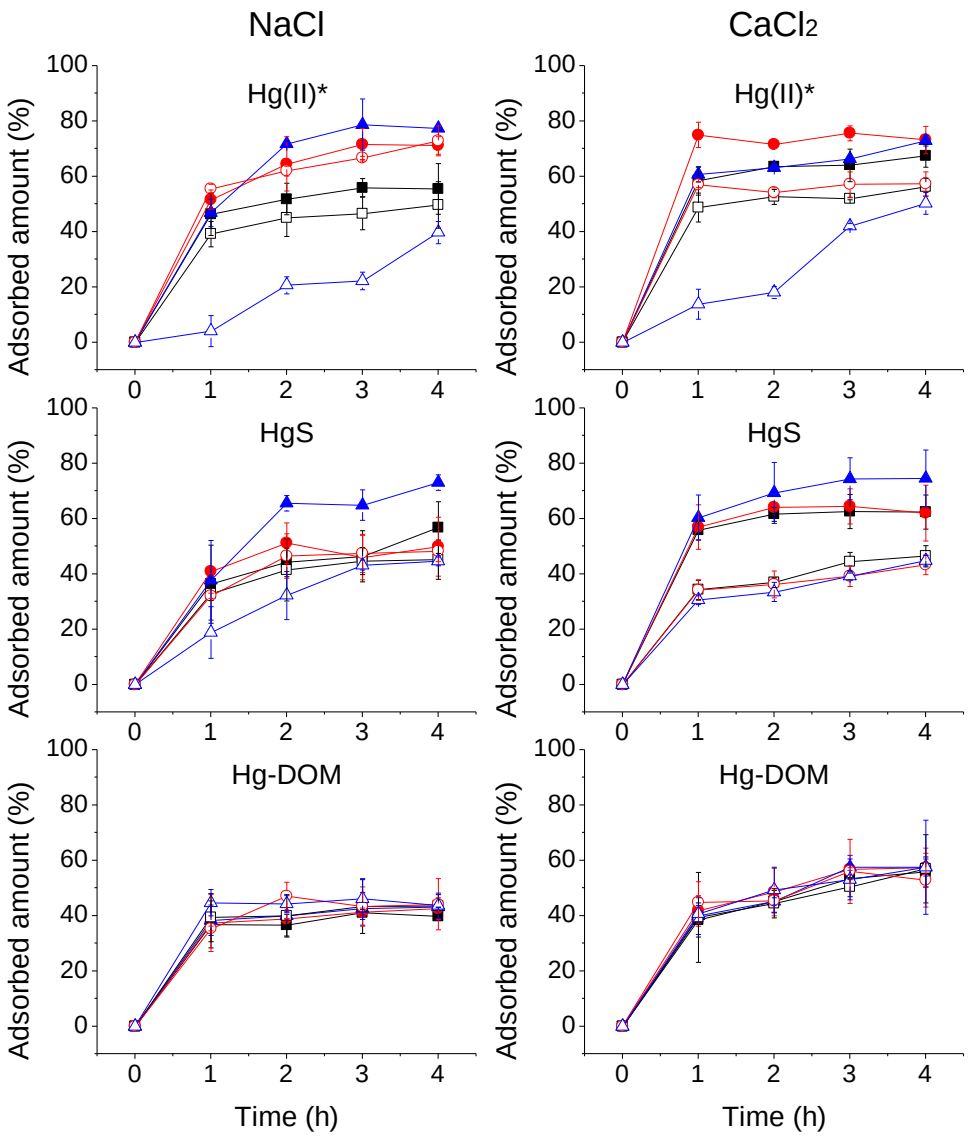

Figure 3.2. Effect of DOM on the removal of mercury species in 5 mM NaCl (left column) and 1.7 mM $CaCl_2$ (right column) solution, respectively**.** ■: Calgon activated carbon; ●: Calgon sulfur-impregnated activated carbon; ▲: CETCO organoclay. Solid symbol: Without HA; Open symbol: With DOM at 1 mg C/L.

The identity of the ion in solution also affected the sorption of Hg species. effect of added DOM on the adsorption of Hg(II)* and HgS nanoparticles for both activated carbon sorbents was greater using Ca^{2+} than for Na^{+} even though both solutions had the same ionic strength (Figure 3.2 and Table B1). Ca^{2+} can bridge the DOM with the negatively charged adsorbent surface (Electrophoretic mobility under 1.7 mM $CaCl_2$ solution: -0.23 ± 0.03μm cm/Vs for AC, -0.17 ± 0.03 μm cm/Vs for CSC, +1.11 ± 0.08 μm cm/Vs for OC) to enhance the adsorption of DOM on adsorbents, while sodium does not have this effect[85, 86]. The greater adsorption of DOM onto the adsorbents in Ca^{2+} solution lowers the adsorbed amount of Hg species because more adsorption sites are occupied by DOM molecules. In contrast to the activated carbon, there was limited effects of cation type on the sorption of Hg(II)* and HgS species to organoclay. This could be a result of an overall higher affinity of organoclay for NOM, which masks the effect of Ca^{2+}. There was no apparent effect of added HA on the removal of the Hg-DOM species. However, this was an artifact of the experimental design. The prepared Hg-DOM species had a Hg/C molar ratio of 0.00007 mol Hg/mol C[72], meaning that 100 ppb Hg-DOM would introduce about 8.6 mg C/L in the system. Thus additional 1 mg C/L did not significantly change the solution conditions and therefore did not significantly impact the removal results for Hg-DOM. But from Table B1 (q_e values), Ca^{2+} was shown to enhance the removal of Hg-DOM species in comparison with Na^{+} regardless of the presence of additional HA in the solution.

3.4.4 Effect of Ionic Strength on the Removal of Hg Species

For both NaCl and $CaCl_2$ solutions, the effect of ionic strength on the removal of each Hg species is shown in Figure 3.3. By comparing q_e values in Table B1, increased ionic strength reduced the adsorption of Hg(II)* in NaCl. A similar trend was previously reported for Hg(II)

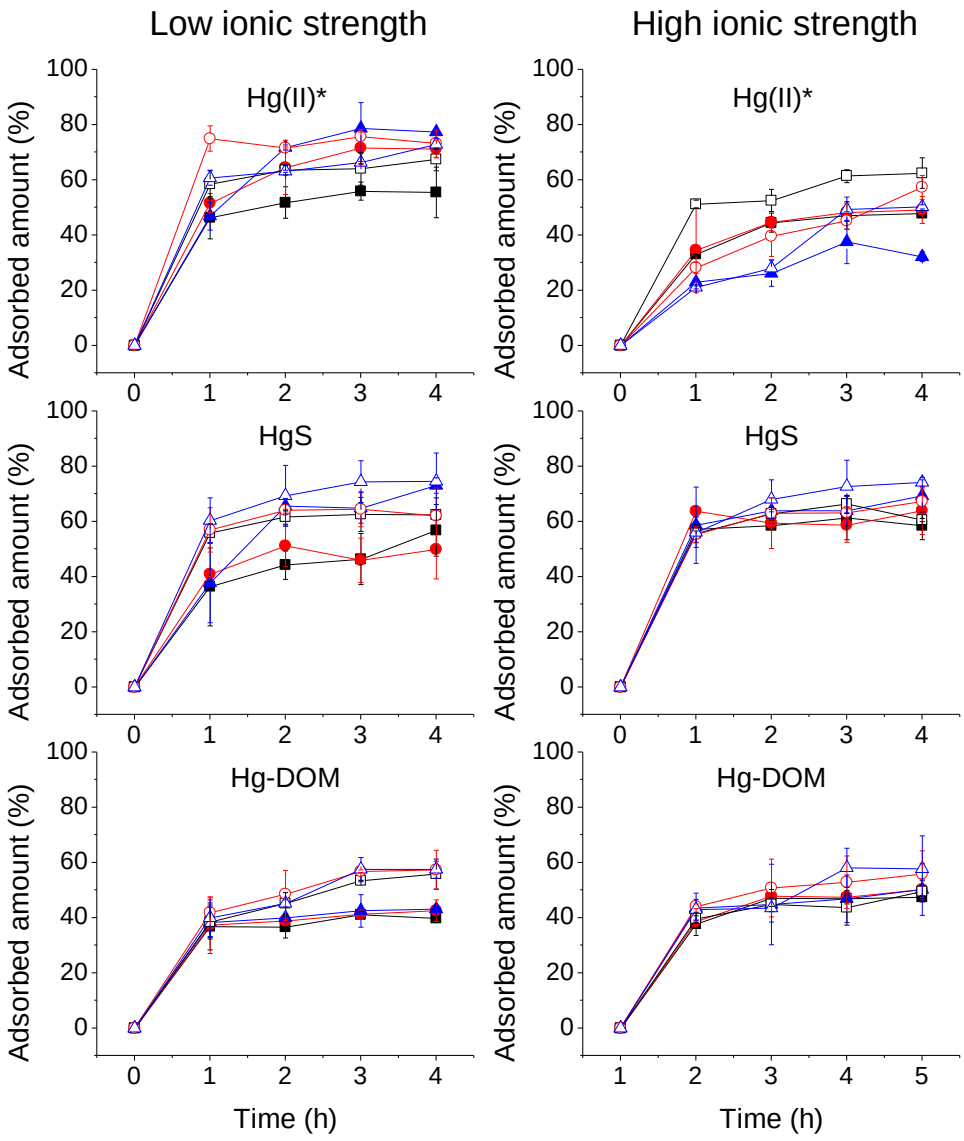

Figure 3.3. Effect of ionic strength on the removal of mercury species under low ionic strength (5 mM NaCl or 1.7 mM $CaCl_2$) (left column) and high ionic strength (200mM NaCl or 66.7mM $CaCl_2$) (right column) solution conditions, respectively. ■: Calgon activated carbon; ●: Calgon sulfur-impregnated activated carbon; ▲: CETCO organoclay. Solid symbol: NaCl solution condition; Open symbol: $CaCl_2$ condition.

adsorption studies, and these were attributed to changes in mercury activities and electrostatic interactions[87, 88]. This is also likely because the Hg(II)* species is a function of ionic strength, with uncharged compounds (e.g., $HgClOH_{(aq)}$, $HgCl_{2(aq)}$) being predominant at low ionic strength, and charged compounds (e.g., $HgCl_4^{-2}$, $HgCl_3^-$) being predominant when the Cl^- concentration increased. The uncharged mercury compounds such as $HgClOH_{(aq)}$ and $HgCl_{2(aq)}$ are apparently more likely to adsorb than the charged Hg species. In $CaCl_2$ solutions, there is a lower amount of negatively charged Hg(II)* species (Figure 3.1), corresponding to a greater adsorbed amount of Hg(II)* relative to NaCl at the same ionic strength.

Increasing ionic strength was expected to decrease the surface charge of HgS nanoparticles and therefore increase the nanoparticles heteroaggregation with the adsorbents. While there is a modest increase in removal of HgS NPs at higher ionic strength in NaCl, there is less increase observed for $CaCl_2$. Ca^{2+} is more efficient at screening charge on the particles than Na^+. So it is likely that the Ca^{2+} ions had effectively screened the charge at 1.7 mM, and no increase in this screening was observed at 66.7mM.

3.4.5 Comparison of Adsorbents

The impregnation of activated carbon with sulfur is designed to increase its affinity for Hg. However, for the aqueous conditions used here, the sulfur-impregnated activated carbon did not show better removal efficacy than activated carbon for Hg-DOM or HgS nanoparticles. There was some improvement seen for Hg(II)* under low ionic strength conditions. At high ionic strength in $CaCl_2$ solution (Figure 3.2), activated carbon showed higher removal rates for dissolved Hg(II)* species than either sulfur-impregnated activated carbon or organoclay.

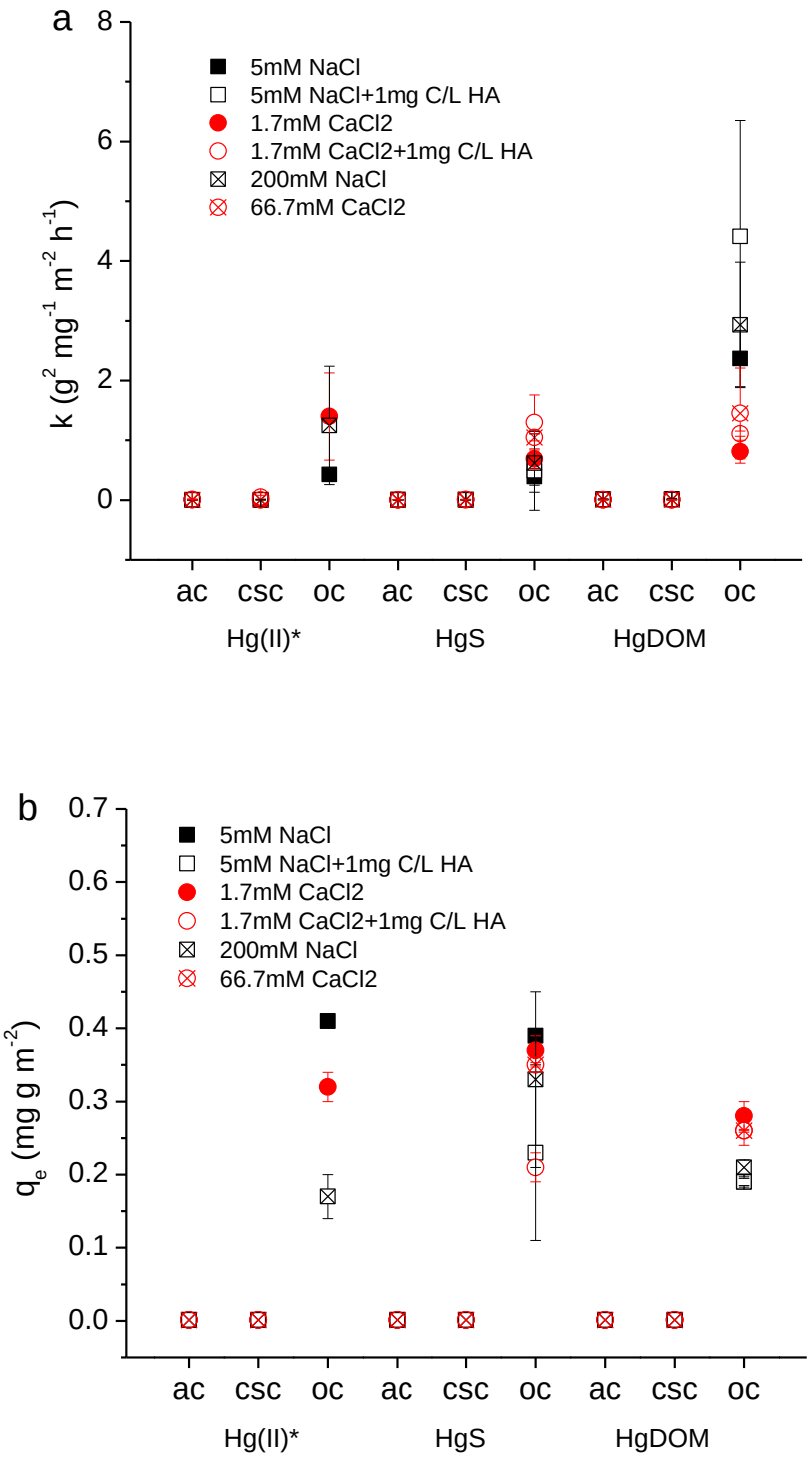

Figure 3.4. Surface area normalized k values (a) and q_e values (b) fitted by pseudo second order kinetic model.

In order to further explore the differences in Hg removal rates and mechanism, the pseudo-first-order model fitting results in Table B1 were normalized by specific surface area values of adsorbents (Table B2). The surface area normalized k and q_e values are also plotted in Figure 3.4a and 3.4b. There were differences between the sorbent types. For all Hg species, the fitted values (k and q_e) for the organoclay were statistically significantly higher than for the activated carbons (Prob>F <0.0001). There were no differences observed between the two activated carbon samples. This is in contrast to that reported for disulfide treated activated carbons. The reasons for this difference are unclear, but could be due to differences in the species of S present on the carbon, or because the sulfur impregnation for CSC decreased the available surface area for our materials. These data indicate that organoclay can provide more efficient in Hg removal than the activated carbon samples per unit surface area.

3.4.6 Characterization of Hg-DOM Adsorbed onto Absorbents

Differences in the speciation of adsorbed mercury were evaluated for Hg-DOM species using XAS. Differences in final Hg speciation on the sorbents may explain the greater apparent affinity of organoclay over the activated carbon samples.

The EXAFS spectra at Hg L(III)-edge and their fits are provided in Figure 3.5 and Table B3, respectively. For both activated carbon samples, Hg(II)-thiol model compounds provide the best fitting results. Because Hg is associated with-DOM by forming Hg-S bonds, it has the same XAS signal as a Hg-thiolated ligand complex. These results suggest that Hg-DOM is mainly physically absorbed onto the surface of activated carbon. A similar result is observed for sulfur-impregnated activated carbon, with most Hg present being most like the Hg-thiol (Hg-S-R) model compound. However, there is a small shift in the Hg speciation towards a Hg-cysteine

model compound which tends to form two-coordinated (R-S-Hg-S-R) species. This shift suggests that some of the impregnated sulfur is indeed reactive with the adsorbed Hg-DOM species. Conversely, the Hg speciation for Hg-DOM adsorbed onto organoclay shows that Hg-DOM is completely transformed to β–HgS, indicating that sulfur content on the surface of the organoclay was reactive with the Hg-DOM complex to form a more thermodynamically stable

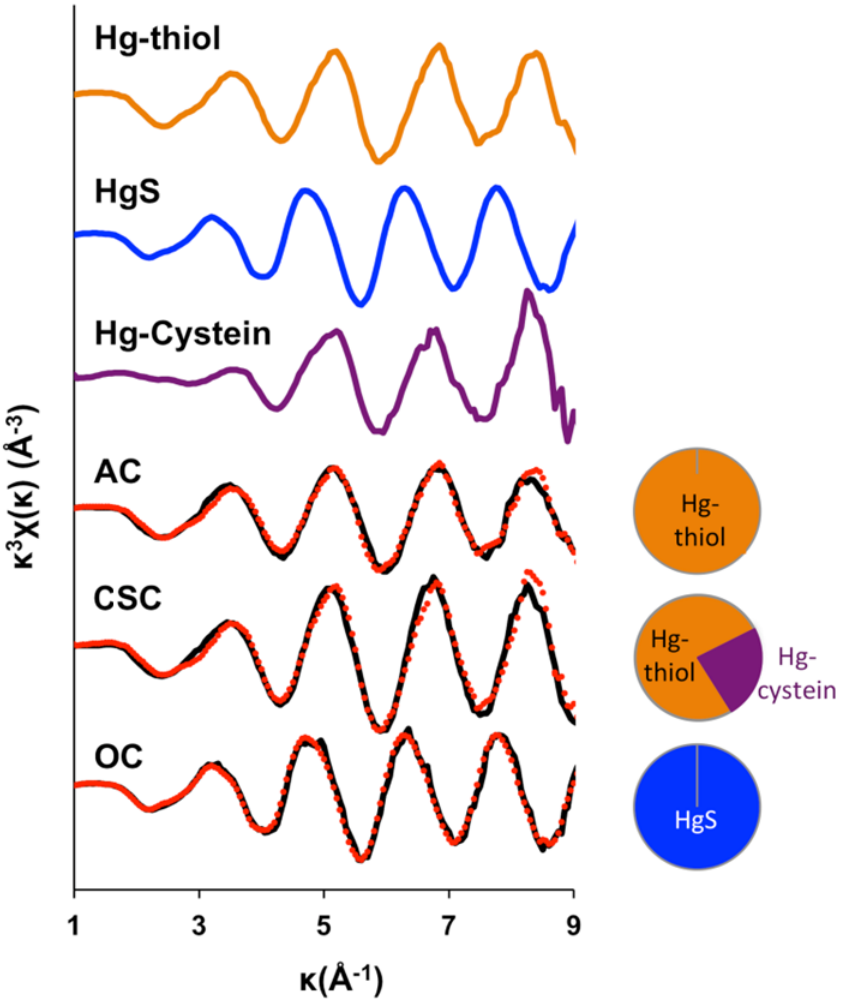

Figure 3.5. XAS experimental results for adsorption of Hg-DOM on adsorbents. AC: Calgon activated carbon; CSC: Calgon sulfur-impregnated activated carbon; OC: CETCO organoclay.

β-HgS species. This is consistent with the higher reactivity of the organoclay surface compared to the activated carbon. The different reactivity of Hg with the sulfur-impregnated activated carbon compared to the organoclay may be due to the different form of sulfur present on those surfaces; elemental sulfur is present on the activated carbon surfaces (per discussion with a Calgon representative) whereas a more reactive dithiocarbamate is likely present on the organoclay. This form of sulfur is not confirmed on organoclay as this is proprietary. The differences in reactivity with Hg may also have resulted from the different distributions of sulfur on the particles. For sulfur-impregnated activated carbon, the sulfur deposited into pores may not be available to react with large-sized Hg-DOM species. However, the impregnated sulfur on organoclay is mainly on the surface of the clay particles and is more readily accessible to the Hg-DOM species.

3.5 Conclusions and Implications

The results from these tests provide important insights into the effects of Hg speciation and water quality parameters on Hg removal by activated carbon and organoclay. It was shown that Hg speciation affected its removal differently depending on the water quality parameters, including the presence of DOM, cation type, and ionic strength. The presence of DOM reduced the removal of Hg(II)* and HgS nanoparticles. Increasing the ionic strength decreased the removal of Hg(II)* species. Organoclay could remove Hg species better than activated carbon or sulfur impregnated activated carbon in terms of unit surface area. However, OC was more susceptible to fouling by NOM in the water. Despite a prior report that carbon disulfide treated activated carbon enhanced aqueous mercury adsorption, the differences between activated carbon and sulfur-impregnated activated carbon samples used in this study were not significant.

XAS results show that organoclay has a highly reactive surface, forming an inorganic HgS phase from adsorbed Hg-DOM, whereas Hg-DOM on the AC surface was not changed.

Dissolved Hg(II) species have been widely used as a model compound to assess the performance of different Hg sorbents. However, dissolved Hg(II) species are not the most dominant Hg species present. This study showed that, except for AC in 1.7 mM $CaCl_2$ solution, Hg speciation affected the removal efficiency. This indicates that using dissolved Hg(II) as a "surrogate" species for assessing removal efficiency may not provide reliable estimates. The magnitude of the error will depend on both the Hg species and the solution conditions.

Therefore, both the expected Hg speciation and the water quality parameters (NOM content, ionic strength, and ionic composition) need to be considered when designing sorbent based emission controls to meet Hg removal targets, especially for flow-through systems commonly used in the field because they have a fixed contact time. For wastewater containing high salinity, e.g., produced water, dissolved Hg(II) species will be more difficulty to remove so increasing the adsorbent dosage may be necessary. Similarly, in solutions containing nominal NOM concentrations as low as 1 mg C/L, the Hg removal efficiency of Hg is expected to decrease, especially for organoclay.

The high surface reactivity of organoclay with Hg-DOM, and the resulting formation of a metacinnabar (β-HgS) phase, may make the use of organoclays an attractive alternative for Hg sorption. The formed β-HgS phase is stable with low aqueous solubility, and a relatively lower bioavailability than other more labile Hg species including Hg-DOM and other dissolved phase Hg species. This benefit may be offset by the greater sensitivity of OC to NOM fouling.

3.6 References

1. Lowry, G.V.; Shaw, S.; Kim, C.S.; Rytuba, J.J.; Brown, G.E., Macroscopic and microscopic observations of particle-facilitated mercury transport from New Idria and Sulphur Bank mercury mine tailings. *Environmental science & technology* **2004,** *38* (19), 5101-5111.
2. Ravichandran, M., Interactions between mercury and dissolved organic matter—a review. *Chemosphere* **2004,** *55* (3), 319-331.
3. Ravichandran, M.; Aiken, G.R.; Ryan, J.N.; Reddy, M.M., Inhibition of precipitation and aggregation of metacinnabar (mercuric sulfide) by dissolved organic matter isolated from the Florida Everglades. *Environmental science & technology* **1999,** *33* (9), 1418-1423.
4. Ravichandran, M., Interactions between mercury and dissolved organic matter - a review. *Chemosphere* **2004,** *55* (3), 319-331.
5. Mierle, G.; Ingram, R., The role of humic substances in the mobilization of mercury from watersheds. *Water, Air, & Soil Pollution* **1991,** *56* (1), 349-357.
6. Kim, C.S.; Brown Jr, G.E.; Rytuba, J.J., Characterization and speciation of mercury-bearing mine wastes using X-ray absorption spectroscopy. *Science of the Total Environment* **2000,** *261* (1–3), 157-168.
7. Smuleac, V.; Butterfield, D.; Sikdar, S.; Varma, R.; Bhattacharyya, D., Polythiol-functionalized alumina membranes for mercury capture. *Journal of Membrane Science* **2005,** *251* (1), 169-178.
8. Biester, H.; Schuhmacher, P.; Müller, G., Effectiveness of mossy tin filters to remove mercury from aqueous solution by Hg(II) reduction and Hg(0) amalgamation. *Water research* **2000,** *34* (7), 2031-2036.
9. Huttenloch, P.; Roehl, K.E.; Czurda, K., Use of copper shavings to remove mercury from contaminated groundwater or wastewater by amalgamation. *Environmental science & technology* **2003,** *37* (18), 4269-4273.
10. Chojnacki, A.; Chojnacka, K.; Hoffmann, J.; Gorecki, H., The application of natural zeolites for mercury removal: from laboratory tests to industrial scale. *Minerals Engineering* **2004,** *17* (7), 933-937.

11. Oehmen, A.; Viegas, R.; Velizarov, S.; Reis, M.A.; Crespo, J.G., Removal of heavy metals from drinking water supplies through the ion exchange membrane bioreactor. *Desalination* **2006,** *199* (1), 405-407.

12. Evangelista, S.M.; DeOliveira, E.; Castro, G.R.; Zara, L.F.; Prado, A.G., Hexagonal mesoporous silica modified with 2-mercaptothiazoline for removing mercury from water solution. *Surface science* **2007,** *601* (10), 2194-2202.

13. Fábrega, F.d.M.; Mansur, M.B., Liquid–liquid extraction of mercury (II) from hydrochloric acid solutions by Aliquat 336. *Hydrometallurgy* **2007,** *87* (3), 83-90.

14. Lopes, C.; Otero, M.; Coimbra, J.; Pereira, E.; Rocha, J.; Lin, Z.; Duarte, A., Removal of low concentration Hg^{2+} from natural waters by microporous and layered titanosilicates. *Microporous and mesoporous materials* **2007,** *103* (1), 325-332.

15. Park, H.G.; Kim, T.W.; Chae, M.Y.; Yoo, I.-K., Activated carbon-containing alginate adsorbent for the simultaneous removal of heavy metals and toxic organics. *Process biochemistry* **2007,** *42* (10), 1371-1377.

16. Vieira, M.A.; Ribeiro, A.S.; Curtius, A.J.; Sturgeon, R.E., Determination of total mercury and methylmercury in biological samples by photochemical vapor generation. *Analytical and bioanalytical chemistry* **2007,** *388* (4), 837-847.

17. Chakrabarty, K.; Saha, P.; Ghoshal, A.K., Separation of mercury from its aqueous solution through supported liquid membrane using environmentally benign diluent. *Journal of Membrane Science* **2010,** *350* (1), 395-401.

18. Olkhovyk, O.; Jaroniec, M., Ordered Mesoporous Silicas with 2,5-Dimercapto-1,3,4-Thiadiazole Ligand: High Capacity Adsorbents for Mercury Ions. *Adsorption* **2005,** *11* (3-4), 205-214.

19. Kostal, J.; Mulchandani, A.; Gropp, K.E.; Chen, W., A temperature responsive biopolymer for mercury remediation. *Environmental science & technology* **2003,** *37* (19), 4457-4462.

20. Mahmoud, M.E.; Gohar, G.A., Silica gel-immobilized-dithioacetal derivatives as potential solid phase extractors for mercury (II). *Talanta* **2000,** *51* (1), 77-87.

21. Lisha, K.; Pradeep, T., Towards a practical solution for removing inorganic mercury from drinking water using gold nanoparticles. *Gold Bulletin* **2009,** *42* (2), 144-152.

22. Lo, S.-I.; Chen, P.-C.; Huang, C.-C.; Chang, H.-T., Gold Nanoparticle–Aluminum Oxide Adsorbent for Efficient Removal of Mercury Species from Natural Waters. *Environmental science & technology* **2012,** *46* (5), 2724-2730.

23. Leopold, K.; Foulkes, M.; Worsfold, P.J., Gold-coated silica as a preconcentration phase for the determination of total dissolved mercury in natural waters using atomic fluorescence spectrometry. *Analytical chemistry* **2009,** *81* (9), 3421-3428.

24. Pradeep, T., Noble metal nanoparticles for water purification: a critical review. *Thin Solid Films* **2009,** *517* (24), 6441-6478.

25. Liu, C.; Huang, Y.; Naismith, N.; Economy, J.; Talbott, J., Novel polymeric chelating fibers for selective removal of mercury and cesium from water. *Environmental science & technology* **2003,** *37* (18), 4261-4268.

26. Nabais, J.V.; Carrott, P.; Carrott, M.; Belchior, M.; Boavida, D.; Diall, T.; Gulyurtlu, I., Mercury removal from aqueous solution and flue gas by adsorption on activated carbon fibres. *Applied Surface Science* **2006,** *252* (17), 6046-6052.

27. Gash, A.E.; Spain, A.L.; Dysleski, L.M.; Flaschenriem, C.J.; Kalaveshi, A.; Dorhout, P.K.; Strauss, S.H., Efficient recovery of elemental mercury from Hg (II)-contaminated aqueous media using a redox-recyclable ion-exchange material. *Environmental science & technology* **1998,** *32* (7), 1007-1012.

28. Chiarle, S.; Ratto, M.; Rovatti, M., Mercury removal from water by ion exchange resins adsorption. *Water research* **2000,** *34* (11), 2971-2978.

29. Noh, Y.D.; Komarneni, S., Mercury (II) exchange by highly charged swelling micas, Sodium Engelhard titanosilicate-4, and Sodium titanosilicate. *Environmental science & technology* **2011,** *45* (16), 6954-6960.

30. Manohar, D.; Anoop Krishnan, K.; Anirudhan, T., Removal of mercury (II) from aqueous solutions and chlor-alkali industry wastewater using 2-mercaptobenzimidazole-clay. *Water research* **2002,** *36* (6), 1609-1619.

31. Hakami, O.; Zhang, Y.; Banks, C.J., Thiol-functionalised mesoporous silica-coated magnetite nanoparticles for high efficiency removal and recovery of Hg from water. *Water research* **2012,** *46* (12), 3913-3922.

32. Hutchison, A.; Atwood, D.; Santilliann-Jiminez, Q.E., The removal of mercury from water by open chain ligands containing multiple sulfurs. *Journal of hazardous materials* **2008,** *156* (1), 458-465.

33. Navarro, R.R.; Sumi, K.; Fujii, N.; Matsumura, M., Mercury removal from wastewater using porous cellulose carrier modified with polyethyleneimine. *Water research* **1996,** *30* (10), 2488-2494.

34. Antochshuk, V.; Jaroniec, M., 1-Allyl-3-propylthiourea modified mesoporous silica for mercury removal. *Chem. Commun.* **2002** (3), 258-259.

35. Rao, M.M.; Reddy, D.H.K.; Venkateswarlu, P.; Seshaiah, K., Removal of mercury from aqueous solutions using activated carbon prepared from agricultural by-product/waste. *Journal of environmental management* **2009,** *90* (1), 634-643.

36. Kadirvelu, K.; Kavipriya, M.; Karthika, C.; Vennilamani, N.; Pattabhi, S., Mercury (II) adsorption by activated carbon made from sago waste. *Carbon* **2004,** *42* (4), 745-752.

37. Namasivayam, C.; Periasamy, K., Bicarbonate-treated peanut hull carbon for mercury (II) removal from aqueous solution. *Water research* **1993,** *27* (11), 1663-1668.

38. Yardim, M.; Budinova, T.; Ekinci, E.; Petrov, N.; Razvigorova, M.; Minkova, V., Removal of mercury (II) from aqueous solution by activated carbon obtained from furfural. *Chemosphere* **2003,** *52* (5), 835-841.

39. Namasivayam, C.; Kadirvelu, K., Uptake of mercury (II) from wastewater by activated carbon from an unwanted agricultural solid by-product: coirpith. *Carbon* **1999,** *37* (1), 79-84.

40. Zhu, J.; Deng, B.; Yang, J.; Gang, D., Modifying activated carbon with hybrid ligands for enhancing aqueous mercury removal. *Carbon* **2009,** *47* (8), 2014-2025.

41. Zhang, F.-S.; Nriagu, J.O.; Itoh, H., Mercury removal from water using activated carbons derived from organic sewage sludge. *Water research* **2005,** *39* (2), 389-395.

42. Filho, N.L.D.; Carmo, D.R.d.; Rosa, A.H., Selective sorption of mercury (II) from aqueous solution with an organically modified clay and its electroanalytical application. *Separation Science and Technology* **2006,** *41* (4), 733-746.

43. Say, R.; Birlik, E.; Erdemgil, Z.; Denizli, A.; Ersöz, A., Removal of mercury species with dithiocarbamate-anchored polymer/organosmectite composites. *Journal of hazardous materials* **2008,** *150* (3), 560-564.

44. Dias Filho, N.L.; do Carmo, D.R., Study of an organically modified clay: selective adsorption of heavy metal ions and voltammetric determination of mercury (II). *Talanta* **2006,** *68* (3), 919-927.
45. Ioannidou, O.; Zabaniotou, A., Agricultural residues as precursors for activated carbon production—A review. *Renewable and Sustainable Energy Reviews* **2007,** *11* (9), 1966-2005.
46. Namasivayam, C.; Kavitha, D., Removal of Congo Red from water by adsorption onto activated carbon prepared from coir pith, an agricultural solid waste. *Dyes and pigments* **2002,** *54* (1), 47-58.
47. Kadirvelu, K.; Thamaraiselvi, K.; Namasivayam, C., Removal of heavy metals from industrial wastewaters by adsorption onto activated carbon prepared from an agricultural solid waste. *Bioresource technology* **2001,** *76* (1), 63-65.
48. Hadi, P.; To, M.-H.; Hui, C.-W.; Lin, C.S.K.; McKay, G., Aqueous mercury adsorption by activated carbons. *Water research* **2015,** *73*, 37-55.
49. Korpiel, J.A.; Vidic, R.D., Effect of Sulfur Impregnation Method on Activated Carbon Uptake of Gas-Phase Mercury. *Environmental science & technology* **1997,** *31* (8), 2319-2325.
50. Liu, W.; Vidic, R.D.; Brown, T.D., Optimization of high temperature sulfur impregnation on activated carbon for permanent sequestration of elemental mercury vapors. *Environmental science & technology* **2000,** *34* (3), 483-488.
51. Wang, J.; Deng, B.; Wang, X.; Zheng, J., Adsorption of aqueous Hg (II) by sulfur-impregnated activated carbon. *Environmental Engineering Science* **2009,** *26* (12), 1693-1699.
52. Cai, J.H.; Jia, C.Q., Mercury removal from aqueous solution using coke-derived sulfur-impregnated activated carbons. *Industrial & engineering chemistry research* **2010,** *49* (6), 2716-2721.
53. Mohan, D.; Gupta, V.; Srivastava, S.; Chander, S., Kinetics of mercury adsorption from wastewater using activated carbon derived from fertilizer waste. *Colloids and Surfaces A: Physicochemical and Engineering Aspects* **2001,** *177* (2), 169-181.
54. Schuster, E., The behavior of mercury in the soil with special emphasis on complexation and adsorption processes-a review of the literature. *Water Air & Soil Pollution* **1991,** *56* (1), 667-680.

55. Haitzer, M.; Aiken, G.R.; Ryan, J.N., Binding of mercury (II) to aquatic humic substances: Influence of pH and source of humic substances. *Environmental science & technology* **2003,** *37* (11), 2436-2441.

56. Haitzer, M.; Aiken, G.R.; Ryan, J.N., Binding of mercury (II) to dissolved organic matter: the role of the mercury-to-DOM concentration ratio. *Environmental science & technology* **2002,** *36* (16), 3564-3570.

57. Hesterberg, D.; Chou, J.W.; Hutchison, K.J.; Sayers, D.E., Bonding of Hg (II) to reduced organic sulfur in humic acid as affected by S/Hg ratio. *Environmental science & technology* **2001,** *35* (13), 2741-2745.

58. Xia, K.; Skyllberg, U.; Bleam, W.; Bloom, P.; Nater, E.; Helmke, P., X-ray absorption spectroscopic evidence for the complexation of Hg (II) by reduced sulfur in soil humic substances. *Environmental science & technology* **1999,** *33* (2), 257-261.

59. Hurley, J.P.; Benoit, J.M.; Babiarz, C.L.; Shafer, M.M.; Andren, A.W.; Sullivan, J.R.; Hammond, R.; Webb, D.A., Influences of watershed characteristics on mercury levels in Wisconsin rivers. *Environmental science & technology* **1995,** *29* (7), 1867-1875.

60. Ravichandran, M.; Aiken, G.R.; Reddy, M.M.; Ryan, J.N., Enhanced dissolution of cinnabar (mercuric sulfide) by dissolved organic matter isolated from the Florida Everglades. *Environmental science & technology* **1998,** *32* (21), 3305-3311.

61. Szalóki, G.; Czégény, I.; Nagy, G.; Bánfalvi, G., *Removal of Heavy Metal Sulfides and Toxic Contaminants from Water*, in *Cellular Effects of Heavy Metals***2011,** Springer. p. 333-346.

62. Wilhelm, S.M.; Kirchgessner, D.A., *Mercury in Petroleum and Natural Gas--estimation of Emissions from Production, Processing, and Combustion*. **2001**: United States Environmental Protection Agency, National Risk Management Research Laboratory.

63. Fillo, J.; Evans, J., Characterization and management of produced waters from underground natural gas storage reservoirs. *American Gas Association Operation Section Proceedings* **1990,** *448459*.

64. (USEPA)., U.S.E.P.A., EPA Office of Compliance Sector Notebook Project: Profile of the Oil and Gas Extraction Industry. **2000.,** *EPA/310-R-99-006*.

65. Powell, K.J.; Brown, P.L.; Byrne, R.H.; Gajda, T.; Hefter, G.; Sjöberg, S.; Wanner, H., Chemical speciation of Hg (II) with environmental inorganic ligands. *Australian journal of chemistry* **2004,** *57* (10), 993-1000.

66. GuangLiang, L.; Yong, C.; O'Driscoll, N.; Liu, G.; Cai, Y., *Environmental chemistry and toxicology of mercury*. **2012**.

67. French, R.A.; Jacobson, A.R.; Kim, B.; Isley, S.L.; Penn, R.L.; Baveye, P.C., Influence of Ionic Strength, pH, and Cation Valence on Aggregation Kinetics of Titanium Dioxide Nanoparticles. *Environmental science & technology* **2009,** *43* (5), 1354-1359.

68. Slowey, A.J.; Rytuba, J.J.; Brown, G.E., Speciation of Mercury and Mode of Transport from Placer Gold Mine Tailings. *Environmental science & technology* **2005,** *39* (6), 1547-1554.

69. Knox, A.S.; Paller, M.H.; Milliken, C.E.; Redder, T.M.; Wolfe, J.R.; Seaman, J., Environmental impact of ongoing sources of metal contamination on remediated sediments. *Science of the Total Environment* **2016,** *563*, 108-117.

70. Knox, A.S.; Paller, M.H.; Reible, D.D.; Ma, X.; Petrisor, I.G., Sequestering agents for active caps—remediation of metals and organics. *Soil & Sediment Contamination* **2008,** *17* (5), 516-532.

71. Wang, Z.H.E., IL, US), Abraham, Robert (Bolingbrook, IL, US), *Sulfur-impregnated organoclay mercury and/or arsenic ion removal media*, **2008,** AMCOL International Corporation (Arlington Heights, IL, US): United States.

72. Gai, K.; Hoelen, T.P.; Hsu-Kim, H.; Lowry, G.V., Mobility of Four Common Mercury Species in Model and Natural Unsaturated Soils. *Environmental science & technology* **2016,** *50* (7), 3342-3351.

73. Wang, H.; Zhang, J.-R.; Zhu, J.-J., A microwave assisted heating method for the rapid synthesis of sphalrite-type mercury sulfide nanocrystals with different sizes. *Journal of Crystal Growth* **2001,** *233* (4), 829-836.

74. Cook, D.; Newcombe, G.; Sztajnbok, P., The application of powdered activated carbon for MIB and geosmin removal: predicting PAC doses in four raw waters. *Water research* **2001,** *35* (5), 1325-1333.

75. Fakhru'l-Razi, A.; Pendashteh, A.; Abdullah, L.C.; Biak, D.R.A.; Madaeni, S.S.; Abidin, Z.Z., Review of technologies for oil and gas produced water treatment. *Journal of hazardous materials* **2009,** *170* (2), 530-551.

76. Ho, Y.S.; McKay, G., Pseudo-second order model for sorption processes. *Process biochemistry* **1999,** *34* (5), 451-465.

77. Sparks, D.L., *Kinetics of soil chemical processes*. **2013**: Academic Press.

78. Ke, F.; Qiu, L.-G.; Yuan, Y.-P.; Peng, F.-M.; Jiang, X.; Xie, A.-J.; Shen, Y.-H.; Zhu, J.-F., Thiol-functionalization of metal-organic framework by a facile coordination-based postsynthetic strategy and enhanced removal of Hg 2+ from water. *Journal of hazardous materials* **2011,** *196*, 36-43.

79. Li, B.; Zhang, Y.; Ma, D.; Shi, Z.; Ma, S., Mercury nano-trap for effective and efficient removal of mercury(II) from aqueous solution. *Nat Commun* **2014,** *5*.

80. http://www.calgoncarbon.com/wp-content/uploads/product-literature/HGR_MercuryRemoval.pdf. [cited 2017 March 9].

81. Huang, C.; Blankenship, D., The removal of mercury (II) from dilute aqueous solution by activated carbon. *Water research* **1984,** *18* (1), 37-46.

82. Karatza, D.; Lancia, A.; Musmarra, D.; Zucchini, C., Study of mercury absorption and desorption on sulfur impregnated carbon. *Experimental Thermal and Fluid Science* **2000,** *21* (1-3), 150-155.

83. Dentel, S.K.; Jamrah, A.I.; Sparks, D.L., Sorption and cosorption of 1, 2, 4-trichlorobenzene and tannic acid by organo-clays. *Water research* **1998,** *32* (12), 3689-3697.

84. Louie, S.M.; Tilton, R.D.; Lowry, G.V., Critical review: impacts of macromolecular coatings on critical physicochemical processes controlling environmental fate of nanomaterials. *Environmental Science: Nano* **2016,** *3* (2), 283-310.

85. Roy, S.B.; Dzombak, D.A., Na^{+}-Ca^{2+} Exchange effects in the detachment of latex colloids deposited in glass bead porous media. *Colloids and Surfaces A: Physicochemical and Engineering Aspects* **1996,** *119* (2), 133-139.

86. Cornelissen, E.; Moreau, N.; Siegers, W.; Abrahamse, A.; Rietveld, L.; Grefte, A.; Dignum, M.; Amy, G.; Wessels, L., Selection of anionic exchange resins for removal of natural organic matter (NOM) fractions. *Water research* **2008,** *42* (1), 413-423.

87. Krishnan, K.A.; Anirudhan, T.S., Removal of mercury(II) from aqueous solutions and chlor-alkali industry effluent by steam activated and sulphurised activated carbons prepared from bagasse pith: kinetics and equilibrium studies. *Journal of hazardous materials* **2002,** *92* (2), 161-183.

88. Feng, Q.G.; Lin, Q.Y.; Gong, F.Z.; Sugita, S.; Shoya, M., Adsorption of lead and mercury by rice husk ash. *Journal of colloid and interface science* **2004,** *278* (1), 1-8.

Chapter 4. Hg Speciation in Oil-Water Separator Effluent from Produced Water Treatment and Effect of Hg Speciation on its Removal

4.1 Abstract

Produced water from oil and gas production can contain mercury (Hg) that may need to be removed to meet location-specific requirements for disposition or beneficial reuse. However, Hg speciation in produced water is not fully understood and may influence the efficacy of its removal by adsorbents. The current study used series filtration and solid phase extraction to determine the native Hg species in two produced water samples. Results suggest that Hg was primarily hydrophobic and particle-associated, with a broad nominal size range between 450 nm and 3 kDa. Three representative Hg species, dissolved inorganic Hg(II) (denoted as Hg(II)*), Hg-DOM and HgS nanoparticles, were then added to the two produced water samples to study the influence of the produced water composition on Hg speciation and hydrophobicity. Added Hg(II)* species became more hydrophobic with time in the produced water; Hg-DOM and HgS nanoparticles were unaffected by the components of produced water. The hydrophobic Hg species formed in produced from adding ionic Hg(II)* were less strong than Hg-glutathione complexes (K=10^{30}). Hg removal by adsorbents was measured for Hg(II)* amended produced water samples. Lower removal was observed for Hg in produced water as it transformed from hydrophilic to hydrophobic species. These findings suggest that chemical reaction with a filterable sorbent containing strong Hg competing functional groups (e.g., thiol), followed by filtration, can enhance the removal of Hg species from produced water.

4.2 Introduction

Produced water is water separated from reservoir fluids during crude oil and natural gas production[1]. It can contain dissolved and dispersed hydrocarbons, dissolved salts, formation material, metals and production chemicals[2]. Produced water can be disposed of through injection in a reservoir or discharge to surface waters, or it can be used for beneficial reuse[3] . The characteristics of produced water vary significantly depending on the geological formation, production operational conditions and processes[4]. Mercury as well as various other heavy metals have been detected in some produced water samples[2, 5, 6]. The variable speciation of Hg in the produced waters leads to Hg species with different physicochemical properties that may be removed with different efficiency for filters and sorbents used to treat the water.

There are many ligands present in natural waters and wastewater than can affect Hg speciation, e.g., natural organic matter (NOM), thiols, and inorganic sulfide. Similar ligands are present in produced waters[7-9]. The different Hg species have different lability, i.e., Hg^{2+} ions and weak Hg(II) complexes are more labile than HgS. Competitive ligand exchange has been used to track the slow decrease of liable Hg species) when Hg was exposed to NOM in water [10, 11]. Competing ligand exchange-solid phase extraction (CLE-SPE) can be used to evaluate the binding strength of the different Hg(II)-complexing ligands present in waste water. This is achieved by reacting the Hg in a sample with ligands of different strength. The ligand exchange changes the Hg species from hydrophilic to hydrophobic. A reverse phase SPE column is then used to separate the hydrophilic Hg species from hydrophobic Hg species[12-14]. Changes in hydrophobicity correlate with the ligand exchange. NOM became associated with Hg(II) species to form hydrophilic Hg(II) complexes, and inorganic sulfide reacted with Hg(II) species to form strongly hydrophobic Hg(II) species (i.e., mononuclear HgS)[12]. However, HgS nanoparticles

instead of mononuclear HgS could be present. The HgS particles would have charged surfaces[15, 16] and therefore be hydrophilic. Therefore, SPE analysis can be used to assess any changes in hydrophobicity of different Hg species when they are added to produced water. This is important to know because the hydrophobicity of resulting Hg species can affect Hg bioavailability,[17] and potentially its ability to be removed from water.

A variety of hydrocarbons can naturally be present in produced water, including benzene, toluene, ethylbenzene, xylenes (BTEX), naphthalene, phenanthrene, dibenzothiophene, organic acids, polycyclic aromatic hydrocarbons, and phenols[4]. The majority of hydrocarbon compounds are commonly dispersed rather than dissolved in produced water[18]. The amounts of hydrocarbon dispersed or dissolved in oil and gas produced water depends on many factors including chemical composition of the oil, pH, salinity, total dissolved solids, temperature, and oil/water ratio[2]. Produced water pH typically ranges from 3.1 to 10 in oilfield and natural gas produced water[19-21]. Salts in produced water consist mostly of sodium and chloride, with concentration as high as 300,000 mg/L[22-24]. All of these factors, ligands, pH, salinity, and ionic composition can affect Hg speciation (see Chapter 3).

With abundant organic compounds (e.g., carboxylic acids[25], benzothiophene and dibenzothiophene[26]) in produced water, a variety of Hg(II) complexes are hypothesized to be present. However, the speciation of Hg(II) species in produced water has not been studied. I hypothesize that the he differences in the hydrophobicity of the Hg species will affect the distribution of Hg in produced water, and will likely impact the choice of technologies used for Hg removal from produced water. This study assesses the Hg speciation in two produced water samples collected from oil wells. The produced water samples were collected after primary separation and additional oil water separation with proprietary chemicals. Serial filtrations and

SPE experiments were used to identify the Hg species originally present in produced water. To further study the effect of Hg speciation on its removal, additional well-defined Hg species were added to produced water and the hydrophobicity of the added Hg was determined by SPE experiments. Finally, the influence of Hg speciation on its removal from produced water was studied by batch adsorption experiments using commercial adsorbents; activated carbon and organoclay. The results of this study will contribute to the understanding of the effect of Hg speciation in produced water, and on the ability of adsorbents to remove these Hg species in produced water streams. It will help in the selection of appropriate treatment methods for Hg in produced water.

4.3 Materials and Methods

4.3.1 Produced Water Samples

Two produced water samples were procured and collected from an oil/water separator at two produced-water treatment plants (Figure C1). Both produced water samples were stored at 4°C prior to use. Because of the heterogeneity of the produced water samples, the water was vigorously mixed in the storage tank before sampling. One liter of produced water was taken from the storage tank for further experiments. This large volume was used to minimize the variance of results due to sample heterogeneity. Produced water sample 1 (PW1) had a larger amounts of solids than produced water sample 2 (PW2). Thus, additional Hg distribution experiments were conducted on PW1 to study the Hg concentration associated with these solids.

4.3.2 Hg Distributions in Produced Water

PW1 contained a visible amount of solid particles associated with yellow flocs were suspended in this sample (Figure C1). Those solids were easily separated from the water phase

by settling (Figure C2). The mercury mass distribution in water and solid phases of the produced water was measured after separating the solid fraction by sedimentation overnight. For that separation, 30 mL of the produced water sample was separated into 28 mL supernatant (water phase) and 2 mL of sediment (water phase with concentrated solids). Digestion was conducted for samples collected from both phases. Briefly, 2 mL of the produced water sample (with or without solids) was digested with 20 mL aqua regia overnight, and the digestant was diluted for total Hg analysis using a Hg analyzer (Brooks Rand) according to EPA method 1631. The total Hg concentration in the solid phase (C_{solid}) was determined by mass balance (equation 4.1),

$$C_1 * V' = C_2 * V' + C_{solid} * V * \frac{M_{solid}}{V_{total}} \qquad \text{(eqn 4.1)}$$

where, C_1 is the total Hg concentration in the water phase with concentrated flocs mixed, C_2 is the total Hg concentration in the supernatant, C_{solid} is the total Hg concentration in the solid phase (mainly flocs), V' is the volume of the water phase with concentrated flocs, V is the total volume of produced water used. M_{solid}/V_{total} is the ratio of solid mass per volume of water, and this ratio is determined as follows. A filter paper was firstly weighed, and then 2 mL of well mixed produced water was dropped onto a filter paper and total weight of filter paper with water was recorded. The filter paper was dried at 60°C overnight and then it was weighed again, the weight of solids in the 2 mL produced water is obtained by subtracting filter weight from the total weight of filter and dried solids. All experiments were conducted in either duplicate or triplicate depending on the amount of variation expected.

4.3.3 Characteristics of Produced Water

The water phase separated from concentrated solids in PW1 and PW2 were collected for characterization and further experiments. Specific conductance and pH were measured while the

water sample was mixed by magnetic stirring using conductivity and pH probes (Fisher Scientific), respectively. TOC was determined by Sievers InnovOx TOC (GE). The surface charge of the suspended solids in the produced water after sedimentation of large particles overnight was characterized by Zetasizer (Malvern, UK), respectively. Other properties in Table 4.1 were provided by our industry partner.

4.3.4 Series Filtration

A series of filtrations were performed to differentiate particulate Hg (HgS nanoparticles or Hg species associated with particles) from dissolved Hg species. Four filters with different pore sizes were used for a series of filtration. They are 0.45 µm PTFE filter (BioExcell), 0.2 µm polypropylene filter (VWR), 0.02 µm filter (Anotop, Whatman) and 3kDa filter (Amicon, Sigma-Aldrich). The potential for Hg impacts on the selected filters was tested by passing 4 mL Milli-Q water through the filter to detect the total Hg in the filtrates. No Hg was detected in the filtrates, indicating minimal potential for impacts. The potential for losses of Hg on the filters (false negative) due to sorption was also assessed by passing 4 mL of a 100 ppb Hg standard solution through the filter. The results show that <1% of total Hg was lost to the filters used. Produced water samples were vigorously shaken before analysis. The total Hg in the produced water samples was measured by digesting 1 mL of the produced water sample with 9 mL of aqua regia. The digestant was diluted and measured according to EPA method 1631. Series filtration experiments followed the order: 0.45 µm filter, 0.2 µm filter, 0.02 µm filter and finally 3kDa filter. For filtrates filtered with a 0.45 µm filter, 0.2 µm filter and 0.02 µm filter, the same aqua regia digestion procedure was used before total Hg analysis. For filtrates that were filtered with the 3kDa filter, the total Hg was directly measured using EPA method 1631 since we assumed the Hg species passing through the 3kDa filter were truly dissolved Hg species. The results of

these experiments are summarized in Table 4.2. We hypothesized that particulate and nanoparticulate Hg species would be the dominant Hg species in the PW samples.

4.3.5 Solid Phase Extraction Experiments

Solid phase extraction (SPE) was conducted to differentiate the hydrophobicity of the Hg species in produced water samples. Produced water samples were filtered with a 0.45um filter before the SPE experiments. After filtration, 64% of total Hg in PW1 and 41% of total Hg in PW2 were removed (Table 4.2), indicating that Hg species was largely associated with particles present in produced water. C18 SPE columns (Sep-Pak, Waters) were used to separate the remaining dissolved or nanoparticulate Hg species. Hydrophobic Hg species are retained in the column while hydrophilic Hg species can pass through the SPE column. 3 mL of produced water samples were slowly passed through the column by pressing the sample through the column using a syringe, and total Hg of the effluents collected were measured according to EPA 1631 methods. With the total Hg mass of produced water samples, the hydrophobic Hg species mass can be calculated by subtracting the Hg mass in the C18 column effluent from total Hg in produced water.

To test the influence of produced water components on the hydrophobicity of different Hg species, HgS nanoparticles, Hg-DOM species, and Hg(II)* species was added to both produced water samples in Teflon containers to provide a total Hg concentration of 600 ppb. The samples were mixed by magnet-stirring (~100 rpm). Hydrophobicity of the Hg species was monitored over time using C18 SPE columns. Control experiments were conducted by adding the same concentration of Hg species to Milli-Q water.

Competing ligand exchange (CLE)-SPE experiments were conducted to distinguish between weak and strong Hg(II) complexes. This method quantifies the concentration of 'weak' Hg(II)-DOM complexes and differentiates them from 'strong' Hg-sulfide nanoparticles. Strong Hg(II) complexes (e.g., mononuclear HgS) initially formed in the produced water are expected to be retained in the C18 column, and hydrophilic Hg species (e.g., Hg(II)-DOM) are expected to elute. When the competing ligands (e.g., glutathione) are added, weak Hg(II) complexes will dissociate and complex with those competing ligands. So the weakly hydrophobic Hg complex that initially existed in the sample can be transformed to a hydrophilic Hg complex. These were only done for Hg(II)*-amended produced water samples because the Hg-DOM and HgS mercury species were unaffected by the PW, as discussed later in the paper. The ligand exchange occurs after addition of a competing ligand glutathione (GSH) to the filtered sample, followed by separation of Hg(II)-ligand complexes by C_{18}- SPE as previously described[13]. Upon addition of glutathione to Hg(II) species, $HgH_2(GSH)_2^{2-}$ complexes (K=10^{30}, at pH=7.4[13, 27])can be formed and are measured as hydrophilic Hg species[13]. The produced water samples were amended with Hg(II) and allowed to react for 60 h before the CLE-SPE experiments. GSH (10 µM) was added as a competing ligand, and the PW was mixed by magnet-stirring (~100 rpm). Aliquots were sampled overtime for SPE experiments.

4.3.6 Hg Removal Experiments

The removal of Hg species in produced waters by commercial adsorbents was evaluated using batch experiments. The adsorbents included activated carbon (D/S React-A, Calgon Corporation, Pittsburgh, PA)(denoted as AC), sulfur-impregnated activated carbon (HGR, 4X10, Calgon Corporation, Pittsburgh, PA)(denoted as CSC) and organoclay (MR2, CETCO Hoffman Estates, IL)(denoted as OC). Adsorbents were ground and dry sieved, and the size fraction

between 74-150 μm was used for the adsorption experiments. Both of the produced water samples were filtered with 0.45 um filter before 600 ppb Hg(II)* was added. Hg amended produced waters were collected after one hour and 60 hours, respectively, for Hg removal experiments. The removal experiments of Hg species were conducted in Teflon beakers with magnetic stirring (~150 rpm). 10 ± 0.1 mg of adsorbent was added to 15 mL of produced water in Teflon beakers without added buffer. The pH of produced water was also measured at the end of the experiment, and no change of pH was observed. Four hour removal experiments were selected based on the typical contact time of common powdered activated carbon processes[28]. To separate unabsorbed Hg species from Hg species associated with adsorbents, the adsorbents were allowed to settle quiescently for 2 min at each sampling time point prior to analyzing the water for total Hg. The relatively large sorbent particles were readily settled in this time period. Aliquots were sampled and digested using aqua regia at different time points over four hours. Digestants were measured according to EPA method 1631 using a mercury analyzer (Brooks-Rand Model MERX).

4.4 Results and Discussion

4.4.1 Hg Distribution and Speciation in Produced Water

Large amounts of solids were observed in PW1 sample (Figure C2). Those solids were associated with flocs and were easily removed by sedimentation. The Hg concentration in the solid phase was calculated from a mass balance according to eqn 1. The result (Table C1) shows that the Hg concentration in the solid phase is 1.03 μg/g, indicating that the solids have a high affinity for the Hg species present in the produced water samples. The Hg concentration in water

phase is ~ 15 times lower at 0.07 µg/mL. However, the water phase represents 99.2 wt% of the produced water sample so the majority of the mass of Hg remained in the water phase.

Table 4.1. Properties of produced water samples.

	PW1	**PW2**
pH	7.40	7.07
Conductivity (mS/cm)	29.33	32.48
TOC (mg/L)	94.9 ± 19.8	172 ± 15
Total dissolved solids (TDS)	18.6%wt/wt	20.5%wt/wt
Zeta potential	-14.4 ± 0.4 mV	-18.3 ± 0.3 mV
Hydrogen sulfide	0-0.001%wt/wt	0-0.001%wt/wt

Table 4.2. Hg speciation determined by series filtration (particulate vs. dissolved)

	PW1 (ppb)	**PW1 (% of Hg mass in sample)**	**PW2 (ppb)**	**PW2 (% of Hg mass in sample)**
Solid phase separated by sedimentation		10%		
Before filtration	49.6 ± 7.1	90%	107.8 ± 12.7	100%
Size fraction:				
>0.45 µm	31.6 ± 3.5	57%	44.2 ± 23.4	41%
0.2 µm-0.45 µm	2.3	4%	17.6 ± 4.8	16%
0.02 µm-0.2 µm	0	0%	31.7 ± 1.1	30%
3kDa filter-0.02 µm	13.3 ± 1.6	24%	12.9 ± 0.1	12%
<3kDa filter	2.7 ± 1.6	5%	1.4 ± 0.1	1%

Hg speciation determined by serial filtration is shown in Table 4.2. The results show that PW2 has a higher Hg concentration than PW1. For PW1 over 60% of Hg can be filtered via 0.45 μm filter. The 0.2 μm filter and 0.02 μm filter did not significantly reduce the Hg concentration in the sample compared with the 0.45 μm filter. The truly dissolved Hg species determined by the 3kDa filters was about 6% of the total Hg, suggesting that majority of the Hg species in PW1 sample were particle-associated that was trapped on the 0.45 micron filter for PW1 and a 0.2 micron filter for PW2. PW2 had a wider range of particle sizes than PW1. However, the particle concentration in these filtrate samples were too low for dynamic light scattering (DLS) experiments so no particle size distribution could be determined for filtrates. In both samples, a 3kDa filter could remove nearly all of the Hg species, suggesting that both samples contained very small amounts of truly dissolved Hg species. These could include molecular Hg complexes, e.g., $HgCl_2(aq)$ or Hg-DOM with a molecular weight lower than 3kDa.

4.4.2 Hydrophobicity of Hg Species in Produced Water

Hg species can be either hydrophilic or hydrophobic in nature. Hydrophilic Hg species could include dissolved Hg(II) species with or without hydrophilic ligands (e.g., Hg(II)-DOM complexes). Hydrophobic Hg species could include mononuclear Hg species associated with hydrophobic ligands (e.g., inorganic sulfide to form HgS). However, nanoparticulate β-HgS would be charged particles that are relatively hydrophilic. However, if the β-HgS nanoparticles are over-coated with hydrocarbons they may be hydrophobic. Under sulfidic conditions at neutral pH, α-HgS can be dissolved to form $Hg(SH)_2^0$, $HgS(SH)^-$ and HgS_2^{2-}[29] depending on the total dissolved sulfide concentration[30]. If the b-HgS particles in the produced water were also reactive with these sulfur species, this could also potentially change the hydrophobicity of Hg species.

The hydrophobicity of Hg species originally present in produced water was analyzed by SPE experiments. Produced water samples were filtered through 0.45 μm filter to removal large particles before SPE experiments. According to Table 4.3, only 18% of Hg species in PW1 and about 28% of Hg species in PW2 were hydrophilic, suggesting that most native Hg species are associated with hydrophobic ligands due to the presence of hydrocarbon. Based on the series filtration results in Table 4.2, most Hg species could be removed with a 3kDa filter, so it is also possible that the particle associated Hg species in PW could be retained in the SPE column due to the size of particulate Hg species instead of hydrophobicity. However, the HgS nanoparticles (hydrodynamic diameter measured by DLS: 20 nm diameter in Milli-Q water) were not retained in the SPE column, even after they had been added to the relatively high ionic strength PW where they would be expected to aggregate into larger particles. In addition, the synthesized Hg-DOM species was found to be about 25% hydrophobic, which is significantly less than for the PW samples. This result suggests that particulate Hg species in produced water passing a 0.45 micron filter were most likely associated with hydrophobic coatings. However, it cannot be ruled out that the particles in the PW were retained in the SPE column because they were larger than the synthesized HgS particles

Table 4.3. Hg speciation determined by SPE experiments (Hydrophobic vs. hydrophilic).

	PW1 (ppb) **(filtered by 0.45 μm filter)**	**PW2 (ppb)** **(filtered by 0.45 μm filter)**
Total	18 ± 3.5	63.6 ± 23.4
Hydrophilic Hg	3.2 ± 0.3	17.7 ± 3
Hydrophobic Hg	14.8	45.9

.

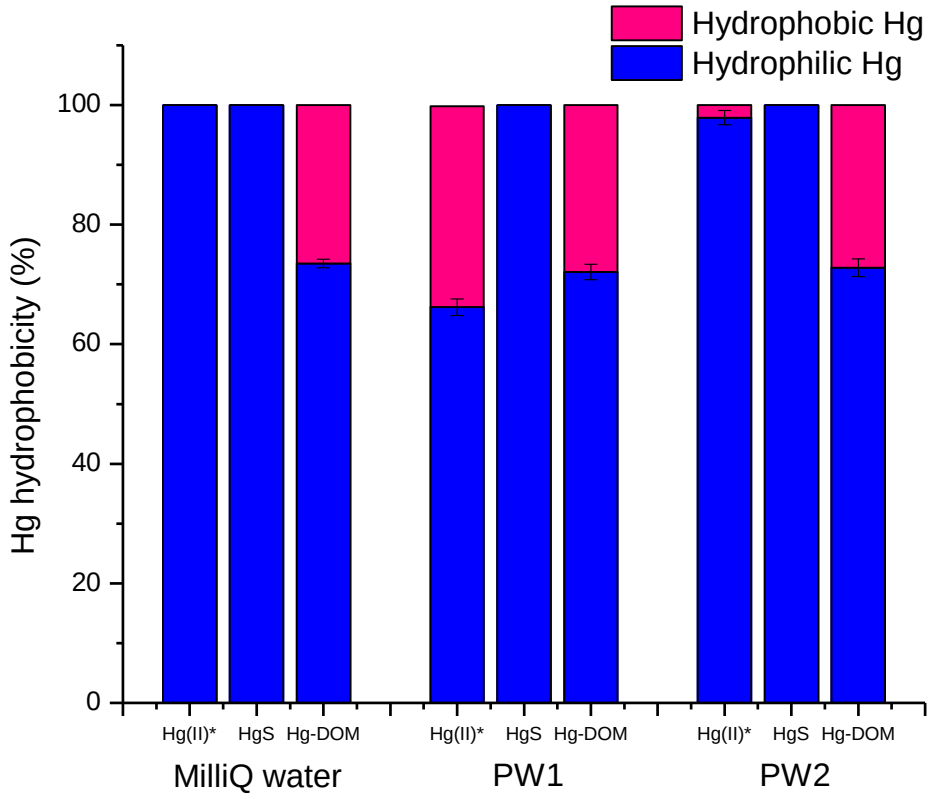

Figure 4.1. Hydrophobicity of three Hg species (Hg(II)*, HgS nanoparticles and Hg-DOM) amended in Milli-Q water, PW1 and PW2 for 60 hours.

To test the effect of the produced water composition on the hydrophobicity of selected Hg species, 600 ppb Hg(II)*, HgS nanoparticles or Hg-DOM were added to both produced water samples. They were allowed to stand for 60 h and then the hydrophobicity of the Hg species was analyzed in SPE experiments. Control experiments were conducted by using 600 ppb Hg species in Milli-Q water. Figure 4.1 shows that the hydrophobicity of HgS nanoparticles and Hg-DOM species was not altered by the ligands in the PW. This is evidenced by the absence of a change in distribution between hydrophilic and hydrophobic Hg species compared to Milli-Q water after 60

h. HgS has a high stability constant[31] and is not likely to be affected by ligands in wastewater streams[12]. Hg-DOM is usually formed via thiol and O-containing functional groups and a previous study showed that strong ligands could ligate the Hg^{2+} to form hydrophobic Hg(II) complexes[12]. Results shown in Figure 4.1 suggest the absence of strong competing ligands in produced that can sequester Hg from Hg-DOM species and change its hydrophobicity.

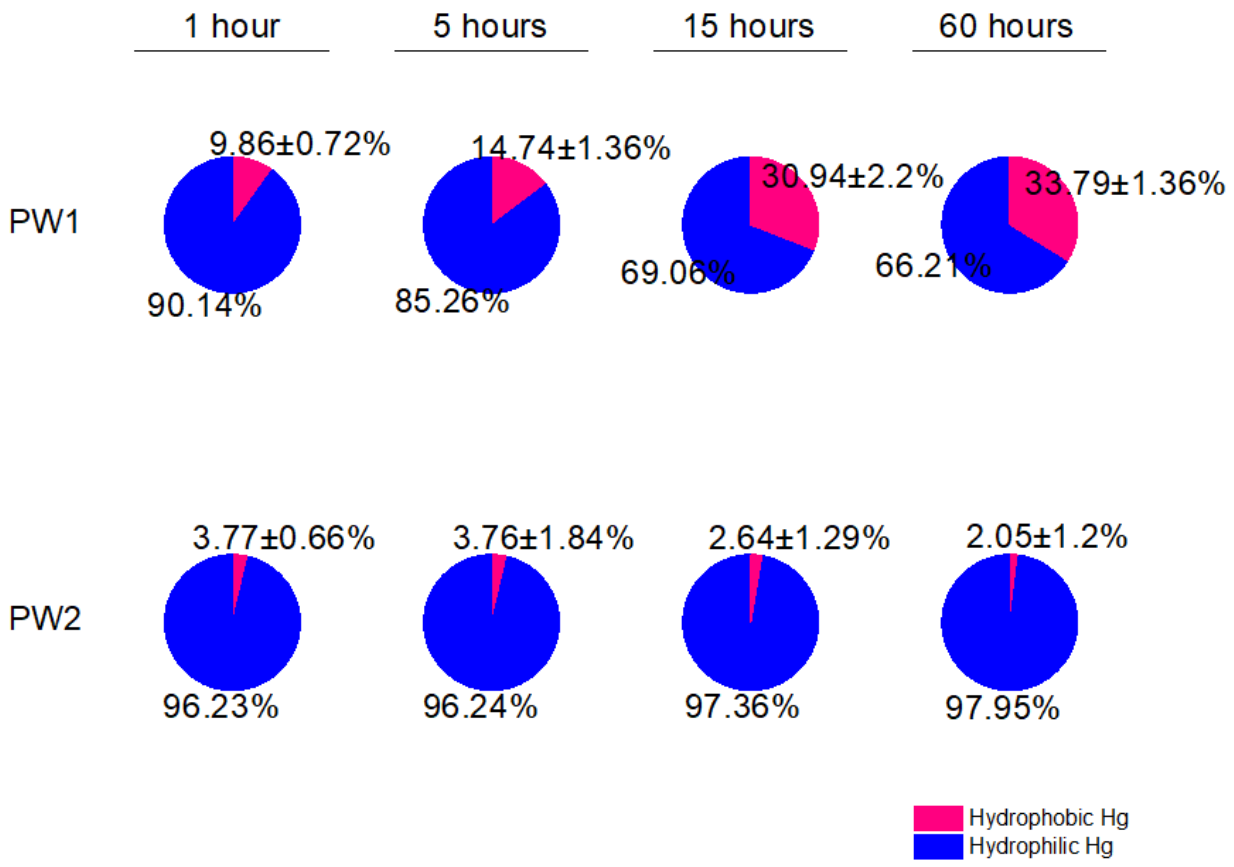

Figure 4.2. Hydrophobicity of Hg species in produced water as a function of time. 600 ppb of inorganic Hg(II)* species ($Hg(NO_3)_2$) was added. Values are averages of duplicate measurements that yielded less than 1% error between the measurements.

In contrast, an increased amount of hydrophobic Hg species was detected when Hg(II) species was amended in both PW1 and PW2 for 60 hours. This suggests that Hg binding ligands exist in produced water samples, but they are weaker ligands than DOM. Despite PW1 having fewer hydrocarbons than PW2 as measured by TOC (Table 4.1), there was a greater shift in hydrophobicity of the Hg species in PW 1 compared to PW2. This suggests that the differences in the resulting hydrophobic Hg species may be a result of the different ligands present in produced water samples.

The increase in hydrophobicity of the Hg species occurs relatively quickly (time scale of hours to 10's of hours), but not instantaneously (Figure 4.2). In PW2, about 3% of the added Hg(II) ions are rapidly converted to hydrophobic Hg species, and no additional change was observed over the course of experiment. In comparison with PW2, the amount of hydrophobic Hg species increased over time and 33% of the added Hg(II) ions became hydrophobic Hg species in PW1 after 60 h of mixing. The relatively slow complexation process suggests that the ligands in PW1 are not likely to be strong ligands such as inorganic sulfide. Slow formation of Hg-DOM complexes in water has been attributed to the presence of a number of different moieties and functional groups on NOM[11]. However, small amounts of partially oxidized sulfur species (e.g., polysulfide[32]) may exists in both produced water samples and can complex with Hg(II)* to form hydrophobic HgS_x species (e.g., HgS_5)[33].

CLE-SPE experiments were conducted to compare the strength of Hg-binding ligands in produced water (PW1) with GSH. The hydrophobicity of the Hg species present in aliquots of PW1 was measured in SPE experiments over time (Figure 4.3). Over 95% of the Hg species became hydrophilic, indicating that $HgH_2(GSH)_2^{2-}$ complexes have a higher stability constant than most of the hydrophobic Hg(II) complexes formed in produced water samples. This implies

that Hg may also be complexing weakly with some organic acids via carboxyl groups in PW1. Thus, adsorbents and flocculants containing thiol groups might be effective candidates for Hg removal from produced water with similar hydrocarbon and ligand composition as used here.

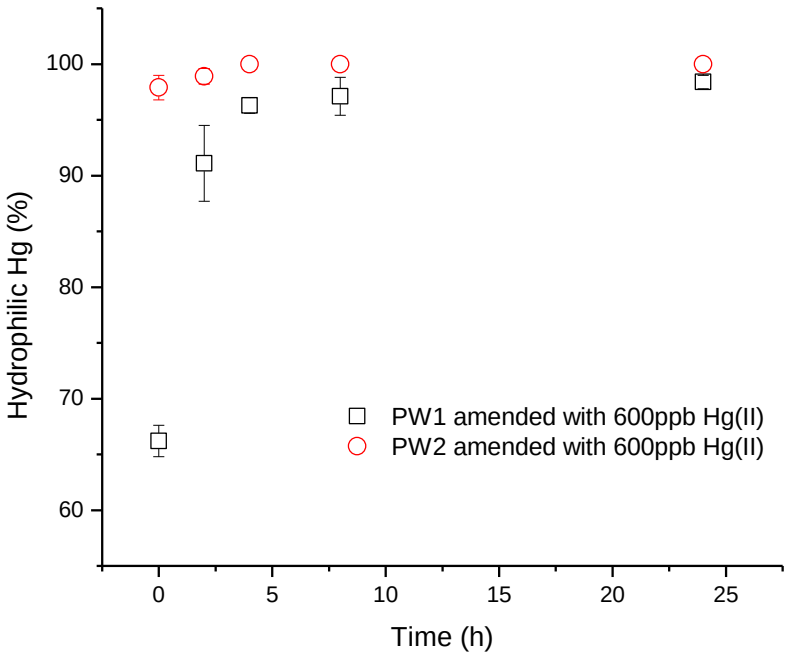

Figure 4.3. Hydrophilic Hg(II) determined after 10 µM GSH was added to produced water samples. Both produced water samples were amended by 600 ppb Hg(II) for 60 h before GSH was added. Error bars represent one standard deviation of duplicate measurements.

4.4.3 Effect of Hg Speciation on its Removal in Produced Water

The Hg speciation in PW1 changed to more hydrophobic species over time. In contrast, the Hg speciation in PW2 remained primarily hydrophilic. The removal of Hg in the produced

water samples by three adsorbents (activated carbon (AC), sulfur impregnated carbon (CSC) and organoclay (OC)) was measured after addition of 600 ppb of Hg(II) and mixing for 1 h and 60 h. Measuring the Hg removal at these two time points allow determination of the impacts of hydrophobicity of the Hg species because they are changing significantly in PW 1 over this time period, but not for PW2 (Figure 4.2). Figure 4.4a shows that over 60% of the Hg(II) species in PW1 were removed by adsorbents after 1 h. After 60 h, when a greater amount of hydrophobic Hg species were present in PW1, the removal rate and extent of the Hg species was significantly lower. In the water phase, hydrophobic compounds are expected to be more easily removed by adsorption to AC than hydrophilic ones due to the higher driving force for hydrophobic species to leave the water phase. So the results obtained here contradicted expectations. However, there are significant amounts of hydrocarbon (TOC) in produced water (Table 4.1). It is possible that the hydrophobic Hg species are trapped in hydrocarbon micro emulsions and thus more difficult to be removed. The large size of the ligated (hydrophobic) Hg species associated with micro emulsions could also reduce the accessibility of Hg species to the micropores of activated carbon samples and lead to lowered adsorption[34]. In contrast to PW1, two samples prepared by adding Hg(II) species to PW2 for 1 h and 60 h (Figure 4.4b) showed no significant change in Hg removal. This corresponds well with the lack of change in the hydrophobicity of the Hg species for PW2 (Figure 4.2). This suggests that the change in Hg speciation to more hydrophobic species may be responsible for the lower removal efficiency.

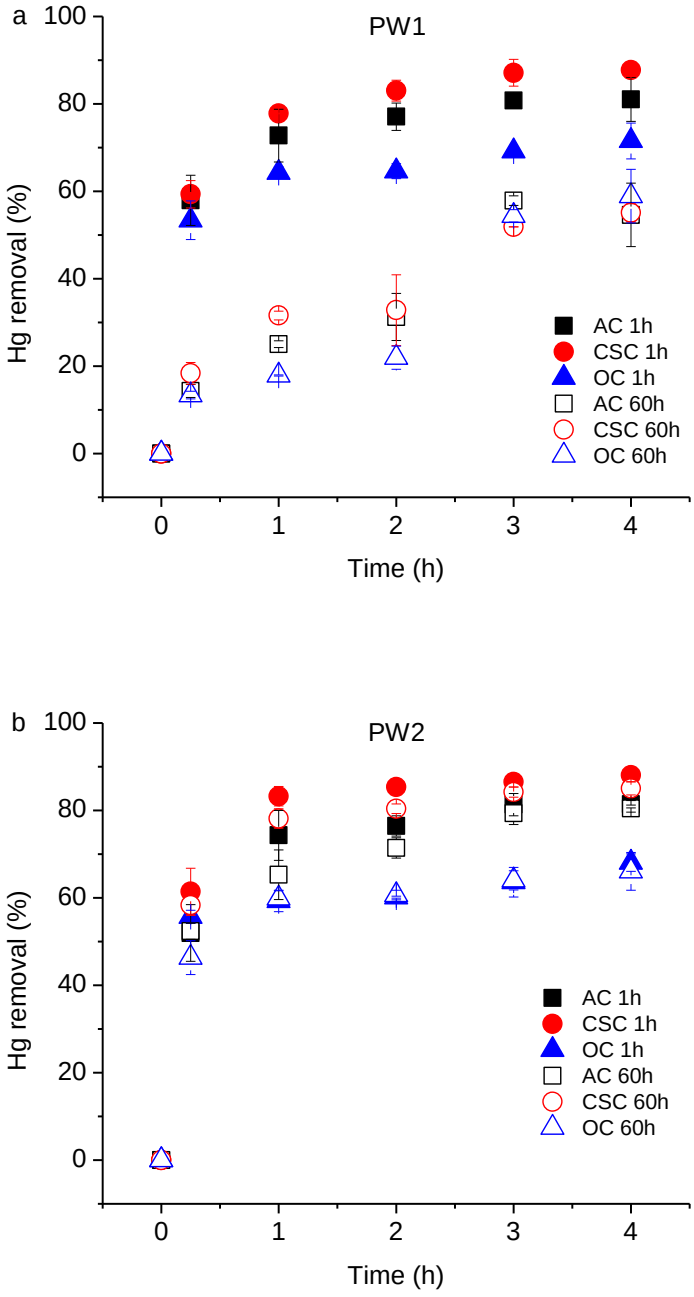

Figure 4.4. Removal of Hg species after 600 ppb Hg(II) was mixed in (a) PW1 and (b) PW2 for 1 h and 60 h, respectively.

It is also noteworthy that organoclay had a lower sorption capacity for the Hg species in produced water than AC. This is likely a result of fouling by the organic compounds present in the PW samples. A similar trend was found when natural organic matter was present in water as shown in Chapter 3. Organoclays are also known for hydrocarbon removal, and the adsorption capacity of organoclay for hydrophobic organic compounds is affected by the way organoclay is produced[35]. Long-chain organoclays are reported to have better sorption performance for highly hydrophobic materials than short-chain organoclays[36]. It may be possible to tune the surfaces of OC for optimal performance in both Hg and hydrocarbon removal from produced water, but this was not assessed here.

4.5 Conclusions and Implications

While the majority of the Hg mass is present in water phase for the produced water samples studied here, Hg can be highly concentrated in a small amount of large solids present in those samples. In the water phase, Hg species are primarily associated with naturally occurring negatively charged particles, indicating that 43% to 59% of the Hg can be removed by removing particles greater than 0.45 microns from produced water. The size distribution of particle-associated Hg passing the 0.45 micron filter was PW-dependent. Less than 5% of the Hg was truly dissolved, i.e., could pass a 3kDa filter.

The native Hg species in produced water samples were mainly hydrophobic, suggesting an association with hydrophilic hydrocarbon components. The added HgS nanoparticles and Hg-DOM remained hydrophilic in produced waters, suggesting that the native hydrophobic Hg species in produced waters were different from our model Hg species. The formation of hydrophobic Hg species from Hg(II) added to PW1 but not in PW2 suggests that the

hydrocarbon composition in produced water sample impacts the speciation of dissolved inorganic Hg(II) species.

The relatively slow complexation process determined in the time dependent SPE experiments suggested that the ligands in PW1 were not likely to be strong ligands such as inorganic sulfide. And CLE-SPE experiments corroborated this, showing that the Hg species were ligated less strongly than in $HgH_2(GSH)_2^{2-}$ complexes ($K_{GSH}=10^{30}$). The results indicate that adding inorganic sulfide can potentially transform dissolved Hg(II) species present in produced water into HgS particulate species ($K_{HgS}=10^{52}$), which would remain hydrophilic and could be removed by filtration if they become large enough. These results also suggest, it would be possible to extract dissolved Hg species from produced water by materials with thiolated surfaces.

The change in Hg speciation to more hydrophobic species decreased the removal efficiency by the adsorbents used here. Activated carbon provided better removal than organoclay in PW, likely due to fouling of the OC from the hydrocarbons present in the samples. This study suggests that filtration, followed by chemical treatment to convert hydrophobic Hg species into hydrophilic species to improve the efficacy of an adsorbent-based polishing step, and could be a more effective way to reduce the Hg concentration to meet the local treatment goals. Alternatively, filtration aids with a high affinity for hydrophobic Hg species could potentially work well.

4.6 References

1. Veil, J.A.; Puder, M.G.; Elcock, D.; Redweik Jr, R.J., *A white paper describing produced water from production of crude oil, natural gas, and coal bed methane*, **2004**, Argonne National Lab., IL (US).

2. Hansen, B.; Davies, S., Review of potential technologies for the removal of dissolved components from produced water. *Chemical engineering research & design* **1994,** *72* (2), 176-188.

3. Burant, A.; Lowry, G.V.; Karamalidis, A.K., Measurement and Modeling of Setschenow Constants for Selected Hydrophilic Compounds in NaCl and $CaCl_2$ Simulated Carbon Storage Brines. *Accounts of Chemical Research* **2017**.

4. Fakhru'l-Razi, A.; Pendashteh, A.; Abdullah, L.C.; Biak, D.R.A.; Madaeni, S.S.; Abidin, Z.Z., Review of technologies for oil and gas produced water treatment. *Journal of hazardous materials* **2009,** *170* (2), 530-551.

5. Gallup, D.L.; Strong, J.B. *Removal of mercury and arsenic from produced water*. in *13th Annual International Petroleum Environmental Conference*. 2006.

6. Utvik, T.I.R., Chemical characterisation of produced water from four offshore oil production platforms in the North Sea. *Chemosphere* **1999,** *39* (15), 2593-2606.

7. Jiang, Y.; Qi, H.; Zhang, X.M.; Chen, G.X., Inorganic impurity removal from waste oil and wash-down water by Acinetobacter johnsonii. *Journal of hazardous materials* **2012,** *239*, 289-293.

8. Witter, A.E.; Jones, A.D., Comparison of methods for inorganic sulfur speciation in a petroleum production effluent. *Environmental Toxicology and Chemistry* **1998,** *17* (11), 2176-2184.

9. Fatema, J.; Bhattacharjee, S.; Pernitsky, D.; Maiti, A., Study of the Aggregation Behavior of Silica and Dissolved Organic Matter in Oil Sands Produced Water Using Taguchi Experimental Design. *Energy & Fuels* **2015,** *29* (11), 7465-7473.

10. Miller, C.L.; Liang, L.; Gu, B., Competitive ligand exchange reveals time dependant changes in the reactivity of Hg–dissolved organic matter complexes. *Environmental Chemistry* **2012,** *9* (6), 495-501.

11. Miller, C.L.; Southworth, G.; Brooks, S.; Liang, L.; Gu, B., Kinetic Controls on the Complexation between Mercury and Dissolved Organic Matter in a Contaminated Environment. *Environmental science & technology* **2009,** *43* (22), 8548-8553.

12. Hsu-Kim, H.; Sedlak, D.L., Similarities between inorganic sulfide and the strong Hg (II)-complexing ligands in municipal wastewater effluent. *Environmental science & technology* **2005,** *39* (11), 4035-4041.

13. Hsu, H.; Sedlak, D.L., Strong Hg (II) complexation in municipal wastewater effluent and surface waters. *Environmental science & technology* **2003,** *37* (12), 2743-2749.
14. Black, F.J.; Bruland, K.W.; Flegal, A.R., Competing ligand exchange-solid phase extraction method for the determination of the complexation of dissolved inorganic mercury (II) in natural waters. *Analytica chimica acta* **2007,** *598* (2), 318-333.
15. Gai, K.; Hoelen, T.P.; Hsu-Kim, H.; Lowry, G.V., Mobility of Four Common Mercury Species in Model and Natural Unsaturated Soils. *Environmental science & technology* **2016,** *50* (7), 3342-3351.
16. Deonarine, A.; Hsu-Kim, H., Precipitation of mercuric sulfide nanoparticles in NOM-containing water: Implications for the natural environment. *Environmental science & technology* **2009,** *43* (7), 2368-2373.
17. Chiasson-Gould, S.A.; Blais, J.M.; Poulain, A.J., Dissolved Organic Matter Kinetically Controls Mercury Bioavailability to Bacteria. *Environmental science & technology* **2014,** *48* (6), 3153-3161.
18. Ekins, P.; Vanner, R.; Firebrace, J., Zero emissions of oil in water from offshore oil and gas installations: economic and environmental implications. *Journal of Cleaner Production* **2007,** *15* (13), 1302-1315.
19. Johnson, B.M.; Kanagy, L.E.; Rodgers, J.H.; Castle, J.W., Chemical, physical, and risk characterization of natural gas storage produced waters. *Water, Air, and Soil Pollution* **2008,** *191* (1-4), 33-54.
20. Tibbetts, P.; Buchanan, I.; Gawel, L.; Large, R., *A comprehensive determination of produced water composition*, in *Produced Water***1992,** Springer. p. 97-112.
21. Fillo, J.; Evans, J., Characterization and management of produced waters from underground natural gas storage reservoirs. *American Gas Association Operation Section Proceedings* **1990,** *448459*.
22. Neff, J.M., *Bioaccumulation in marine organisms: effect of contaminants from oil well produced water*. **2002**: Elsevier.
23. Jacobs, R.; Grant, R.; Kwant, J.; Marquenie, J.; Mentzer, E., *The composition of produced water from Shell operated oil and gas production in the North Sea*, in *Produced Water***1992**, Springer. p. 13-21.

24. Pitre, R. *Produced water discharges into marine ecosystems*. in *Offshore Technology Conference*. **1984.** Offshore Technology Conference.
25. Bostick, D.T., *Characterization of soluble organics in produced water*, **2002**, ORNL Oak Ridge National Laboratory (US).
26. Durell, G.; Røe Utvik, T.; Johnsen, S.; Frost, T.; Neff, J., Oil well produced water discharges to the North Sea. Part I: Comparison of deployed mussels (Mytilus edulis), semi-permeable membrane devices, and the DREAM model predictions to estimate the dispersion of polycyclic aromatic hydrocarbons. *Marine Environmental Research* **2006,** *62* (3), 194-223.
27. Oram, P.D.; Fang, X.; Fernando, Q.; Letkeman, P.; Letkeman, D., The formation constants of mercury (II)− glutathione complexes. *Chemical research in toxicology* **1996,** *9* (4), 709-712.
28. Cook, D.; Newcombe, G.; Sztajnbok, P., The application of powdered activated carbon for MIB and geosmin removal: predicting PAC doses in four raw waters. *Water research* **2001,** *35* (5), 1325-1333.
29. Benoit, J.M.; Gilmour, C.C.; Mason, R.P.; Heyes, A., Sulfide controls on mercury speciation and bioavailability to methylating bacteria in sediment pore waters. *Environmental science & technology* **1999,** *33* (6), 951-957.
30. Paquette, K.E.; Helz, G.R., Inorganic speciation of mercury in sulfidic waters: the importance of zero-valent sulfur. *Environmental science & technology* **1997,** *31* (7), 2148-2153.
31. Benjamin, M.M., *Water chemistry*. **2014**: Waveland Press.
32. Luther III, G.W.; Glazer, B.T.; Hohmann, L.; Popp, J.I.; Taillefert, M.; Rozan, T.F.; Brendel, P.J.; Theberge, S.M.; Nuzzio, D.B., Sulfur speciation monitored in situ with solid state gold amalgam voltammetric microelectrodes: polysulfides as a special case in sediments, microbial mats and hydrothermal vent watersPresented at the Whistler 2000 Speciation Symposium, Whistler Resort, BC, Canada, June 25–July 1, 2000. Electronic Supplementary Information available. See http://www. rsc. org/suppdata/em/b0/b006499h. *Journal of Environmental Monitoring* **2001,** *3* (1), 61-66.
33. Jay, J.A.; Morel, F.M.M.; Hemond, H.F., Mercury Speciation in the Presence of Polysulfides. *Environmental science & technology* **2000,** *34* (11), 2196-2200.

34. Dias, J.M.; Alvim-Ferraz, M.C.M.; Almeida, M.F.; Rivera-Utrilla, J.; Sánchez-Polo, M., Waste materials for activated carbon preparation and its use in aqueous-phase treatment: A review. *Journal of environmental management* **2007,** *85* (4), 833-846.

35. Lee, S.Y.; Kim, S.J.; Chung, S.Y.; Jeong, C.H., Sorption of hydrophobic organic compounds onto organoclays. *Chemosphere* **2004,** *55* (5), 781-785.

36. Groisman, L.; Rav-Acha, C.; Gerstl, Z.; Mingelgrin, U., Sorption of organic compounds of varying hydrophobicities from water and industrial wastewater by long- and short-chain organoclays. *Applied Clay Science* **2004,** *24* (3), 159-166.

Chapter 5. Conclusions and Recommendations for Future Research

5.1 Summary

This dissertation focuses on the impact of mercury (Hg) speciation on its transport in porous media and on its removal from wastewater streams. The transport of Hg species in porous media was studied by conducting column experiments using four model inorganic mercury species: Hg(II), Hg-DOM, HgS nanoparticles and Hg(0). Porous media composition and solution chemistry were varied to simulate rainfall and landfill leachate conditions. Removal of inorganic Hg(II), Hg-DOM, and HgS nanoparticles was studied in batch experiments using commercially available activated carbon and organoclay sorbents. The effects of dissolved organic matter, ionic strength and cation type on Hg removal were also tested. Hg speciation in produced water samples were determined by serial filtration and solid phase extraction experiments. The effect of Hg hydrophobicity on its removal from produced water was determined in batch experiments using activated carbon and organoclay as adsorbents to remove Hg from produced water.

The specific objectives of the research were to

- Evaluate the impact of Hg speciation, porous media properties and water chemistry on the transport of Hg species in an unsaturated porous medium,
- Evaluate the impact of Hg speciation, adsorbent type and water chemistry on the removal of Hg species from water,
- Determine the Hg speciation in produced water and assess the influence of Hg speciation on its removal from produced water.

5.2 Conclusions

Conclusions in Chapter 2: Mobility of Four Common Mercury Species in Model and Natural Unsaturated Soils

- *Hg speciation affects its transport in unsaturated porous media.*

The transport of four model Hg species in unsaturated porous media was studied using column experiments. Mercury model compounds included inorganic Hg(II), Hg-DOM, HgS nanoparticles and fine droplets of Hg(0). Among the selected Hg species, the Hg(II)-DOM species had the highest mobility among the four Hg species evaluated, and HgS particles (~230 nm hydrodynamic diameter) had the lowest mobility, for all soil and influent conditions tested. The breakthrough behavior and eluted mass for Hg(0) was distinct from the other Hg species, which may suggest that a slow but continual transport of separate phase liquid elemental Hg(0) is possible in unsaturated porous media, or that dissolved elemental Hg(0) is being mobilized to some degree.

- *DOM in influent solutions facilitates the transport of Hg species in unsaturated porous media.*

The deposition rate constant, $k_{d,mobile}$ of each Hg species was lower in simulated leachate (high ionic strength and high DOM) compared to the simulated rainfall for all tested porous media, indicating that the introduction of DOM facilitated the transport of Hg species in porous media despite the higher ionic strength.

- *Small fines in porous media significantly decrease the mobility of Hg species in unsaturated porous media.*

In a model silica sand medium, the addition of 2 wt% clay particles to sand greatly retarded the transport of all Hg species, especially under simulated rainfall. The clay particles in the medium are highly effective at retarding the transport of particulate Hg species, but less effective on dissolved Hg species, especially with high DOM in the column influent.

- *Higher TOC content in the porous medium (soil organic matter) decreases the transport of Hg species.*

In a high TOC content soil under simulated rainwater, only Hg-DOM showed detectable breakthrough after 11 pore volumes. The results indicate that particulate Hg species (e.g., Hg(0) and HgS nanoparticles) had limited transport in this organic rich porous medium using simulated rainwater. It also suggests that Hg(II)* can become strongly associated with particle-associated organic matter in this soil matrix. Breakthrough of all Hg species was lower than for a low TOC content soil.

Conclusions in Chapter 3: Impact of Hg Speciation on its Removal from Water by Activated Carbon and Organoclay

- *Hg speciation affected its removal from water by adsorbents. However, water quality parameters, including the presence of DOM, cation type, and ionic strength, also affected removal rates.*

The presence of DOM reduced the removal of Hg(II)* and HgS nanoparticles. Increasing the ionic strength decreased the removal of Hg(II)* species. In contrast, no apparent effect of water quality parameters on the removal of Hg-DOM for the tested conditions was observed. This indicates that using dissolved Hg(II) as a "surrogate" species for assessing removal

efficiency may not provide reliable estimates. The magnitude of the reliability will depend on both the Hg species and the solution conditions.

- *Adsorbent type affects the removal of Hg species from water by adsorbents.*

We compared the efficacy of sulfur-impregnated organoclay (OC) with activated carbon and sulfidized activated carbon to remove Hg from water. Organoclay had higher surface reactivity, and could remove Hg species better than activated carbon or sulfur impregnated activated carbon per unit surface area. However, OC was more susceptible to fouling by NOM in water. Hg X-ray absorption spectroscopy results also indicate that the surface of the organoclay is highly reactive with the adsorbed Hg species, resulting in the formation of a β-HgS phase for adsorbed Hg-DOM. Activated carbon did not result in a similar change in Hg speciation for adsorbed Hg-DOM. Despite a prior report that carbon disulfide treated activated carbon enhanced aqueous mercury adsorption, the differences between activated carbon and sulfur-impregnated activated carbon samples used in this study were not significant.

Conclusions in Chapter 4: Hg Speciation in Oil-Water Separator Effluent from Produced Water Treatment and Effect of Hg Speciation on its Removal

The Hg speciation was determined in two different PW samples (PW1 and PW2) using both serial filtration and solid phase extraction methods. The removal of amended Hg(II) by adsorbents was measured to evaluate the effect of Hg speciation on its removal.

- *Hg species in produced water were highly concentrated in solids (floc) present in produced water. However, most Hg was associated with the aqueous phase.*

The distribution of Hg between the phases present in produced water was determined. The Hg concentration in the solid phase is 1.03 μg/g, while the Hg concentration in water phase is ~15 times lower at 0.07 μg/mL. However, the water phase represents 99.2 wt% of the produced water sample so the majority of the mass of Hg is present in the water phase.

- *Hg species in produced water was primarily particulate Hg.*

The speciation of the Hg in produced water was determined. The majority (43% to 59%) of the Hg species in the aqueous phase of PW was either particulate or associated with particles naturally occurring in PW. Five percent or less of the Hg was able to pass through a 3 kDa filter, suggesting that little Hg was not complexed with DOM having a MW>3kDa or associated with solids.

- *Hg species in produced water was mainly hydrophobic Hg.*

Less than a quarter of the native Hg species in PW were hydrophilic, suggesting an association of the Hg with hydrophobic moieties. The native Hg in PW is not likely HgS NPs or Hg-DOM species given that these species are primarily hydrophilic. Moreover, these species were unchanged over time by the PW composition when added to PW at 600 ppb.

- *The ligands present in produced water can complex with Hg(II) to form relatively weak hydrophobic Hg species.*

When 600 ppb hydrophilic Hg(II) species was amended in produced water samples, 33% of the added Hg(II) ions became hydrophobic Hg species in PW1 after 60 h of mixing. The relatively slow complexation process suggests that the ligands in PW1 are not likely to be strong ligands such as inorganic sulfide. When a competing ligand, glutathione, was added to

the Hg(II)-amended produced water, over 95% of the Hg species became hydrophilic, indicating that $HgH_2(GSH)_2^{2-}$ complexes have a higher stability constant than most of the hydrophobic Hg(II) complexes formed in produced water samples. This implies that Hg may also be complexing weakly with some organic acids via carboxyl groups in PW1.

- *The change in Hg speciation to more hydrophobic Hg species decreased its removal efficiency by the adsorbents used here.*

The Hg(II) added to the two different PW samples behaved differently, and this impacted its removal from water by sorbents. In PW1, added Hg(II) slowly became more hydrophobic over time. This increase in hydrophobicity corresponded with a decreased in the ability to removed Hg(II) by adsorption to OC and activated carbon. In contrast, the added Hg(II) in PW2 remained hydrophilic and there was no change in its removal efficiency over time. This suggests that the change in Hg speciation to more hydrophobic species may be responsible for the lower removal efficiency. This study suggests that filtration, followed by chemical treatment to convert hydrophobic Hg species into hydrophilic species to improve the efficacy of an adsorbent-based polishing step, may provide more effective Hg removal than trying to treat hydrophobic Hg species.

- *Activated carbon is a better adsorbent than OC in PW due to fouling of the OC by organics in the PW.*

Organoclay had a lower sorption capacity for the Hg species in produced water than ACs. This is consistent with the results in chapter 3 indicating that the presence of DOM significantly decreased the removal of Hg species by organoclay. This is likely a result of fouling by the organic compounds present in the PW samples since organoclay also has high

affinity for organic compounds. It may be possible to tune the surfaces of OC for optimal performance in both Hg and hydrocarbon removal from produced water, but this was not assessed in the current study.

The novel and most important findings in this dissertation are that: 1) Hg speciation has a significant impact on its transport in unsaturated porous media. Hg-DOM transport in well sorted sandy media with high dissolved organic matter flow through presents the greatest potential risk of vertical migration of Hg. This study suggests that the speciation of Hg in a soil or sediment and the permeability and organic content of the soil should be considered in assessing the potential for migration in an unsaturated porous medium. 2) The Hg speciation (particulate Hg vs. dissolved Hg species, dissolved Hg compound vs. dissolved Hg-DOM complexes, and hydrophobic Hg vs. hydrophilic Hg) influences its removal from water dependent on the environmental factors (e.g., presence of organic matter, ionic strength) and types of adsorbent used. Both Hg speciation and the water quality parameters (organic ligands, ionic strength, and ionic composition) should be considered when designing sorbent based emission controls to meet Hg removal targets.

5.3 Recommendations for Future Research

The results from this research show that Hg speciation impacts transport in porous media and the efficacy of Hg removal by adsorbents. To further understand the effects of Hg speciation on its environmental behavior, future research needs are suggested.

Long term transport experiments are needed to test the mobility and potential transformation of Hg species. As shown in this study, Hg-DOM has the highest mobility under tested unsaturated porous media conditions while HgS nanoparticles have limited transport under

the same conditions. At the same time, a slow but continuous transport was observed for Hg(0) species under the experimental conditions tested. This suggests that in situ transformations of the Hg species (e.g., sulfidation to form β-HgS or complexation with organic matter) after its introduction to the environment may continually change the mobility of the Hg over time. Therefore, experiments to understand the types of transformations, the conditions that lead to those transformations, and the rates of transformation are needed to better understand (or model) the transport and fate of Hg, and to better assess the risk of Hg species in unsaturated porous media.

There are other important parameters (e.g., saturation condition, pH, and Eh) that may affect the transport of Hg species in similar porous media. Research is needed to test the influence of those parameters on the transport of Hg species. The current study suggested that the air-water interface in the unsaturated porous media may capture Hg species. However, the exact flow conditions in unsaturated columns are not clear. Further Hg transport experiments using customized flow chambers to control saturation degree and flow paths can help us understand the role of the soil-air and air-water interfaces on the transport of Hg species under unsaturated porous media. pH will affect the dissolved Hg speciation and greatly impact the surface charge and therefore the stability of HgS nanoparticles under porous media. Under extreme pH conditions, HgS nanoparticles may become well dispersed and demonstrate a high mobility in porous media. The effects of Eh on Hg speciation and transport should also be assessed.

This study showed that both Hg speciation and the water quality parameters (NOM content, ionic strength, and ionic composition) should be considered when designing sorbent based emission controls to meet Hg removal targets. In the field, flow-through treatment systems are commonly used, and the mixing conditions in flow through systems are different from batch

experiments. Thus, experiments conducted in flow-through systems with adsorbents as filtration materials are needed to optimize the operation conditions (e.g., flow rate).

Studies about the toxicity and bioavailability of Hg species in the soil and Hg-associated wastes are also needed to further understand their environmental risk. Hg X-ray absorption spectroscopy shows that Hg-DOM was transformed to β-HgS when sulfur-impregnated organoclays were used as adsorbents. But no transformation was observed for Hg-DOM on sulfur-impregnated activated carbon. The transformation of Hg species may significantly affect its toxicity and bioavailability when those Hg-associated solids are disposed, but this needs to be determined experimentally

This study showed that the hydrocarbon composition of produced water can impact the Hg speciation over time, and such Hg speciation changes determine the efficacy of Hg removal from produced water using adsorbent-based technology. Studies are needed to identify the competing ligands for Hg to help us understand the partitioning of Hg species in produced water phases (water phase vs. micro emulsion). This study also showed that Hg was highly concentrated in solid phase (floc), which likely involves microbial activity. Research to better understand Hg bioavailability in produced water are also recommended to explore potential biological techniques for Hg removal from produced water, or for transformation of those species to other forms.

Appendix A: Supplementary Information for Chapter 2

A1. Tracer Test Analysis

The hydraulic conductivity of the column medium was calculated using the equation A1,

$$K = \frac{VL}{Ath} \quad \text{(eqn A1)}$$

K = Hydraulic conductivity at 20°C (cm/s)

V = Volume of discharge (cm^3)

L = Length of column (cm)

A = Cross section area (cm^2)

t = Time of discharge (s)

h = Hydraulic head difference (cm)

Given the flow rate of 0.37 mL/min and effective porosity determined by tracer test results (Figure A1), the average linear velocity of water was calculated using equation S2,

$$v_x = \frac{Q}{n_e A} \quad \text{(eqn A2)}$$

v_x = Average linear velocity (cm/s)

Q = Flow rate (mL/min)

A = Cross section area (cm^2)

n_e = Effective porosity

Given L, v_x, C/C_0 and t, the coefficient of hydrodynamic dispersion can be determined by least squares fitting of the tracer test breakthrough data using equation S3.

$$C = \frac{C_0}{2}\left[erfc\left(\frac{L-v_x t}{2\sqrt{D_L t}}\right) + \exp\left(\frac{v_x L}{D_L}\right) erfc\left(\frac{L+v_x t}{2\sqrt{D_L t}}\right)\right] \quad \text{(eqn A3)}$$

C = Solute concentration at time *t*

C_0 = Initial solute concentration

L = Transport distance (cm)

D_L = Coefficient of hydrodynamic dispersion

erfc = Complementary error function

A2. Hg(II)* Speciation Analysis

Hg(II)* concentration was calculated by assuming the added Hg was well mixed in the top layer of the column (eqn A4).

$$C_{Hg(II)} = \frac{M_{(Hg(II)doped)}}{V_{pore\ volume\ in\ the\ top\ layer\ of\ the\ column}} \quad \text{(eqn A4)}$$

The Hg speciation was determined using Visual MINTEQ by assuming equilibrium conditions were reached. The Hg-DOM species was calculated by assuming the reaction of below:

Hg(II)*+DOM=Hg-DOM log K=23.4L/kg[1]

Table A1. Column experiment parameters and calculated deposition rates.

Column media	Influent solution	Hg species	$\frac{q}{N_0}\int_0^{t_f} C(t)dt^{a}$	$k_{d,overall}$ (min^{-1})	$k_{d,mobile}$ (min^{-1})
#50sand	5 mM NaCl	Hg(II)*	39%	0.0207	0.0165 ±0.0014
		Hg-DOM	25%	0.0298	0.0249 ±0.003
		Hg(0)	26%	0.0295	0.0158 ±0.0005
		HgS	0.4%	0.1406	0.0837 ±0.0036
	200 mM NaCl, 147 mg C/L humic acid	Hg(II)*	96%	0.0009	0.0007 ±0.0001
		Hg-DOM	88%	0.0029	0.0022 ±0.0001
		Hg(0)	94%	0.0014	0.0003 ±0
		HgS	12%	0.0479	0.0298 ±.002
#50sand+clay	5 mM NaCl	Hg(II)*	6%	0.0611	0.0377 ±0.0083
		Hg-DOM	14%	0.0414	0.0345 ±0.0013
		Hg(0)	0.04%	0.1630	0.0825 ±0.01
		HgS	0%	N/A	0.0925 ±0.0119
	200 mM NaCl, 147 mg C/L humic acid	Hg(II)*	91%	0.0021	0.0023 ±0.0001
		Hg-DOM	81%	0.0054	0.0035 ±0.001
		Hg(0)	22%	0.0327	0.018 ±0.0013
		HgS	5%	0.0656	0.0395 ±0.0027
Low TOC soil	5 mM NaCl	Hg(II)*	2%	0.0826	0.0742 ±0.0037
		Hg-DOM	69%	0.0078	0.0056 ±0.0001
		Hg(0)	42%	0.0183	0.0133 ±0.005
		HgS	5%	0.0632	0.0335 ±0.0034
	200 mM NaCl, 147 mg C/L humic acid	Hg(II)*	45%	0.0169	0.0111 ±0.0008
		Hg-DOM	78%	0.0052	0.0035 ±0.0001
		Hg(0)	52%	0.0138	0.0088 ±0.0001
		HgS	11%	0.0466	0.0279 ±0.0007

Table A1 (continued). Column experiment parameters and calculated deposition rates.

Column media	Influent solution	Hg species	$\frac{q}{N_0}\int_0^{t_f} C(t)dt$ [a]	$k_{d,overall}$ (min^{-1})	$k_{d,mobile}$ (min^{-1})
High TOC soil	5mM NaCl	Hg(II)*	0%	N/A	0.0652 ±.0652
		Hg-DOM	5%	0.0632	0.0382 ±.0382
		Hg(0)	0%	N/A	0.0575 ±.0575
		HgS	0%	N/A	0.0526 ±.0526
	200mM NaCl, 147 mg C/L humic acid	Hg(II)*	13%	0.0431	0.0357 ±0.0031
		Hg-DOM	20%	0.0340	0.0261 ±0.0027
		Hg(0)	11%	0.0466	0.0296 ±0.0032
		HgS	2%	0.0826	0.0431 ±0.067

[a] $\frac{q}{N_0}\int_0^{t_f} C(t)dt$ is the percentage of total Hg mass that can break through the column until no detectable Hg can be found in the following effluents;

Table A2. Calculated filtration length needed for removing each Hg species to different targets.

Column media	Influent solution	Hg species	Filter length needed (m)			
			99% removal	99.9% removal	99.99% removal	99.999% removal
#50sand	5 mM NaCl	Hg(II)*	0.55±0.04	0.83±0.07	1.11±0.09	1.38±0.11
		Hg-DOM	0.36±0	0.53±0.01	0.71±0.01	0.89±0.01
		Hg(0)	0.57±0.02	0.86±0.07	1.15±0.04	1.43±0.05
		HgS	0.13±0.01	0.19±0.01	0.25±0.01	0.32±0.01
	200 mM NaCl, 147 mg C/L humic acid	Hg(II)*	12.81±1.2	19.22±1.81	25.63±2.41	32.03±3.01
		Hg-DOM	4.18±0.24	6.27±0.35	8.36±0.47	10.44±0.59
		Hg(0)	28.26±0.74	42.39±1.1	56.52±1.47	70.66±1.84
		HgS	0.32±0.02	0.47±0.03	0.63±0.04	0.79±0.05
#50sand+clay	5 mM NaCl	Hg(II)*	0.24±0.05	0.37±0.08	0.49±0.11	0.61±0.14
		Hg-DOM	0.25±0.01	0.38±0.01	0.51±0.02	0.63±0.02
		Hg(0)	0.1±0.01	0.16±0.02	0.21±0.03	0.26±0.03
		HgS	0.1±0.01	0.15±0.02	0.2±0.03	0.25±0.03
	200 mM NaCl, 147 mg C/L humic acid	Hg(II)*	3.94±0.24	5.91±0.36	7.88±0.49	9.85±0.61
		Hg-DOM	3.02±0.1	4.53±0.15	6.04±0.2	7.55±0.25
		Hg(0)	0.5±0.04	0.75±0.05	1±0.07	1.25±0.09
		HgS	0.23±0.02	0.35±0.02	0.46±0.03	0.58±0.04
Low TOC soil	5 mM NaCl	Hg(II)*	0.12±0.01	0.18±0.01	0.24±0.01	0.3±0.01
		Hg-DOM	1.56±0.03	2.35±0.05	3.13±0.06	3.91±0.08
		Hg(0)	0.96±0.04	1.44±0.06	1.92±0.08	2.4±0.1
		HgS	0.15±0.01	0.22±0.01	0.3±0.02	0.37±0.02
	200 mM NaCl, 147 mg C/L humic acid	Hg(II)*	0.79±0.06	1.18±0.08	1.58±0.11	1.97±0.14
		Hg-DOM	2.51±0.06	3.78±0.1	5.03±0.13	6.29±0.16
		Hg(0)	0.99±0.01	1.48±0.02	1.98±0.02	2.47±0.03
		HgS	0.31±0.01	0.47±0.01	0.63±0.01	0.78±0.02
High TOC soil	5 mM NaCl	Hg(II)*	0.14±0.03	0.21±0.04	0.27±0.05	0.34±0.07
		Hg-DOM	0.23±0.05	0.35±0.08	0.47±0.1	0.59±0.13
		Hg(0)	0.15±0.02	0.23±0.03	0.31±0.4	0.38±0.05
		HgS	0.17±0.04	0.26±0.07	0.34±0.09	0.43±0.11
	200 mM NaCl, 147 mg C/L humic acid	Hg(II)*	0.25±0.02	0.38±0.03	0.51±0.04	0.63±0.05
		Hg-DOM	0.34±0.03	0.5±0.05	0.67±0.07	0.84±0.09
		Hg(0)	0.29±0.03	0.44±0.05	0.58±0.06	0.73±0.08
		HgS	0.21±0.03	0.32±0.05	0.42±0.07	0.53±0.08

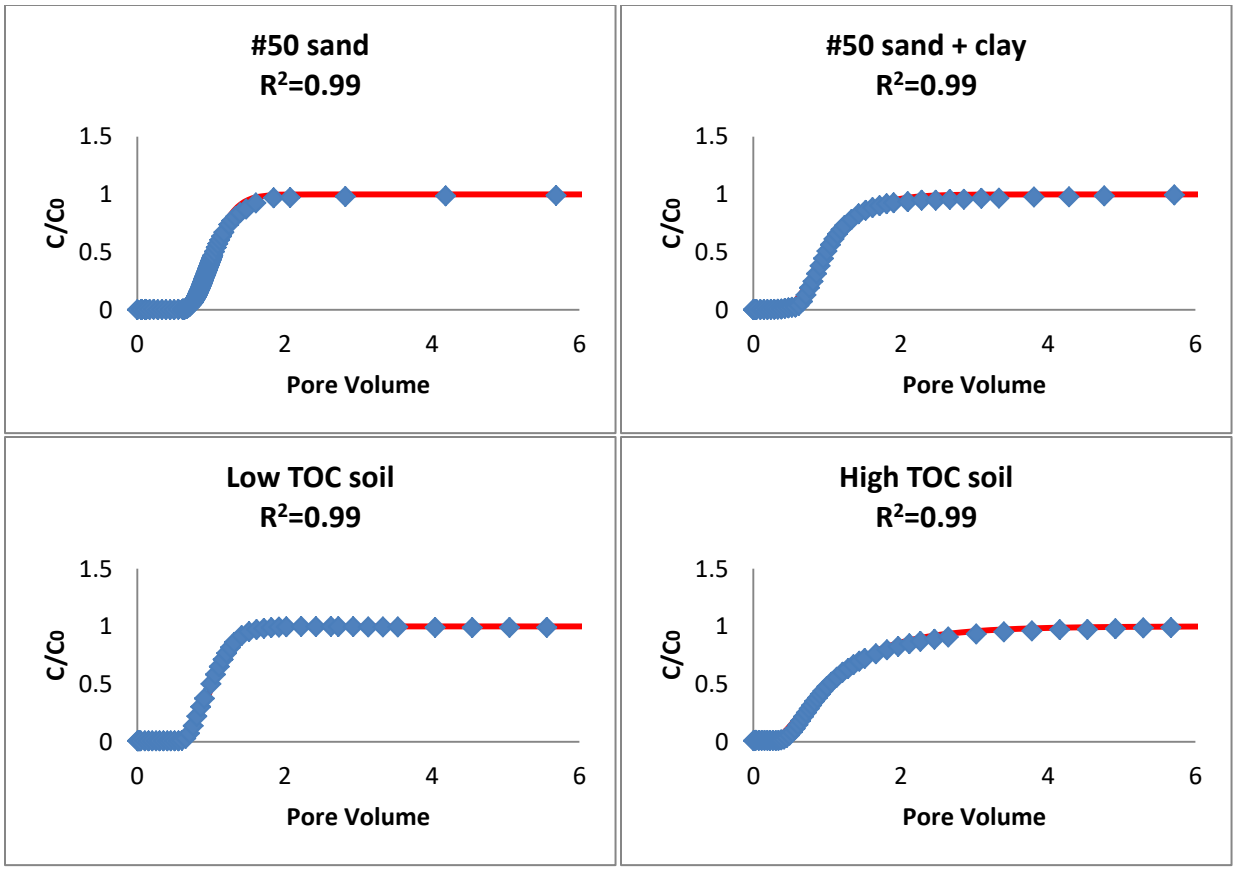

Figure A1. Tracer test breakthrough curves. Tracer: 20 mM NaCl; Blue square symbols are the raw data collected by in-line conductivity detector and the red lines represent the least square fitting of the raw data using eqn S2. The similarity of the breakthrough curve shapes suggests a similar water distribution in the different soils.

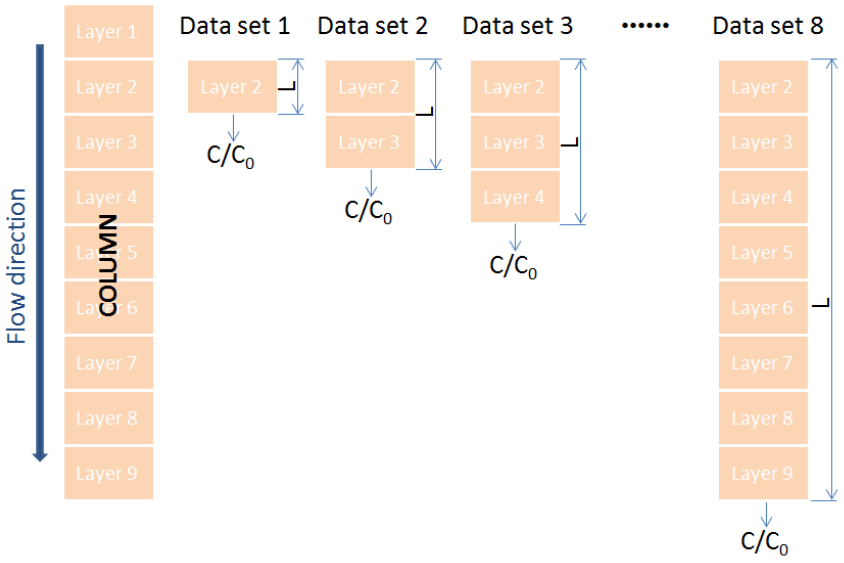

Figure A2. Illustration of the method used to determine the deposition rate coefficient for the mobile Hg mass introduced into Layer 1 for the column transport experiments. C_0 was the mobile Hg concentration determined from the difference in mass of Hg in Layer 1 at the end of the experiment compared to what was initially emplaced in this layer. C was the mobile Hg concentration at the bottom of a layer n (n = 2-9) through a segment length of L. C at the exit of each segment was calculated from a mass balance on that segment and all segments above it, i.e., was determined by subtracting the Hg mass deposited in n segments from total Hg mass entering layer 2. For all Hg species under a specific column condition, a plot of $\ln(C/C_0)$ vs. L was made, and the slope of the line formed was used to determine the mobile deposition rate according to equation 2.2.

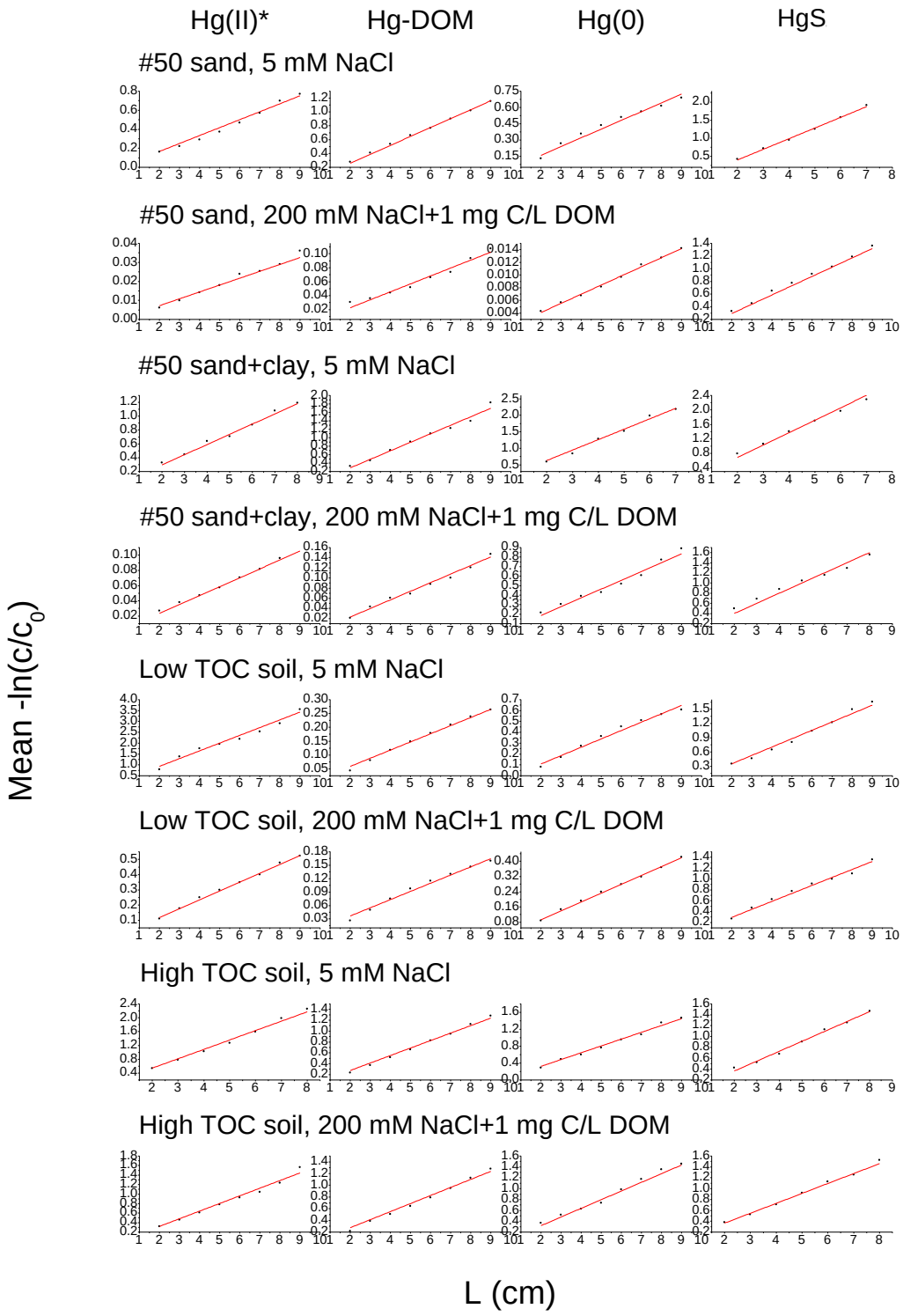

Figure A3. Fitting of mean $-\ln(C/C_0)$ vs. L for Hg species to determine $k_{d,mobile}$.

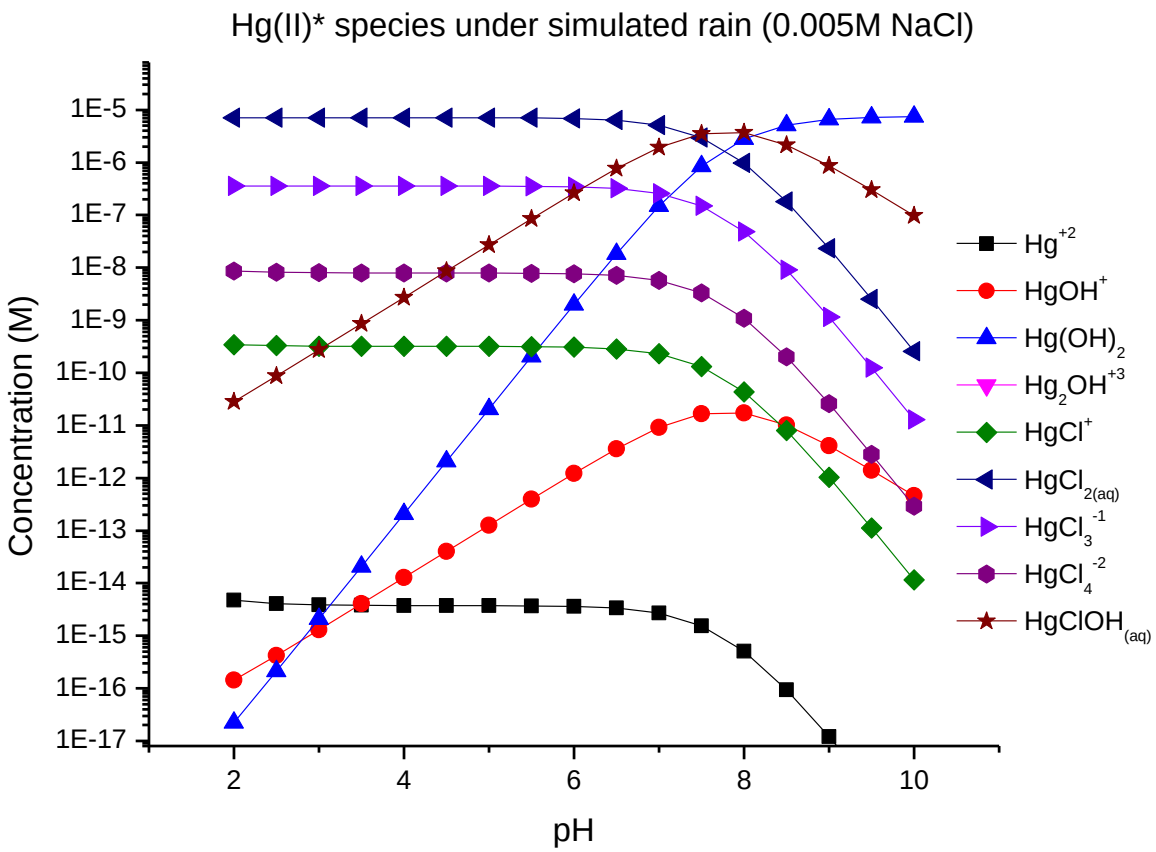

Figure A4. Dissolved Hg(II) species (denoted as Hg(II)*) under simulated rainwater (0.005 M NaCl) condition. See speciation analysis method in A2.

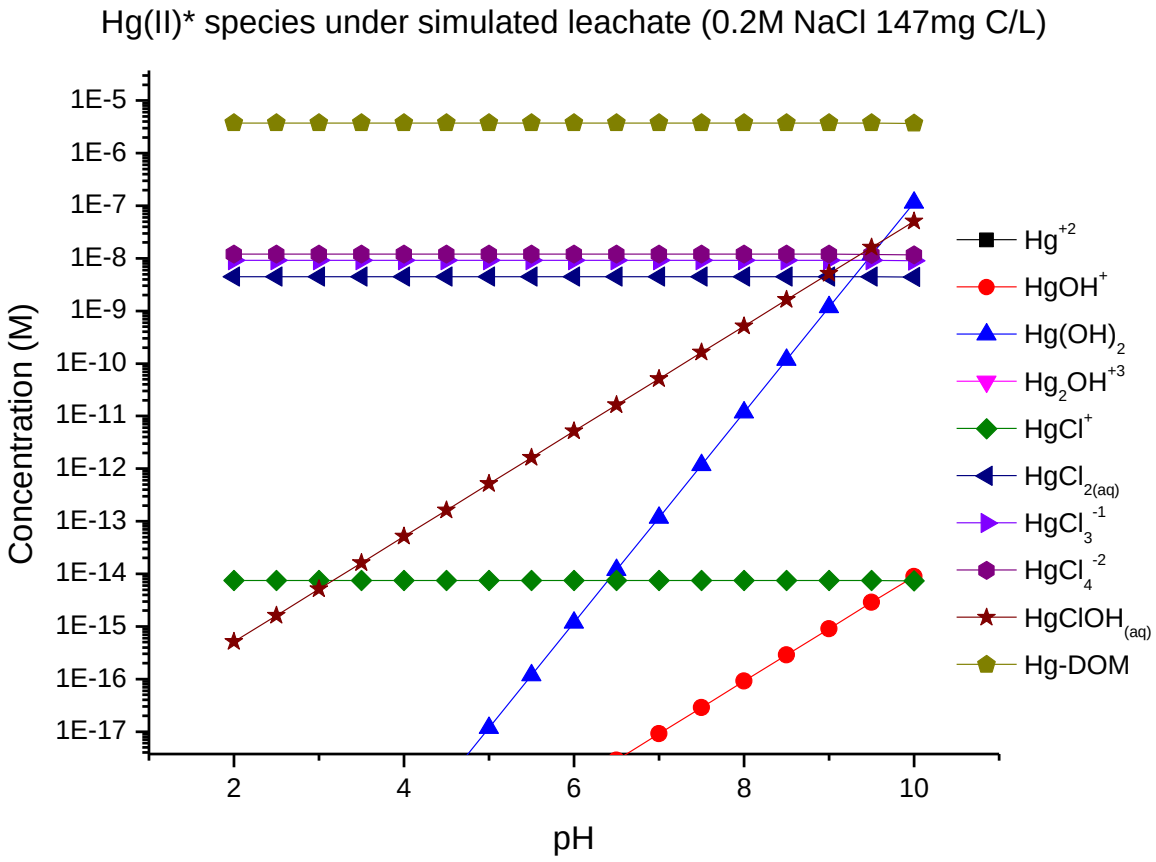

Figure A5. Dissolved Hg(II) species (denoted as Hg(II)*) under simulated leachate (0.2 M NaCl, 147 mg C/L) condition. See speciation analysis method in A2.

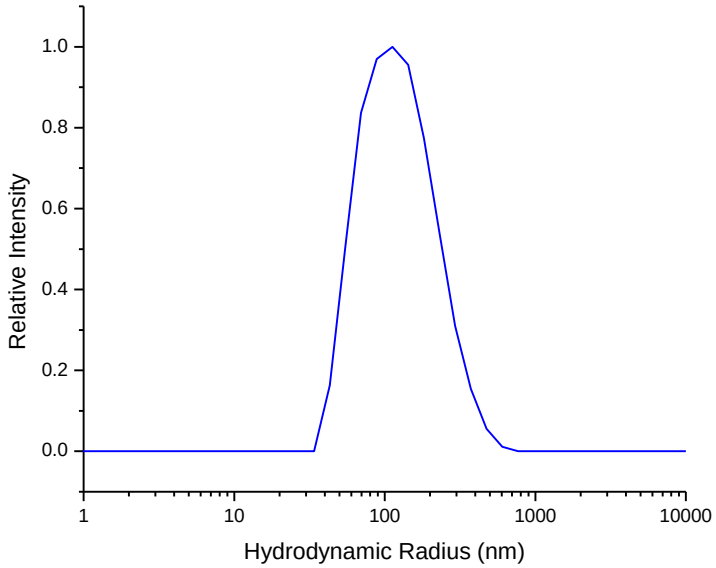

Figure A6. Intensity-weighted hydrodynamic radius of HgS nanoparticle stock solution as determined from DLS (polydispersity index=0.35).

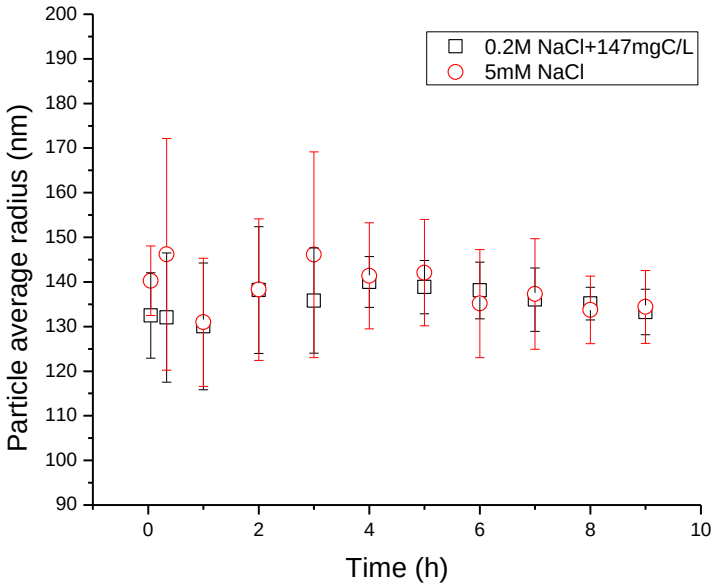

Figure A7. The change in measured hydrodynamic radius vs. time for HgS particles in two different column influent solutions, 1) 5 mM NaCl and 2) 200 mM NaCl + 147 mg carbon per L DOC.

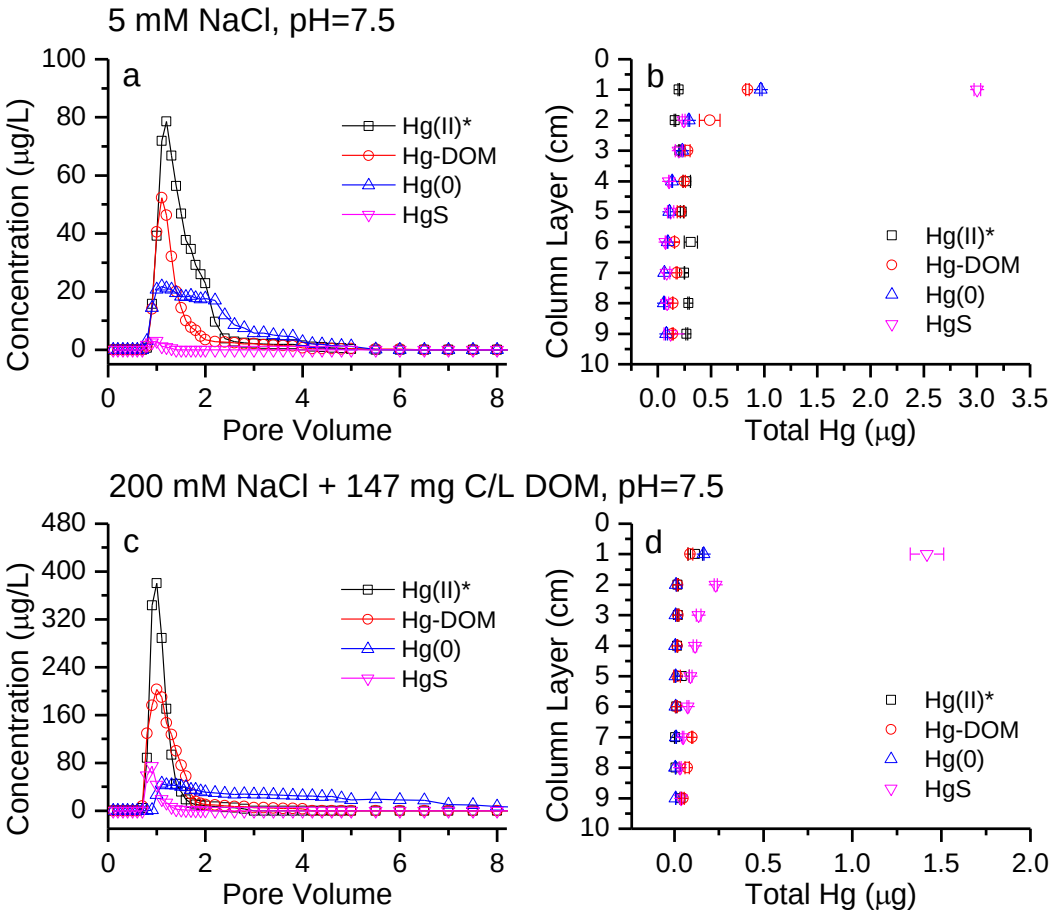

Figure A8. Representative breakthrough curves (a and c) and deposition profiles (b and d) for the four different Hg species in the unsaturated sand column. Column size: 9cm × 2.5cm; Medium: #50 Unimin sand; Influent chemistry for a and b: 0.005 M NaCl, pH 7.5; Influent chemistry for c and d: 200 mM NaCl + 147 mg C/L DOC, pH 7.5. Lines are not model fits of data. They are only meant to guide the eye.

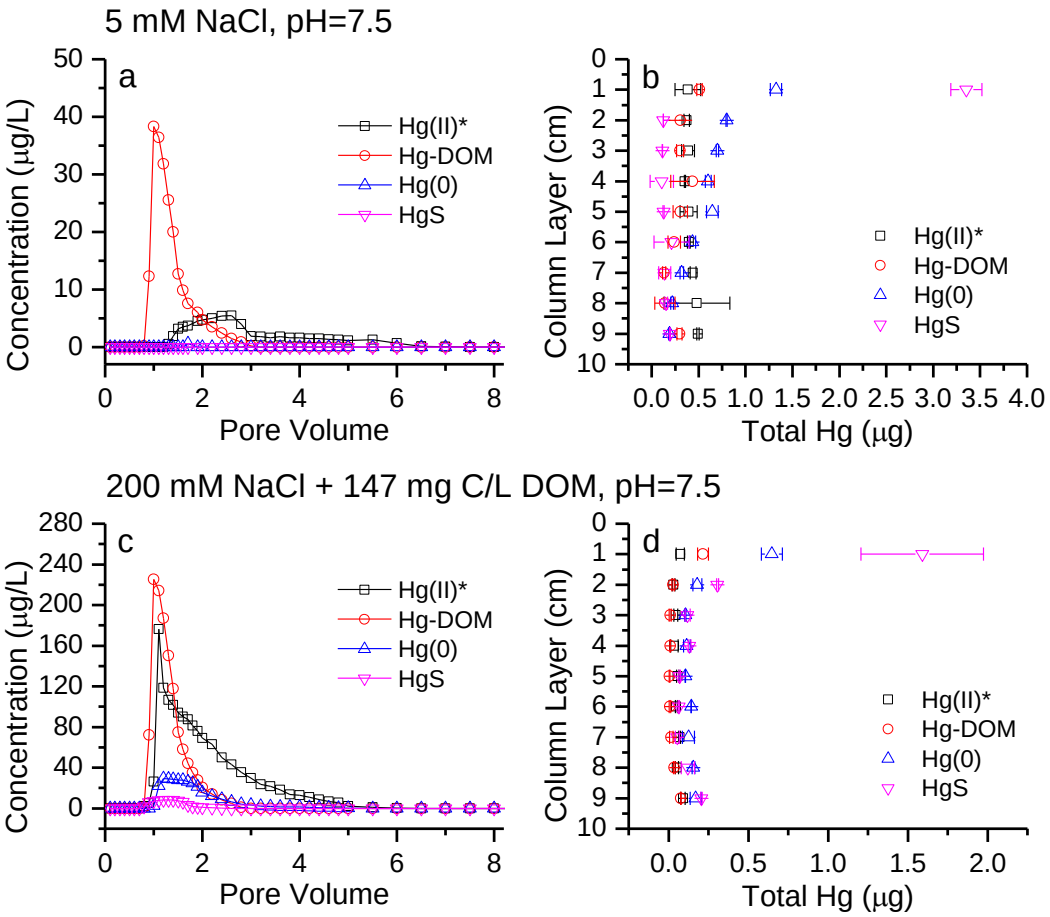

Figure A9. Representative breakthrough curves (a and c) and deposition profiles (b and d) for the four different Hg species in the unsaturated sand column. Column size: 9cm × 2.5cm; Medium: #50 Unimin sand (98 wt%) + clay (2 wt%); Influent chemistry for a and b: 0.005 M NaCl, pH 7.5; Influent chemistry for c and d: 200 mM NaCl + 147 mg C/L DOC, pH 7.5. Lines are not model fits of data. They are only meant to guide the eye.

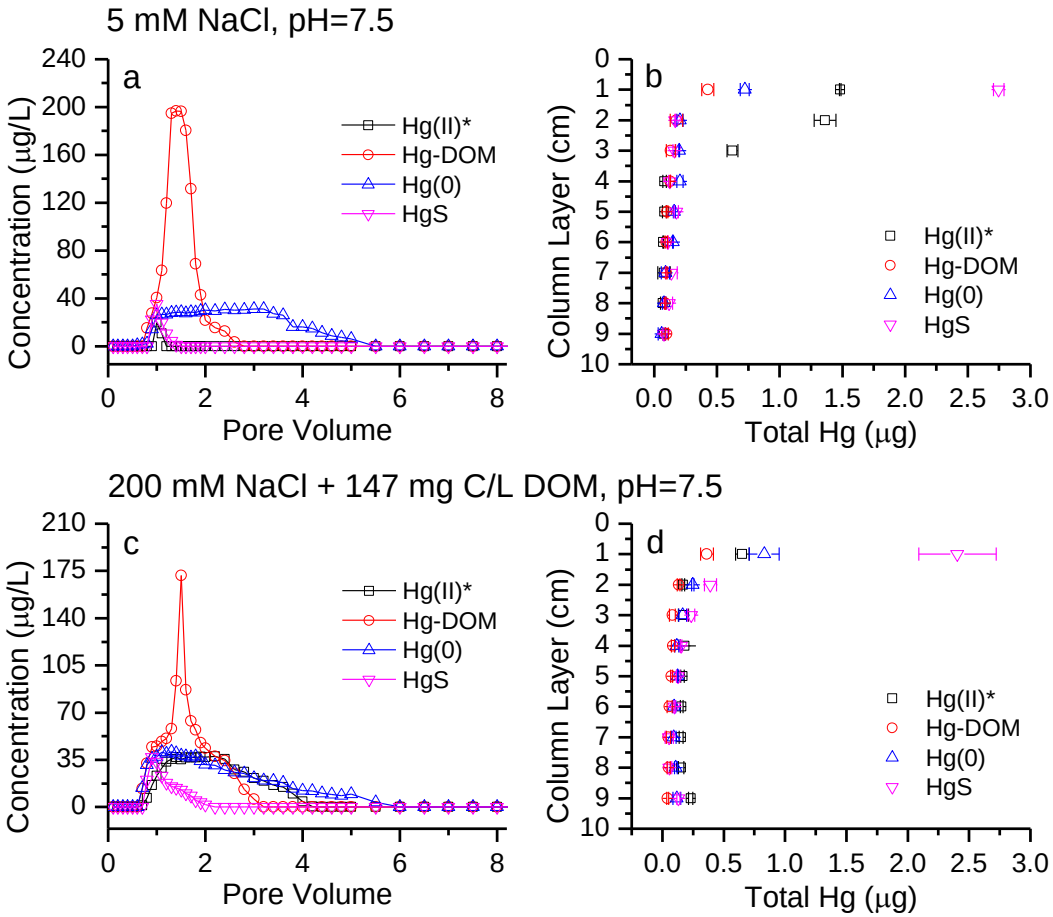

Figure A10. Representative breakthrough curves (a and c) and deposition profiles (b and d) for the four different Hg species in the unsaturated sand column. Column size: 9cm × 2.5cm; Medium: low TOC soil from Alameda point, CA; Influent chemistry for a and b: 0.005 M NaCl, pH 7.5; Influent chemistry for c and d: 200 mM NaCl + 147 mg C/L DOC, pH 7.5. Lines are not model fits of data. They are only meant to guide the eye.

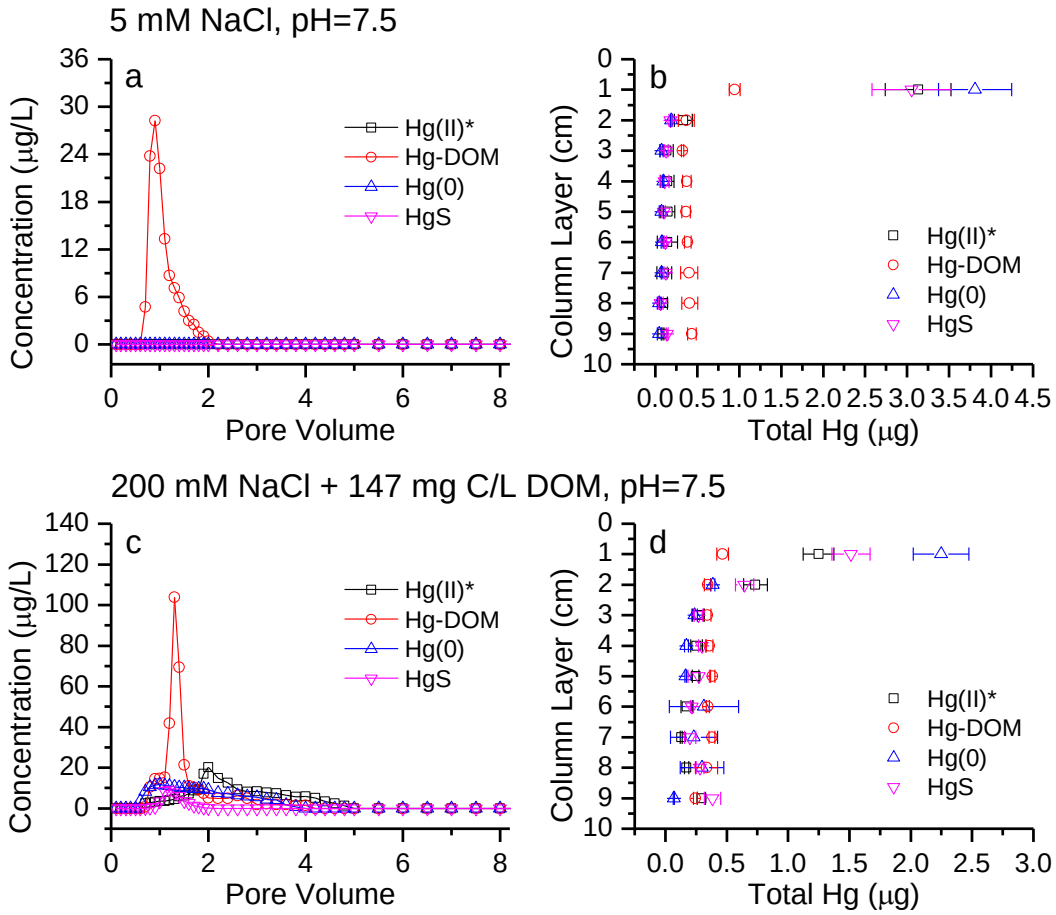

Figure A11. Representative breakthrough curves (a and c) and deposition profiles (b and d) for the four different Hg species in the unsaturated sand column. Column size: 9cm × 2.5cm; Medium: high TOC soil from Pittsburgh, PA; Influent chemistry for a and b: 0.005 M NaCl, pH 7.5; Influent chemistry for c and d: 200 mM NaCl + 147 mg C/L DOC, pH 7.5. Lines are not model fits of data. They are only meant to guide the eye.

Reference

1. Haitzer, M., G.R. Aiken, and J.N. Ryan, *Binding of mercury (II) to dissolved organic matter: the role of the mercury-to-DOM concentration ratio.* Environmental science & technology, 2002. **36**(16): p. 3564-3570.

Appendix B: Supplementary Information for Chapter 3

B1. Reference compounds used for Hg EXAFS fitting

A total of 18 reference compounds containing minerals, salts, or organic species were acquired as model compounds (see EXAFS spectra and provenance of the references in Figure B3) for the LCF, including: α-Hg^0 (slow cooled), cinnabar (α-HgS), metacinnabar (β-HgS), eglestonite ($Hg_6Cl_3O_2H$), schuetite ($Hg_3O_2SO_4$), kleinite ($Hg_2N(Cl, SO_4)$, mosesite ($Hg_2N(Cl, SO_4, MoO_4, CO_3)$), terlinguite ($Hg_2OCl$), $Hg_3S_2Cl_2$, HgCl, HgO, $HgSO_4$, $HgCl_2$, Hg-thiosulfate, Hg-cysteine, Hg-glutathione (Hg-thiol), $Hg(SR)_4$, Hg-phenyl and Hg-DOM. An additional reference spectra contribution was added to the fit if both *(i)* its contribution to the signal was above 10% and *(ii)* it reduced the χ^2 and the R-factor values (i.e., quality factors, the lower their value, the better the fit) by more than 20%. During the LCF, the energy was not allowed to vary, and the fits were not forced to sum 100. The R-factor (R_f), indicates the variations between fit and the data. We considerate a R_f value higher than 0.1 as the indicator of flaws in the fit, or of a low quality data. We also used the chi-square (χ^2) value, assessing the statistical quality of the fit. χ^2 is based on the differences between the data and the fit in comparison to the noise of the spectra. A χ^2 close to 10 (for the spline range we used), indicate that the difference between the fit and the measurement is attributable to measurement uncertainty.

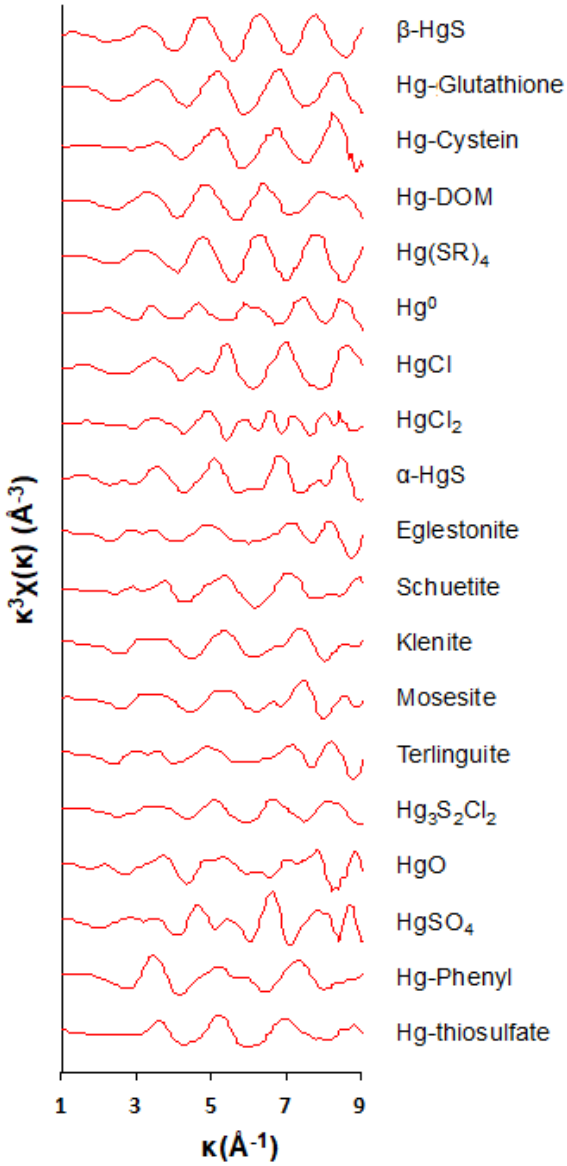

Figure B1. EXAFS spectra $k^3\chi(k)$ at Hg-L(III) edge of the reference compounds used for the linear combination fits. References were either 1) given from the mineral collection by Gordon's Brown lab at Stanford university and has been used and characterized in previous publications[1], 2) Hg-Cysteine[2], Hg-Glutathione[3], $Hg(SR)_4$[4] and β-HgS[5] were synthesized following published protocols, and the rest has been 3) purchased as pure minerals from Sigma Aldrich or Alfa Aesar.

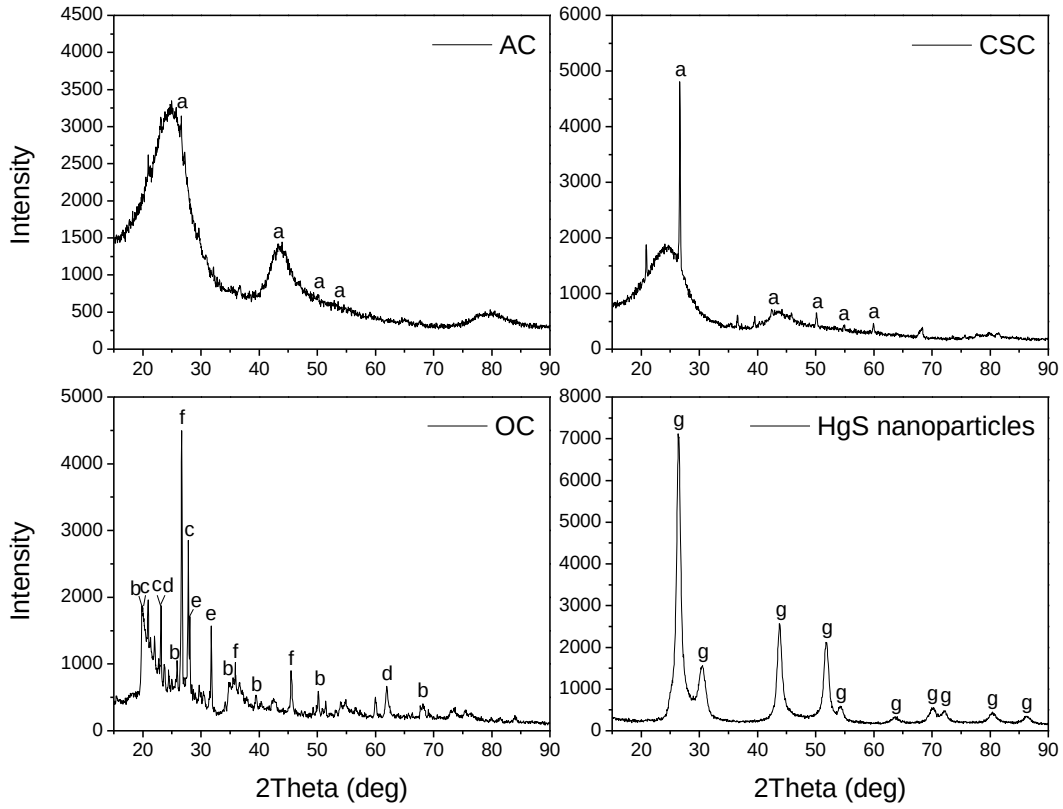

Figure B2. XRD spectra for activated carbon (AC), sulfur-impregnated activated carbon (CSC), organoclay (OC) and HgS nanoparticles. Collected for peaks matching (a): graphite (C), (b) quartz (SiO_2), (c) sulfur (S_{12}), (d) kaolinite ($Al_2Si_2O_5(OH)_4$), (e) tuhualite ($(Na,K)Fe^{2+}Fe^{3+}[Si_6O_{15}]$), (f) potassium hydrogen sulfide (KSH) and (g) metacinnabar (HgS).

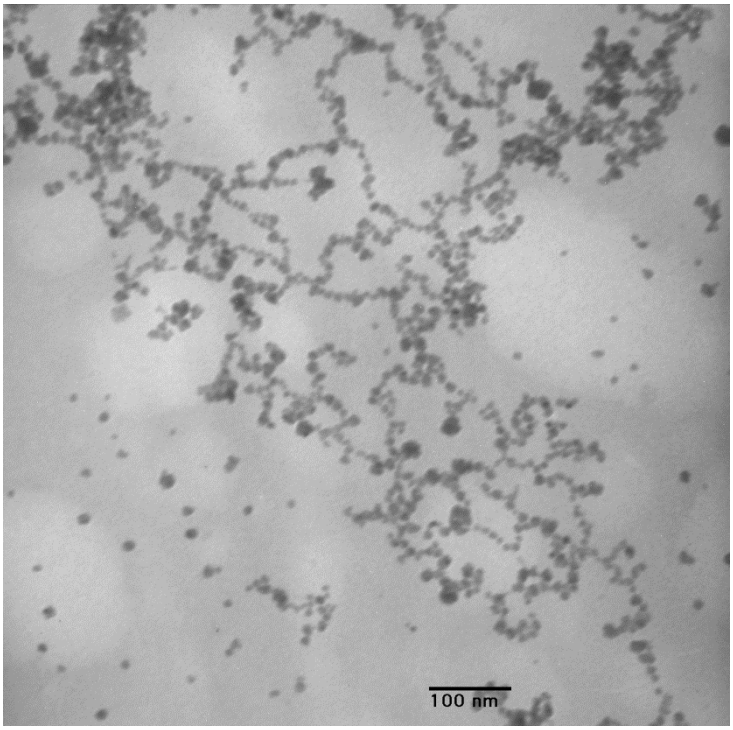

Figure B3. TEM image of synthesized HgS nanoparticles with an average particle size of 10 nm.

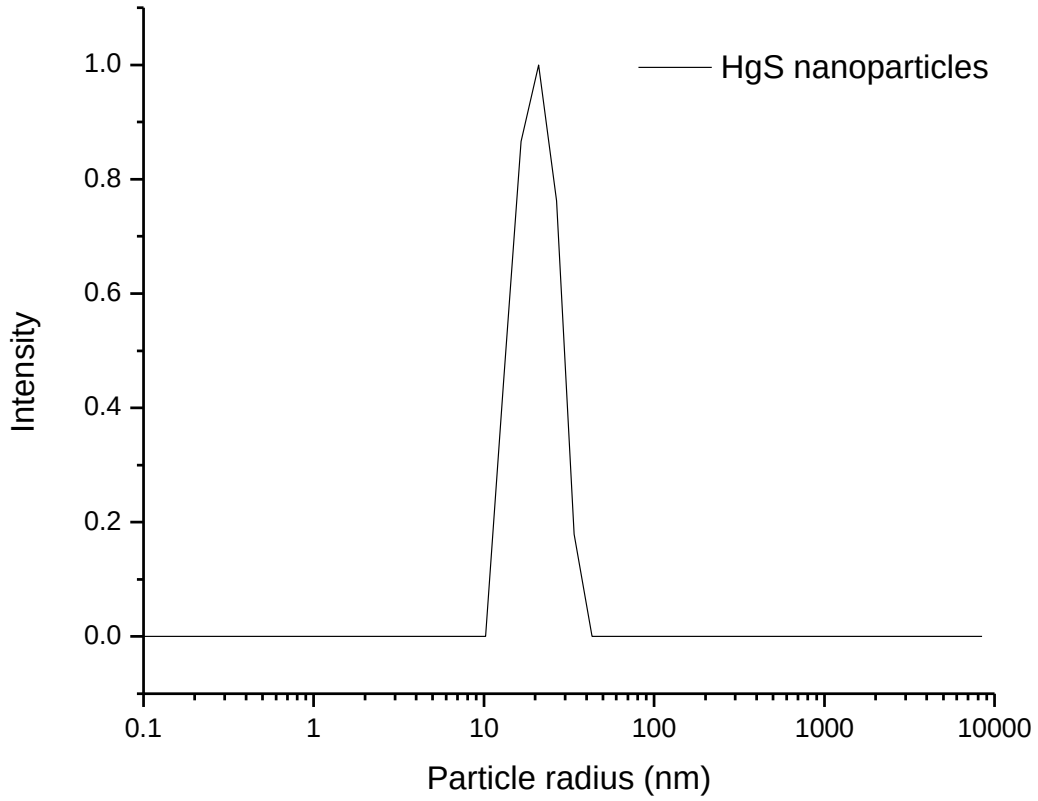

Figure B4. Particle size distribution of synthesized HgS nanoparticles determined by dynamic light scattering.

Table B1. Fitting results for Hg removal experiments using pseudo second order kinetic model.

		5 mM NaCl			5 mM NaCl+1 mg C/L HA		
		k	**q_e**	**R^2**	**k**	**q_e**	**R^2**
Hg(II)*	**AC**	3.2±0.7	0.63±0.03	0.993	3.8±0.5	0.55±0.01	0.998
	CSC	1.5±0.2	0.87±0.03	0.994	1.6±0.3	0.85±0.04	0.991
	OC	1.0±0.2	0.99±0.06	0.984	Cannot be fitted		
HgS	**AC**	1.0 ±0.6	0.72±0.18	0.890	5.4±0.7	0.46±0.01	0.998
	CSC	5±2.7	0.53±0.04	0.976	3.1±0.6	0.56±0.02	0.993
	OC	0.9±0.3	0.93±0.11	0.944	1.2±1.6	0.55±0.29	0.711
Hg-DOM	**AC**	6.6±2	0.44±0.02	0.991	9.7±2.1	0.43±0.01	0.999
	CSC	5.4±0.7	0.47±0.01	0.999	11.3±7.1	0.46±0.02	0.991
	OC	5.7±1.1	0.47±0.01	0.999	11±4.7	0.46±0.02	0.995
		1.7 mM $CaCl_2$			**1.7 mM $CaCl_2$+1 mg C/L HA**		
		k	**q_e**	**R^2**	**k**	**q_e**	**R^2**
Hg(II)*	**AC**	6.3±2.4	0.70±0.02	0.984	7.4±4.4	0.58±0.03	0.989
	CSC	2.3±1.2	0.86±0.09	0.960	29.8±19.3	0.58±0.02	0.982
	OC	3.4±1.8	0.78±0.05	0.983	Cannot be fitted		
HgS	**AC**	2.9±1.0	0.72±0.06	0.983	3.3±0.8	0.52±0.03	0.990
	CSC	3.2±1.5	0.71±0.06	0.973	4.4±1.1	0.47±0.02	0.992
	OC	1.7±0.4	0.89±0.05	0.986	3.1±1.1	0.49±0.04	0.972
Hg-DOM	**AC**	2.2±0.3	0.65±0.02	0.994	2.1±0.4	0.64±0.03	0.991
	CSC	2.3±0.3	0.67±0.02	0.995	3.3±1.1	0.60±0.04	0.985
	OC	1.9±0.5	0.68±0.04	0.985	2.7±0.1	0.63±0.01	0.999
		200 mM NaCl			**66.7 mM $CaCl_2$**		
		k	**q_e**	**R^2**	**k**	**q_e**	**R^2**
Hg(II)*	**AC**	2.9±0.7	0.56±0.03	0.994	3.2±1.5	0.69±0.05	0.985
	CSC	2.0±0.5	0.60±0.04	0.988	0.5±0.2	0.84±0.15	0.913
	OC	3.0±2.4	0.41±0.08	0.883	Cannot be fitted		
HgS	**AC**	3.2±1.5	0.69±0.05	0.999	2.9±1.2	0.63±0.05	0.992
	CSC	2.2±1.9	0.84±0.15	0.990	4.6±1.4	0.71±0.02	0.996
	OC	1.5±1.2	0.80±0.30	0.986	2.5±0.2	0.83±0.01	0.993
Hg-DOM	**AC**	7.4±1.8	0.51±0.01	0.997	6.7±3.3	0.51±0.03	0.988
	CSC	6.2±1.4	0.53±0.01	0.997	5.3±0.8	0.59±0.01	0.998
	OC	7.0±2.5	0.51±0.02	0.994	3.5±1.8	0.62±0.06	0.967

The unit of k is [g mg^{-1} h^{-1}]; the unit of q_e is [mg g^{-1}].

Table B2. Surface area normalized fitting results for Hg removal experimental results using pseudo second order kinetic model.

		5 mM NaCl			5 mM NaCl+1 mg C/L HA		
		k	**q_e**	**R^2**	**k**	**q_e**	**R^2**
Hg(II)*	**AC**	0.005±0.002	0.001±0	0.993	0.005±0.001	0.001±0	0.998
	CSC	0.003±0	0.001±0	0.994	0.003±0	0.001±0	0.991
	OC	0.43±0.09	0.41±0.03	0.984	Cannot be fitted		
HgS	**AC**	0.001±0.001	0.001±0	0.890	0.007±0.001	0.001±0	0.998
	CSC	0.008±0.004	0.001±0	0.976	0.005±0.001	0.001±0	0.993
	OC	0.39±0.14	0.39±0.05	0.944	0.49±0.66	0.23±0.12	0.711
Hg-DOM	**AC**	0.01±0.003	0.001±0	0.991	0.014±0.003	0.001±0	0.999
	CSC	0.009±0.001	0.001±0	0.999	0.018±0.011	0.001±0	0.991
	OC	2.37±0.47	0.19±0.005	0.999	4.41±1.94	0.19±0.007	0.995
		1.7 mM $CaCl_2$			**1.7 mM $CaCl_2$+1 mg C/L HA**		
		k	**q_e**	**R^2**	**k**	**q_e**	**R^2**
Hg(II)*	**AC**	0.009±0.003	0.001±0	0.984	0.011±0.006	0.001±0	0.989
	CSC	0.004±0.002	0.001±0	0.960	0.049±0.032	0.001±0	0.982
	OC	1.40±0.73	0.32±0.02	0.983	Cannot be fitted		
HgS	**AC**	0.004±0.002	0.001±0	0.983	0.005±0.001	0.001±0	0.990
	CSC	0.005±0.003	0.001±0	0.973	0.007±0.002	0.001±0	0.992
	OC	0.69±0.17	0.37±0.02	0.986	1.3±0.46	0.21±0.02	0.972
Hg-DOM	**AC**	0.003±0	0.001±0	0.994	0.003±0.001	0.001±0	0.991
	CSC	0.004±0.001	0.001±0	0.995	0.005±0.002	0.001±0	0.985
	OC	0.81±0.19	0.28±0.02	0.985	1.11±0.044	0.26±0.002	0.999
		200 mM NaCl			**66.7 mM $CaCl_2$**		
		k	**q_e**	**R^2**	**k**	**q_e**	**R^2**
Hg(II)*	**AC**	0.004±0.001	0.001±0	0.994	0.005±0.002	0.001±0	0.985
	CSC	0.003±0.001	0.001±0	0.988	0.001±0	0.001±0	0.913
	OC	1.25±0.99	0.17±0.03	0.883	Cannot be fitted		
HgS	**AC**	0.005±0.002	0.001±0	0.999	0.004±0.002	0.001±0	0.992
	CSC	0.004±0.003	0.001±0	0.990	0.007±0.002	0.001±0	0.996
	OC	0.62±0.49	0.33±0.12	0.986	1.05±0.06	0.35±0.003	0.993
Hg-DOM	**AC**	0.011±0.003	0.001±0	0.997	0.01±0.005	0.001±0	0.988
	CSC	0.01±0.002	0.001±0	0.997	0.009±0.001	0.001±0	0.998
	OC	2.93±1.05	0.21±0.01	0.994	1.45±0.76	0.26±0.02	0.967

The unit of k is [g^2 mg^{-1} m^{-2} h^{-1}]; the unit of q_e is [mg g^{-1} m^{-2}].

Table B3. Linear combination Fit results. Rf : R-factor is a quality factor. The lower the value the better the fit.

Initial speciation	Adsorbent	Hg-thiol (%)	Hg-Cysteine (%)	HgS(%)	Sum (%)	Rf
Hg-DOM	AC	92 ± 3			92	0.04
	SAC	88 ± 6	27 ± 4		115	0.07
	OC			107 ± 5	107	0.02

References

1. Jew, A.D.; Kim, C.S.; Rytuba, J.J.; Gustin, M.S.; Brown Jr, G.E., New technique for quantification of elemental Hg in mine wastes and its implications for mercury evasion into the atmosphere. *Environmental science & technology* **2010,** *45* (2), 412-417.
2. Jalilehvand, F.; Leung, B.O.; Izadifard, M.; Damian, E., Mercury (II) cysteine complexes in alkaline aqueous solution. *Inorganic chemistry* **2006,** *45* (1), 66-73.
3. Mah, V.; Jalilehvand, F., Mercury (II) complex formation with glutathione in alkaline aqueous solution. *JBIC Journal of Biological Inorganic Chemistry* **2008,** *13* (4), 541-553.
4. Warner, T.; Jalilehvand, F., Formation of Hg (II) tetrathiolate complexes with cysteine at neutral pH. *Canadian journal of chemistry* **2016,** *94* (4), 373-379.
5. Wang, H.; Zhu, J.-J., A sonochemical method for the selective synthesis of α-HgS and β-HgS nanoparticles. *Ultrasonics sonochemistry* **2004,** *11* (5), 293-300.

Appendix C: Supplementary Information for Chapter 4

Table C1. Total mass distribution of Hg in each phase of produced water.

Sample	**Total Hg**	**Percentage of Total Hg in each phase**
Water phase (99.2%wt/wt)	0.07 ± 0.02 µg/mL	89.5%
Solid phase (0.8%wt/wt)	1.03 ± 0.35 µg/g	10.5%

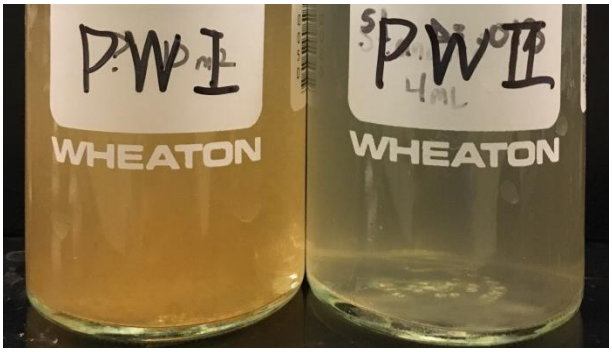

Figure C1. Produced water samples.

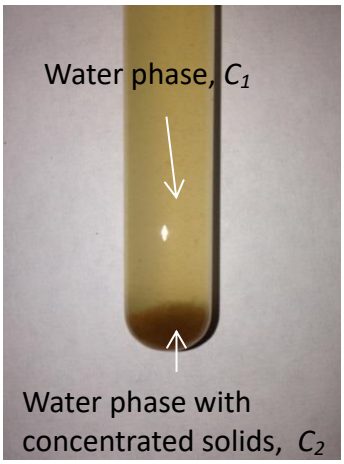

Figure C2. Produced water one (PW1) phase separation.